

Copyright
by
Kimberly Kershea Roberts
2013

**The Dissertation Committee for Kimberly Kershea Roberts Certifies that this is the
approved version of the following dissertation:**

HOST RESPONSE TO RIFT VALLEY FEVER VIRUS INFECTION

Committee:

Michael R. Holbrook, Ph. D., Supervisor

Alexander N. Freiberg, Ph. D.,
Co-Supervisor

Brian Gowen, Ph. D.

Tetsuro Ikegami, Ph. D.

Gregg N. Milligan, Ph. D.

Dean, Graduate School

HOST RESPONSE TO RIFT VALLEY FEVER VIRUS INFECTION

by

Kimberly Kershea Roberts, B.S., M.S.

Dissertation

Presented to the Faculty of the Graduate School of

The University of Texas Medical Branch

in Partial Fulfillment

of the Requirements

for the Degree of

Doctor of Philosophy

The University of Texas Medical Branch

August 2013

Dedication

For my family who has endured this long journey with me, especially those who are not here to see the end of the ride.

Acknowledgements

First I would like to thank mentors, Drs. Mike Holbrook and Alex Freiberg. Mike, thank you for accepting me into your lab and starting me out on this journey, even when I didn't know who Dr. Holbrook was. Thank you for being my Orwellian "Big Brother". Alex, thank you for continuing this journey with me, helping bring it to a close and serving as a surrogate when needed.

Next I would like to thank my committee members, Drs. Brian Gowen, Tetsuro Ikegami, and Gregg Milligan. Each of you eagerly served on my committee and brought your expertise to each meeting. There were times when I felt that this time would never end and each of you, in one way or the other, encouraged me and told me the end was near.

I want to thank all the past and present members of the Holbrook/Freiberg Lab, (in no particular order) Terry Juelich, Colette Pietzsch, Jennifer Smith, Bersabeh Tigabu, Terence Hill, Tanya Yun, Sara Woodson, Missy Worthy, LiHong Zhang, and Joe Bertrand. All the laughs and support provided throughout the years have all been appreciated. I want to say a special thank you to everyone who devoted their time and talents in the BSL4. You all worked long and late hours to help me to achieve my goals and there is no way I could thank you enough.

Next, I would like to thank my family, Mom, Pops, Rene, Clarence, Sue, Rochelle and all my countless nieces and nephews. It has been a long tough journey but this chapter in my life is finally coming to a close. You all will never know how much I love you and what your unwavering support has meant to me.

I also have to thank my husband, Darrin, who has been extremely patient with me especially these last few months. You didn't realize that I like to work through the night

into the wee hours of the morning until it was too late. I want to thank my son, Kayden, for showing me to always smile and have fun, even on rainy days

Last, but not least, I want to thank The Almighty. Without my faith to help me climb the mountains in this journey, it all would have been in vain.

Host response to Rift Valley fever virus infection

Publication No. _____

Kimberly Kershea Roberts, Ph. D.

The University of Texas Medical Branch, 2013

Supervisor: Michael R. Holbrook

Co-Supervisor: Alexander N. Freiberg

Rift Valley fever virus (RVFV) has the ability to cause severe disease (in the form of encephalitis or hemorrhagic fever) in humans and animals. RVFV is endemic to parts of Africa and the Arabian Peninsula, but there is significant concern regarding its potential introduction into non-endemic regions and the potentially devastating effect to livestock populations with concurrent infections of humans. The lack of licensed vaccines or therapeutics contributes to the designation of RVFV as a category A agent on the NIAID list of priority pathogens. During outbreaks in livestock, a nearly 100% abortion rate in infected pregnant animals can be observed with up to a 60% mortality rate in adult animals. Until recently, limited information has been published on the host response to infection by RVFV. To date, there is little detailed data directly comparing the host response to infection with RVFV and correlation with viral pathogenesis. My goal was to be able to discern the host response to infection and to correlate the response with

development of RVFV-induced pathogenesis. My efforts have centered on understanding how host immune-modulatory cells respond to infection.

In the first part of my project, primary mouse bone marrow derived (BMD) macrophages were infected with MP-12 (attenuated vaccine strain), rMP-12 Clone13 type virus (a recombinant virus resembling a naturally occurring attenuated strain), and ZH501 (pathogenic wild type strain). The cytokines and chemokines examined show a larger increase after MP-12 or rMP12-C13type infection when compared to the increase of the same cytokines after ZH501 infection. Since ZH501 does not induce secretion of cytokines in macrophage cells, it may be using these cells for transport and as initial replication site.

The second part of my project involved characterizing clinical and systemic immune responses to infection with ZH501 or MP-12 in the C57BL/6 mouse. Animals infected with MP-12 survived productive viral infection with little evidence of clinical disease and minimal cytokine response in evaluated tissues. In contrast, ZH501 infection was lethal, caused depletion of lymphocytes and platelets and elicited a strong, systemic cytokine response which correlated with high virus titers and significant tissue pathology.

TABLE OF CONTENTS

List of Tables	xi
List of Figures	xii
List of Abbreviations	xv
Chapter 1 Introduction	1
Brief History	1
Distribution and Impact	1
Virus transmission	3
Viral structure and protein function.....	5
Viral Replication.....	9
Smithburn strain.....	10
MP-12	11
Clone13	12
rMP-12 Clone13 type virus.....	12
Formalin-inactivated	13
Virus-like particles.....	13
DNA Vaccines	14
Wild type RVFV	15
Disease presentation	15
Humans	16
Livestock.....	17
Rodents	18
Non-human primates (NHPs)	21
Host Response to RVFV	22
Cell signaling during RVFV infection.....	22
Cytokine response during RVFV infection.....	23
Justification of Studies.....	26
Specific Aims of Dissertation	28

Chapter 2 Materials and Methods	29
Established cell lines.....	29
Primary cells	29
Viruses	32
Virus titration.....	32
Cell infection.....	33
Mouse challenge studies	33
Bio-Plex assay.....	34
ELISA	36
Clinical evaluation of infected mice	37
Immunohistochemistry (IHC) on mouse tissues.....	37
Statistical analysis.....	38
Chapter 3 The response of immunomodulatory cells to RVFV infection	39
Results.....	40
Cell-signaling response in immortalized mouse macrophage cells (RAW 264.7)	40
Cell-signaling response in immortalized mouse dendritic cells (DC 2.4)	48
Cell-signaling response in primary mouse macrophage cells.....	52
Cell-signaling response in primary mouse dendritic cells	58
Discussion.....	60
Chapter 4 Cytokine secretion that is affected following RVFV infection.....	68
Results.....	69
Cytokine response in RAW 264.7 cells	69
Cytokine response in DC 2.4 cells	73
Cytokine response in primary macrophage cells	77
Cytokine response in primary BMD DCs.....	86
Discussion.....	86
Chapter 5 Chemotatic and Inflammatory Responses in the Liver and Brain are associated with Pathogenesis of Rift Valley Fever Virus Infection in the Mouse	91
Results.....	93

Clinical observations.....	93
Complete Blood Counts (CBCs).....	94
Plasma Chemistry	99
Virus Distribution	101
Cytokine Profiles	103
Histopathology	114
Discussion.....	116
Chapter 6 Conclusions and Future Studies	126
Overview.....	126
Cell Signaling	127
Cytokine Secretion.....	129
<i>In vivo</i>	132
Future Studies	136
In Summary.....	137
References.....	139
Vita	158

List of Tables

Table 3.1: Phosphorylation Sites	44
Table 5.1. Complete blood counts.....	98
Table 6.1. Comparison of the host response to MP-12 and ZH501 infections ...	135

List of Figures

Figure 1.1. RVFV Distribution	3
Figure 1.2. RVFV Transmission cycle.....	5
Figure 1.3. Schematic of RVFV gene organization	6
Figure 3.1. Schematic of signaling pathways examined	41
Figure 3.2. MP-12 growth in RAW 264.7 cells	42
Figure 3.3. Total protein levels in RAW 264.7 cells.....	43
Figure 3.4. Protein levels of STAT proteins in RAW 264.7 cells	46
Figure 3.5. Protein levels in RAW 264.7 cell of JNK.....	47
Figure 3.6. Phosphoprotein levels in RAW 264.7 cells of p53, p38 MAPK, and NF-κB	48
Figure 3.7. MP-12 growth in the DC 2.4 cell line.....	49
Figure 3.8. Phosphorotein levels in DC 2.4 cells.....	51
Figure 3.9. Viral titers in BMD macrophages after infection.....	53
Figure 3.10. Primary BMD macrophages 1 or 72 HPI.....	55
Figure 3.11. Phosphoprotein levels in primary macrophage cells.....	57
Figure 3.12. Viral titers in BMD dendritic cells after infection.....	59

Figure 3.13. Photographs of primary dendritic cells 1 or 72 HPI	61
Figure 3.14. Protein levels in primary BMD dendritic cells	65
Figure 4.1. Th1 cytokines secreted by RAW 264.7 cells	71
Figure 4.2. TNFα secreted by RAW 264.7 cells.....	72
Figure 4.3. Chemokines secreted by RAW 264.7 cells.....	74
Figure 4.4. Th1 cytokines secreted by DC 2.4 cells.....	75
Figure 4.5. TNFα secreted by DC 2.4 cells.....	76
Figure 4.6. Chemokines secreted by DC 2.4 cells after infection.....	77
Figure 4.7. Th1 cytokines secreted by primary macrophages	78
Figure 4.8. TNFα secreted by primary macrophages.....	80
Figure 4.9. Cytokines secreted by primary macrophages	82
Figure 4.10. G-CSF and GM-CSF secreted by primary macrophages	83
Figure 4.11. Pro/Anti-inflammatory cytokines secreted by primary macrophages	84
Figure 4.12. Interleukins secreted by primary macrophage cells	85
Figure 5.1. Mouse survival after RVFV infection.....	95
Figure 5.2. Mouse daily weight and temperature	96

Figure 5.3. Hematology results	96
Figure 5.4. Liver function enzymes	100
Figure 5.5. Viral Distribution	102
Figure 5.6. Serum Cytokines.....	105
Figure 5.7. Liver Cytokines.....	107
Figure 5.8. Spleen Cytokines.....	109
Figure 5.9. Brain Cytokines	112
Figure 5.10. IFN-β concentration folowing infection.....	113
Figure 5.11. Liver and spleen pathology	115

List of Abbreviations

ALT	Alanine aminotransferase
AST	Aminotransferase
BMD	Bone marrow derived
BSL	Biosafety level
CBC	Complete blood count
CPE	Cytopathic effect
DC	Dendritic cell
DIC	Disseminated intravascular coagulation
DMEM	Dulbecco's Modified Eagle's Media
DPI	Days post infection
eIF2 α	Eukaryotic initiation factor 2 α
EtOH	Ethanol
G-CSF	Granulocyte colony-stimulating factor
GM-CSF	Granulocyte macrophage colony-stimulating factor
HPI	Hours post infection
HSAEC	Human small airway epithelial cells
IFN	Interferon
IHC	Immunohistochemistry
IL	Interleukin
JAK	Janus activated kinase
LEW	Lewis rat strain

LPS	Lipopolysaccharide
MCP	Monocyte chemoattractant protein
MEF	Mouse embryonic fibroblast
MIP	Macrophage inflammatory protein
MOI	Multiplicity of infection
MP-12	Vaccine strain of Rift Valley fever virus
MPI	Minutes post infection
NHP	Non-human primate
NIAID	National Institute for Allergy and Infectious Disease
PFU	Plaque-forming units
PKR	dsRNA-dependent protein Kinase
RBC	Red blood cells
	Recombinant strain of RVFV, has the backbone of MP-12 and resembles
rMP12-C13type	the naturally attenuated strain Clone 13
RNP	Ribonucleoprotein
RVF	Rift Valley fever
RVFV	Rift Valley fever virus
SAP30	Sin3A-Associated Protein 30
STAT	Signal transducers and activators of transcription
TFIIH	Transcription factor II H
TNF α	Tumor necrosis factor α
USAMRIID	United States Army Medical Research Institute of Infectious Disease
USDA	United States Department of Agriculture

VLP	Virus like particles
WBC	White blood cells
WF	Wistar-Furth rat strain
ZH501	Wild type strain of Rift Vally fever virus

Chapter 1 Introduction¹

BRIEF HISTORY

Rift Valley fever (RVF) virus (RVFV) (family *Bunyaviridae*, genus *Phlebovirus*) is a highly pathogenic mosquito-borne virus that can cause lethal disease in both humans and, particularly, ruminant animals (Findlay 1931; Schwentker and Rivers 1934). RVFV is endemic to sub-Saharan Africa, Egypt, and the Arabian Peninsula (Saudi Arabia and Yemen) (Bird, Ksiazek *et al.* 2009). Humans are typically infected during disease outbreaks in animals. The clinical picture of RVF in humans can vary from a self-limiting febrile disease, to more severe symptoms, such as hemorrhagic fever, encephalitis, and retinitis, and can even result in death. Major outbreaks in human populations vary in size, intensity and location with these parameters dependent upon rainfall and mosquito abundance (Gear 1977; Davies, Linthicum *et al.* 1985; WHO 2007). Most outbreaks of RVFV can be linked to a period of high rainfall that increases the number of breeding sites for *Aedes* species mosquitoes (Meegan 1988; Davies 2003). RVFV is classified by the National Institute for Allergy and Infectious Diseases (NIAID) as a category A priority pathogen and is a United States Department of Agriculture (USDA) high priority pathogen.

DISTRIBUTION AND IMPACT

The first known outbreak of RVFV was in sheep in 1930 in the Great Rift Valley in Kenya near Lake Naivasha (Daubney 1931). On a farm in the area, many sheep, lambs, and ewes became sick and died. Since then, the disease has been seen in many

¹Portions of this chapter have been previously published. K.K. Gray, M. N. Worthy, *et al.* (2012). "Chemotactic and inflammatory responses in the liver and brain are associated with pathogenesis of Rift Valley fever virus infection in the mouse." *PLoS Negl Trop Dis* 6(2): e1529

different African countries (Figure 1.1). The largest recorded outbreak of RVF was in Egypt in 1977 while only 598 fatalities were reported, 20,000 to 200,000 human infections were estimated (Abdel-Wahab 1978; Laughlin, Meegan *et al.* 1979; Meegan, Hoogstraal *et al.* 1979). RVFV is historically endemic in sub-Saharan Africa, but the virus increased its range and spread to the Arabian Peninsula in 2000 and the island of Madagascar in 2008. It is believed the virus spread either by wind-blown mosquitoes or transportation of infected livestock from East Africa (Shoemaker, Boulianne *et al.* 2002). The outbreak in 2000 was the first documented outbreak of RVFV outside of Africa. In this outbreak, 14% and 11% of individuals that reported infections died in a five-month span in Saudi Arabia and Yemen, respectively (Shoemaker, Boulianne *et al.* 2002). The higher than normal mortality rates found on the Arabian Peninsula are thought to be due to the virus being introduced into a naïve population. Recent outbreaks in South Africa and Mauritania have shown a higher mortality rate than previous ones have. A 2010-2011 outbreak in South Africa resulted in over 250 laboratory confirmed cases with an approximate case fatality rate of 11% (NICD 2011). The outbreak in the fall of 2012 in Mauritania resulted in 34 reported cases with 17 deaths (WHO 2013). This increase could be due to more awareness of the disease and better detection methods and therefore a higher rate of reported mortality.

RVFV infection in ruminants causes a more catastrophic disease than in humans. Pregnant ruminants that become infected with RVFV can have nearly a 100% abortion rate and some might have permanent reproductive problems (Baskerville, Hubbard *et al.* 1992; Flick and Bouloy 2005). An outbreak of RVFV causes significant agricultural problems to an area. It is thought that in the first year of an outbreak, 40-100% of pregnant animals that become infected will abort their fetuses and 90-100% of all animals younger than 14 days old that become infected will also succumb to the disease (Hartley, Rinderknecht *et al.* 2011). After an outbreak, trade restrictions can be placed on live animals, meat and meat products, as well as milk and milk products. In the United States,

susceptible livestock and competent mosquito vectors are present (Davies 2003; Swanepoel 2004; Kasari, Carr *et al.* 2008) and an outbreak of RVF could be a substantial setback to the agricultural industry as many animals would be sacrificed to limit the spread of the disease and animal as well as animal product exports would be severely restricted. The estimated cost of an outbreak to the livestock industry is in the billions.



Figure 1.1. RVFV Distribution²

The dark green countries indicate reported outbreaks of RVFV. The lighter green countries represent areas where the virus has been isolated (Ikegami 2012).

VIRUS TRANSMISSION

While the virus has been detected in 23 species of mosquitoes (including *Aedes*, *Anopheles*, and *Culex* spp. mosquitoes) as well as other vectors such as sandflies, RVFV is transmitted primarily by floodwater *Aedes mcintoshii* mosquitoes (Smithburn, Haddow *et al.* 1949; Swanepoel 1994; Fontenille, Traore-Lamizana *et al.* 1998; Moutailler, Krida *et al.* 2008). These mosquitoes increase in number after heavy rainfalls that result in a

² Modified and reprinted from Ikegami, T. (2012). "Molecular biology and genetic diversity of Rift Valley fever virus." *Antiviral Res* **95**(3): 293-310 with permission from Elsevier.

larger number of accessible breeding sites and stimulate dormant eggs to hatch. The virus survives during the dry season due to transovarial transmission. Infected mosquitoes lay eggs that are infected with the virus. When it rains, the mosquito eggs hatch and infected mosquitoes are released. Outbreaks have been shown to follow times of abundant rainfall or after new dams have been constructed (Linthicum, Davies *et al.* 1985; Meegan 1988; Digoutte and Peters 1989). *Aedes* mosquitoes are found throughout the world, including the United States and Europe, making the potential introduction of RVFV into naïve populations a very serious public health and agricultural concern as naïve populations have higher morbidity and severe reactions recorded (Al-Hazmi, Ayoola *et al.* 2003; Bird, Ksiazek *et al.* 2009). To support the notion that naïve populations are more susceptible to RVFV infection, recent studies have evaluated RVFV infection in primate species from Africa and South America. These studies found that several African monkey species do not have any febrile response after they are infected with RVFV, while South American monkey species had fever for up to 2 days after infection (Findlay 1932; Easterday 1965; Davies, Clausen *et al.* 1972; Ikegami and Makino 2011; Smith, Bird *et al.* 2012). It appears that the old-world monkey species may have developed a slight natural genetic resistance to infection after dealing with RVFV for over 80 years. This resistance also appears to occur in livestock as indigenous African breeds of sheep, goats, and cattle have no clinical signs of disease, when compared to the European breeds, even though they do have a short viremic period (Davies 2003).

RVFV is generally transmitted to humans through the bite of an infected mosquito, but aerosol transmission or contact with bodily fluids and tissues from infected animals has also been documented (Figure 1.2) (Smithburn, Haddow *et al.* 1949; Smithburn, Mahaffy *et al.* 1949). People who are in close contact with viremic animals, such as farmers, herders, and veterinarians, have an increased risk of contracting RVFV. Aborted fetuses are of special concern as RVFV can maintain its high infectivity in the

protein rich environment of the fetus for an extended period of time (Bouloy 2011). People that are involved in the birthing process are at a particularly high risk due to the contact with infected tissue and possible aerosolized particles from animals. RVFV is thought to be highly infectious in an aerosol and is stable at 4°C for extended periods of time; accordingly, it has the theoretical potential to be used as a biological weapon (Davies and Highton 1980; Peters 2002; Gerdes 2004).

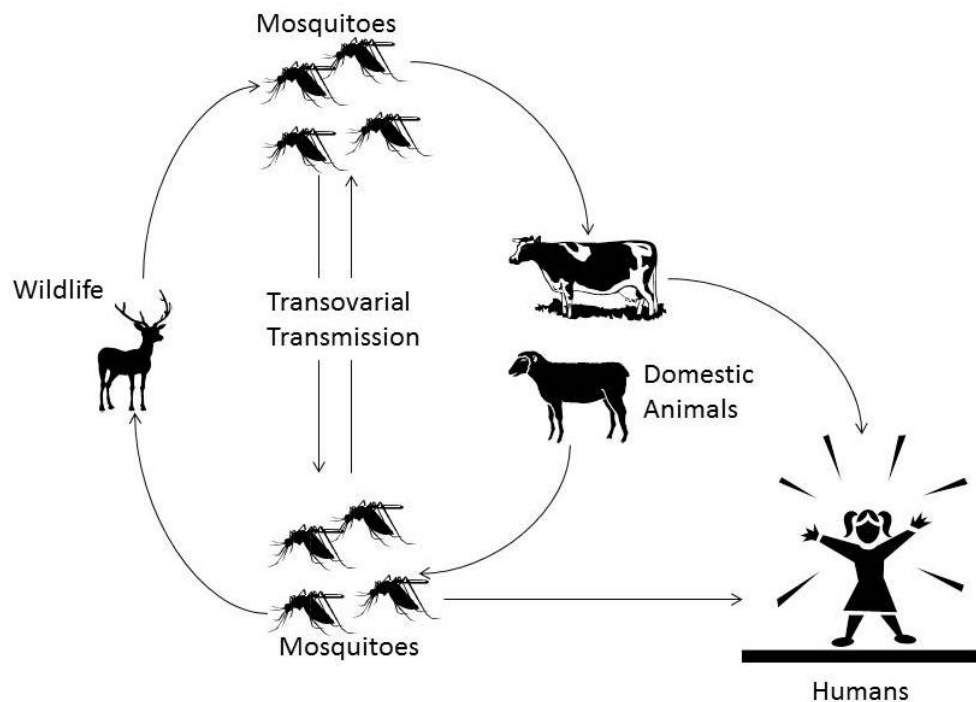


Figure 1.2. RVFV Transmission cycle

Transmission cycle of RVFV. The virus is transmitted by mosquitoes to domestic animals or wildlife. Humans can be infected by mosquitoes or by exposure to infected animal tissue.

VIRAL STRUCTURE AND PROTEIN FUNCTION

RVFV is an icosahedral virus enveloped by a lipid bilayer that is 90-110 nm in diameter and contains a segmented, negative-sense, single-stranded RNA genome (Flick and Bouloy 2005; Schmaljohn 2007; Freiberg, Sherman *et al.* 2008; Huiskonen, Overby *et al.* 2009; Sherman, Freiberg *et al.* 2009). The genome consists of three segments: large

(L), medium (M), and small (S). The L and M segments are of negative polarity (Figure 1.3) while the S segment has an ambisense polarity. The L segment encodes the L protein (viral RNA dependent RNA polymerase), while the M segment encodes Gn and Gc, (surface glycoproteins that extend from the virion surface), NSm (non-structural protein), and a 78 kDa protein. The S segment encodes for two proteins: N (nucleocapsid protein) and NSs (non-structural protein) (Schmaljohn 2007).

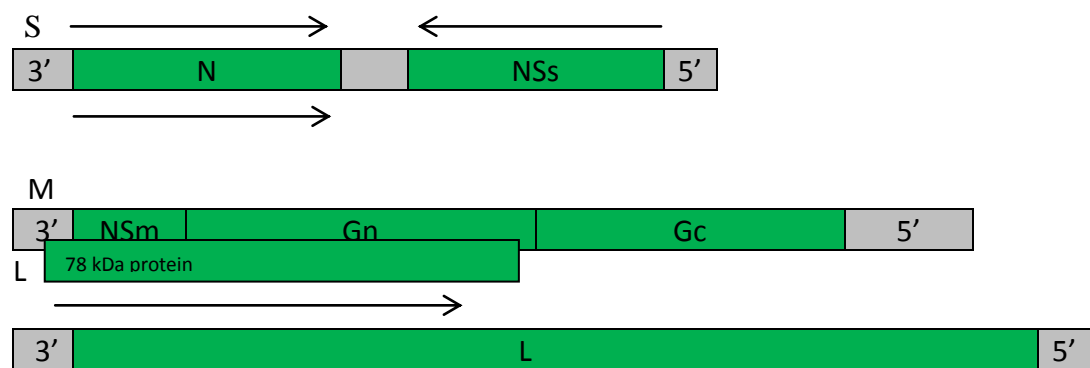


Figure 1.3. Schematic of RVFV gene organization³

The green boxes represent the 6 genes of RVFV. N, Gn, Gc and L represent the 4 structural genes while NSs and NSm represent the 2 non-structural genes. The 78 kDa protein is part of the M-segment, but is shown below the M-segment as it overlaps the NSm and Gn genes. The arrows represent gene polarity. The L and M segments are negative polarity. The S segment is ambisense.

The surface glycoproteins Gn and Gc are transmembrane proteins that are arranged at regular intervals on the viral surface. The virion is covered by 122 glycoprotein capsomers (Sherman, Freiberg *et al.* 2009), which are likely formed by Gn-Gc heterodimers, and form hexamers and pentamers (Freiberg, Sherman *et al.* 2008; Rusu, Bonneau *et al.* 2012). While Gc is required for the virus to fuse with the host cell membrane (Dessau and Modis 2013), the cytoplasmic tail domains of the Gn protein associate with the viral ribonucleoprotein (RNPs) and are thought to act as a matrix protein found in other negative-strand RNA viruses, connecting the viral envelope with

³ Modified and reprinted from Ikegami, T. (2012). "Molecular biology and genetic diversity of Rift Valley fever virus." *Antiviral Res* **95**(3): 293-310 with permission from Elsevier.

its RNA (Piper, Sorenson *et al.* 2011; Strandin, Hepojoki *et al.* 2013). The RNPs are composed of the individual genomic segments of RNA that are encapsidated with the N protein in a string of pearls formation and the viral L protein. The RNA and N protein interact in a similar fashion as DNA and histones (Raymond, Piper *et al.* 2010; Ferron, Li *et al.* 2011; Raymond, Piper *et al.* 2012). The untranslated regions at both the 3' and 5' ends of the genomic RNA are highly conserved and self-associate through non-covalent bonds. The genomic panhandle structured RNA is then packaged into mature virions.

While neither non-structural protein is needed for viral replication, NSs is considered the virulence factor of RVFV (Bouloy, Janzen *et al.* 2001). NSs has several important functions. It has been known for some time that the NSs protein is responsible for the type I interferon (IFN- α and IFN- β) antagonistic properties of RVFV (Billecocq, Spiegel *et al.* 2004; McElroy and Nichol 2012). This property is lacking in the NSs protein of the RVFV mutant clone 13 which has an in-frame deletion of the majority (70%) of the NSs gene and is attenuated in wild type adult mice (Bouloy, Janzen *et al.* 2001; Billecocq, Spiegel *et al.* 2004). NSs interacts with the p44 subunit of transcription factor and Sin3A-Associated Protein 30 (SAP30) (Le May, Dubaele *et al.* 2004; Le May, Mansuroglu *et al.* 2008; Benferhat, Josse *et al.* 2012) and affects the IFN- β pathway at various stages all with the role of evading the host response to viral infection (Ikegami and Makino 2009). NSs interacts with SAP30 and represses the histone acetylation of this protein to prevent the transcriptional activation of the IFN- β promoter and thus prevents the transcription of IFN- β gene (Le May, Mansuroglu *et al.* 2008). It was also found that NSs down regulates general host transcription by interacting with the p44 subunit of transcription factor II H (TFIIH) (Le May, Dubaele *et al.* 2004). TFIIH is a required transcription factor for cellular RNA polymerase I and II. NSs nuclear filaments bind the p44 subunit so that host RNA polymerase cannot be activated because TFIIH assembly is blocked (Le May, Dubaele *et al.* 2004). Since the RNA polymerase cannot be activated, basal level cellular transcription is decreased (Le May, Dubaele *et al.* 2004). NSs has

also been shown to down regulate the p62 subunit of TFIID (Kalveram, Lihoradova *et al.* 2011). NSs is able to inhibit transcription in the host cell, including type I IFN and genes stimulated by IFN, which prevents a proper antiviral response in nearby cells, (Ikegami, Narayanan *et al.* 2009; Ikegami and Makino 2011). By down-regulating host transcription, RVFV can use all the components of the cell to make mature virions.

NSs also promotes proteasome-mediated degradation of PKR (dsRNA-dependent protein kinase) and does not allow for the activation of eukaryotic initiation factor 2 alpha (eIF2 α) (Habjan, Pichlmair *et al.* 2009; Ikegami, Narayanan *et al.* 2009; Ikegami, Narayanan *et al.* 2009). Normally PKR plays an important role in inhibiting cellular and viral protein synthesis and induction of apoptosis after sensing dsRNA. To prevent translational shut-off, NSs promotes the degradation of PKR. This process promotes viral protein synthesis as the degraded PKR cannot inhibit protein synthesis nor induce apoptosis in infected cells (Ikegami, Narayanan *et al.* 2009; Ikegami and Makino 2011).

Even though RVFV replicates in the cytoplasm, NSs forms filamentous structures in the nucleus that bind to specific regions of host DNA (Struthers and Swanepoel 1982). When RVFV binds to these DNA sequences, it leads to segregation defects and chromosome cohesion in mouse cells (Struthers and Swanepoel 1982; Bouloy 2011). These two processes could be the cause of fetal defects and therefore abortions that are seen in RVFV infected ruminants (Bouloy 2011).

NSm is implicated in viral pathogenesis and is thought to have anti-apoptotic properties (Won, Ikegami *et al.* 2007). It has been shown that deletion of NSm from the virus stimulates significant cell die offs through the activation of caspases 3, 8, and 9 in infected cells (Won, Ikegami *et al.* 2007). The suppression of apoptosis by NSm could give the virus a larger window of productivity thereby increasing the viral progeny output by each infected cell (Engdahl, Naslund *et al.* 2012).

VIRAL REPLICATION

After binding to its receptor, the virus enters the cell through receptor-mediated endocytosis (Lozach, Kuhbacher *et al.* 2011). DC-SIGN has been identified as at least one receptor for phleboviruses on DCs (Lozach, Kuhbacher *et al.* 2011). NSs is synthesized very early after viral infection because some S antigenome is present in the mature virion when it initially infects the cell (Ikegami, Won *et al.* 2005). Once inside the cells, viral genomic RNA that is associated with the viral N protein undergoes primary transcription in the cell cytoplasm with the aid of the viral RNA polymerase and produces complementary RNA (cRNA), antigenome and mRNA. The S segment antigenome is the template for NSs mRNA. NSs then begins its interruption of the cellular functions that allows the virus to replicate to high titers in the cell (Billecocq, Spiegel *et al.* 2004; McElroy and Nichol 2012). After NSs has accumulated in the cell, viral replication can begin in a “virus-friendly” environment, where the transcription of antiviral proteins is down-regulated. Host mRNAs are cleaved and the 5'-cap is removed from the host mRNA through the cap-snatching mechanism to initiate viral mRNA synthesis by the L protein which also possesses an endonuclease activity (Patterson, Holloway *et al.* 1984). Initiation of cRNA synthesis begins with 5' nucleoside triphosphates (Simons and Pettersson 1991; Gro, Di Bonito *et al.* 1992).

Viral mRNA for the Gn and Gc proteins is translated into viral protein at the ER. Structural proteins Gn and Gc are transported to the Golgi apparatus due to a Golgi localization signal in the transmembrane domain of the Gn protein. Gn and Gc are glycosylated, and expressed together as a polyprotein. Gc requires the physical interaction with Gn to be transported to the Golgi. Without Gn, Gc remains in the ER due to an ER retention signal it expresses. After replication of RVFV in the cytoplasm, and assembly at the Golgi membrane, the mature virus buds from the Golgi compartment and, in infected hepatocytes, the plasma membrane (Anderson and Smith 1987; Bouloy

2011). When the virus buds from the Golgi complex, Golgi vesicles containing mature virus migrate to the cell surface and fuse with the plasma membrane where mature virus is then released.

Current Vaccines

The easiest way to slow the spread of RVFV is through mosquito control programs. Phlebovirus cases have been shown to decrease after malaria eradication campaigns implemented widespread insecticide spraying in an area (Bouloy 2011). It is possible that decreasing the number of vectors that can transmit RVFV will decrease the number of cases seen annually. This type of proactive method of prevention needs to be implemented in conjunction with a successful vaccine campaign.

Smithburn strain

Although there are currently no licensed vaccines or therapeutics for RVFV infection in humans, several potential vaccine candidates are available and have been tested in animals and clinical trials (Smithburn 1949; Barnard and Botha 1977; Morrill, Jennings *et al.* 1987; Morrill and Peters 2003; Ikegami and Makino 2009; Dungu, Louw *et al.* 2010; Boshra, Lorenzo *et al.* 2011). In Kenya and South Africa the neuroadapted Smithburn RVFV strain is used in an effort to control RVF (Capstick and Gosden 1962). Smithburn used an established method for attenuating the virus. A wild type strain of RVFV isolated in Uganda in 1944 was serially inoculated into mouse brains until it became attenuated in mice (Smithburn 1949). The Smithburn strain provides long lasting protection in sheep as little as 6 days after vaccination (Coackley, Pini *et al.* 1967). However, this strain is not completely avirulent and can cause abortions and birth defects in cows, sheep, and goats (Smithburn 1949; Coetzer and Barnard 1977; Swanepoel 2004; Botros, Omar *et al.* 2006; Kamal 2009). Therefore, the vaccine is only used during an outbreak and is given to female ruminants only if they are not pregnant (Swanepoel

2004). The Smithburn vaccine also has the potential to revert to its virulent form if used in non-endemic countries (Swanepoel 2004).

MP-12

The vaccine strain MP-12 was developed by the United States Army by passaging RVFV ZH548 12 times in the presence of 5-fluorouracil (Caplen, Peters *et al.* 1985). The ZH548 strain was isolated during a major outbreak in Egypt in 1977, which resulted in 200,000 clinical cases and almost 600 deaths (Meegan 1979). Serial passaging resulted in the acquisition of a total of 23 nucleotide mutations in all three viral segments relative to its parent strain ZH548, with eleven mutations resulting in an amino acid change (Vialat, Muller *et al.* 1997; Lokugamage, Freiberg *et al.* 2012). Currently, MP-12 is one of the most promising RVF vaccine candidates because it provides protection from infection with few adverse reactions (Ikegami and Makino 2009). The MP-12 vaccine is currently only available to military personnel and researchers through the Special Immunizations Programs at the US Army Medical Research Institute of Infectious Diseases (USAMRIID) as part of an on-going clinical trial (www.clinicaltrials.gov). The MP-12 vaccine virus has been found to induce high titer neutralizing antibodies in vaccinated ruminants and has been shown to protect animals from subsequent challenge with wild type virus (Morrill, Jennings *et al.* 1987; Morrill, Carpenter *et al.* 1991; Morrill, Mebus *et al.* 1997; Morrill, Mebus *et al.* 1997). MP-12 has also been demonstrated to be apathogenic in adult mice (Vialat, Muller *et al.* 1997; Gray, Worthy *et al.* 2012). While wild type RVFV must be handled in a high or maximum containment facility in many countries, MP-12 is frequently employed in research as a BSL-2 model virus for the highly pathogenic wild type virus.

While MP-12 can be administered to sheep and cows in the late stages of pregnancy with no complications as compared to the Smithburn strain, it has been shown to be teratogenic and to cause abortions in sheep vaccinated at the 28th day of gestation

(Morrill, Carpenter *et al.* 1991; Morrill, Johnson *et al.* 1991; Baskerville, Hubbard *et al.* 1992; Morrill, Mebus *et al.* 1997; Hunter, Erasmus *et al.* 2002). When the vaccine is given to lactating animals, maternal antibodies are spread to nursing lambs, but live virus is not shed in milk (Morrill, Jennings *et al.* 1987; Morrill, Mebus *et al.* 1997). MP-12 can also be given to lambs that are older than 2 days without any adverse effects and the animals produce neutralizing antibodies (Moussa, Abdel-Wahab *et al.* 1986; Hubbard, Baskerville *et al.* 1991; Morrill, Carpenter *et al.* 1991). The NSs of MP-12 has 3 nucleotide mutations from its parent strain. Only one of these mutations leads to an amino acid change in MP-12. These mutations cause the virus to be attenuated. The NSs of MP-12 has IFN antagonist properties (discussed in detail below) (Lokugamage, Freiberg *et al.* 2012)..

Clone13

Clone13 is a live attenuated RVFV strain that resembles wild type RVFV but has a large in frame deletion (approximately 70%) of the NSs gene (Muller, Saluzzo *et al.* 1995). This deletion causes the virus to be attenuated. Due to this large deletion, it is unlikely that the virus can revert to a virulent form. Vaccination with Clone13 provides protection against wild type virus infection by the induction of a high antibody response (Muller, Saluzzo *et al.* 1995). Further, Clone13 does not cause abortions or birth defects, as does the Smithburn strain (Dungu, Louw *et al.* 2010). In recent years, vaccine candidate viruses resembling ZH501 but carrying a deletion in the NSs protein similar to Clone13 have been generated (Bird, Albarino *et al.* 2008).

rMP-12 Clone13 type virus

Using reverse genetics a vaccine candidate resembling Clone13 on the background of MP-12 was created (Ikegami, Won *et al.* 2005). Recent studies have

shown that RVFV NSs mutants are protective 20-30 minutes after exposure to ZH501 in C57BL/6 mice (Gowen, Bailey *et al.* 2013).

Formalin-inactivated

Formalin-inactivated RVF vaccines have been used in Egypt and South Africa (El-Karamany 1981). Vaccination with inactivated viruses generally results in development of high neutralizing antibody titers. While inactivated vaccines are safer for the animals they are not as immunogenic as live virus vaccines and yearly boosters are required to achieve and maintain protective immunity. One such vaccine from The Salk Institute-Government Services Division, TSI-GSD-200, (Kark, Aynor *et al.* 1982) provides protection in 90% of vaccines after three doses but only for a short term. After 9 months, only 50% of the vaccines had Plaque Reduction Neutralizing Test (PRNT)₈₀ values of 1:40 (Pittman 2000). Furthermore, inactivated vaccines are very expensive to produce since they require containment laboratories for virus growth and inactivation needs to be proven for each batch (Kark, Aynor *et al.* 1985; Pittman 2000; Lubroth, Rweyemamu *et al.* 2007). Using a vaccine that requires a yearly booster is not economically feasible in the areas that need a RVFV vaccine, since long time gaps (up to 25 years) can occur between outbreaks.

Virus-like particles

Virus-like particles (VLPs) and DNA vaccines are being developed as an alternative to live and formalin-inactivated vaccines against RVFV (Lagerqvist, Naslund *et al.* 2009; Naslund, Lagerqvist *et al.* 2009). VLPs are formed when structural proteins are expressed and assemble into native-like structure, but no genomic material is present. Since there is no genomic material and thus no RNA polymerase, VLPs are replication deficient and cannot produce progeny virus. The RVF VLP is similar to RVFV in that it has the viral Gc, Gn, and in some cases N-proteins present. Because of structural

similarities between VLPs and native virus, VLPs will bind to the same receptors and cells as the complete virus (Habjan, Penski *et al.* 2009; Ikegami and Makino 2009). VLPs are not replication competent and cannot produce progeny virus due to a lack of viral RNA polymerase. Vaccination with VLPs has been shown to provide protection against viral challenge, but does not cause any birth defects or abortions in vaccinated animals (Habjan, Pichlmair *et al.* 2009; Naslund, Lagerqvist *et al.* 2009; de Boer, Kortekaas *et al.* 2010; Pichlmair, Habjan *et al.* 2010; Koukuntla, Mandell *et al.* 2012). VLPs have been created using recombinant baculoviruses that express the RVFV Gn, Gc and N proteins (Liu, Spurrier *et al.* 2008). At present, RVFV VLP vaccines have a large amount of optimization that still needs to be done for these to be a viable candidate for human vaccine studies (Ikegami and Makino 2009), but studies are quickly moving forward (Habjan, Penski *et al.* 2009; de Boer, Kortekaas *et al.* 2010; Pichlmair, Habjan *et al.* 2010). Since VLPs do not produce progeny, an optimal dose needs to be determined that will result in a development of protective immunity without causing adverse reactions to the inoculum. Also, appropriate cells substrates need to be identified and optimized for production of VLPs as a human vaccine (Ikegami and Makino 2009).

DNA Vaccines

DNA vaccines are relatively inexpensive to generate and do not require the cold-chain storage that is typically required for live vaccines (Belakova, Horynova *et al.* 2007). A vaccine that is not temperature sensitive is a valued commodity in developing countries where it may be difficult to maintain cold storage from receipt to use of the vaccine (Giese 1998). DNA vaccines directed at Gn and Gc have shown protection, albeit incomplete, against lethal challenge with ZH548 (Spik, Shurtleff *et al.* 2006; Wallace, Ellis *et al.* 2006; Lagerqvist, Naslund *et al.* 2009). While a majority of mice

vaccinated with DNA vaccines are protected against lethal challenge, some do not have any protection to wild type infection.

While both VLP and DNA vaccines show promise, in most studies, aside from neutralizing antibodies and lymphocyte proliferation, the cellular immune response following the administration of DNA vaccines has not been reported. Recent studies using a DNA vaccine and alphavirus replicon in tandem caused high neutralizing antibodies to be produced and a cellular immune response to be mounted (Bhardwaj, Heise *et al.* 2010). The immune response in the DNA vaccine study was of mixed T-helper response, but did show a Th2 bias. Splenocytes from mice vaccinated with RVF VLPs have been shown to increase the production of IL-2, -4, -5 and IFN- γ after stimulation with MP-12 (Mandell, Koukuntla *et al.* 2010).

WILD TYPE RVFV

ZH501 and ZH548, the parent strain for MP-12, were both isolated during an outbreak of RVF in Egypt in 1977. ZH501 was isolated from a fatal hemorrhagic case of RVF in a 12-year old female at Zagazig Hospital while ZH548 was as isolated from a non-fatal case in a 52-year old male at the same facility. Both viruses were isolated by inoculating two-day-old suckling mice intracerebrally with the undiluted sera from the patients. Viral stocks were made from mouse brain suspensions (Meegan 1979). The LD50 of ZH501 is approximately 1 PFU (Reed, Lin *et al.* 2013).

DISEASE PRESENTATION

Liver necrosis can contribute to development of disseminated intravascular coagulation (DIC) and death in infected animals. Following RVFV infection, animals across different species have been found to have elevated liver enzymes (alanine aminotransferase (ALT) and aspartate aminotransferase (AST)), decreased white blood cell (WBC) counts, and decreased platelet count (Coetzer and Ishak 1982; Morrill,

Jennings *et al.* 1989; Morrill, Jennings *et al.* 1990; Gray, Worthy *et al.* 2012). Disease pathogenesis has been characterized in various different animal models (Smith, Steele *et al.* 2010). The course of infection has been documented in rodents, ruminants, and non-human primates (NHPs). Some of these animal species (livestock, rodents and NHPs) are discussed in detail below.

Humans

Human disease is usually not as severe as the disease seen in livestock as most humans develop a self-limiting febrile illness. During an outbreak of RVF, which can often be predicted by outbreaks of disease in animals (Daubney 1931; WHO 2007), a large percentage of the infected human population will likely develop an asymptomatic infection.

The incubation period following RVFV infection in humans is 2 to 6 days, with symptoms lasting 2 to 4 days (Bartelloni and Tesh 1976). The symptoms for RVF are common for many febrile illnesses like malaria, bacterial illnesses and even a severe cold: debilitating biphasic fever, chills, malaise, headache, photophobia, back pain, and joint pain (Bartelloni and Tesh 1976; Peters, Liu *et al.* 1989). Due to the similarities between RVF and other common tropical diseases and the swift progression of RVF, the disease can go undetected in many infected people. Generally, only about 1% of patients progress to severe illness (Meegan 1979; Meegan 1989). RVFV infection can result in three severe manifestations: retinal vasculitis, encephalitis, and hemorrhagic fever (Schwentker and Rivers 1934; Meegan 1979; Gerdes 2004). While hemorrhagic fever may present early in the disease course, retinal vasculitis and encephalitis can present weeks to months after the initial phase of disease. Since the virus appears to have been cleared from the organism before these manifestations (retinal vasculitis and encephalitis) first appear, an overactive immune response is thought to be of high importance in their appearance (Peters 1981). Of patients that present with severe manifestations, mortality

has been reported in up to 20% of these cases (Laughlin, Meegan *et al.* 1979; McIntosh, Russell *et al.* 1980; Madani, Al-Mazrou *et al.* 2003; Ikegami and Makino 2011). In populations not previously exposed to RVFV, the severe manifestations of disease are more common and the mortality rate tends to be higher (Shoemaker, Boulianne *et al.* 2002). While the mortality rate is generally accepted as approximately 2%, recent outbreaks have reported mortality rates near 45% (WHO 2007; CDC 2009; Adam, Karsany *et al.* 2010). This increase in mortality could be due to increased surveillance and reporting in rural areas or increased virulence of the virus.

Rift Valley fever patients that progress to the hemorrhagic stages of the disease have been shown to have elevated levels of many liver enzymes, such as aspartate aminotransferase (AST) and alanine aminotransferase (ALT) (Al-Hazmi, Ayoola *et al.* 2003). This elevation in liver enzymes is indicative of liver necrosis associated with the disease. Patients can also have low hemoglobin and platelet counts (Al-Hazmi, Ayoola *et al.* 2003). The low platelet counts could be due to DIC that uses up the platelets in non-specific clotting events. Liver necrosis also contributes to other factors that can cause DIC, since the liver both synthesizes and recycles coagulation factors and releases coagulation factors into the blood stream as necrosis spreads throughout the organ.

Livestock

RVFV outbreaks are often first indicated by “abortion storms” of livestock in an affected area (Daubney 1931; WHO 2007). Cases of RVFV result in abortion in nearly 100% of infected pregnant ruminants (e.g. sheep, cattle, and goats) regardless of the trimester of pregnancy (Flick and Bouloy 2005). These animals develop very high viral titers and are considered an amplifying host for the virus (Gerdes 2004; Bouloy 2011). For newborn lambs and kids, the viral incubation period is 24 to 36 hours and 90-100% of the animals die 24 to 36 hours after the first clinical signs of symptoms, usually from acute hepatitis (Daubney 1931; Flick and Bouloy 2005). Mortality in animals less than 2

weeks old is greater than 90%, but as animals age and develop a stronger immune response, they become more resistant to infection (Easterday 1965). In adult animals, RVFV has an incubation period of 1 to 6 days and the mortality is between 5% and 60% (Gerdes 2004; Flick and Bouloy 2005). The disease is indicated by fever, abdominal pain, lack of appetite, lack of movement, and abortion (Daubney 1931; Flick and Bouloy 2005). In animals that succumb to disease, high viremia is detectable with widespread tissue damage, vasculitis, and hepatic necrosis (Swanepoel, Struthers *et al.* 1986; Cosgriff, Morrill *et al.* 1989).

Rodents

Mice that are infected with RVFV MP-12 survive infection, while RVFV ZH501 is highly lethal in common laboratory strains (Flick and Bouloy 2005; Bhardwaj, Heise *et al.* 2010; Smith, Steele *et al.* 2010; Ikegami and Makino 2011; Gray, Worthy *et al.* 2012). Mice represent a suitable animal model for RVFV because mouse infection with RVFV closely resembles certain aspects of RVFV infection in humans (Ikegami and Makino 2009; Ikegami and Makino 2011). Most mice infected subcutaneously (sc) or intraperitoneally (ip) with ZH501 will succumb to the infection due to liver necrosis and hepatitis 3-5 days post infection (Vialat, Billecocq *et al.* 2000; Bouloy, Janzen *et al.* 2001; Smith, Steele *et al.* 2010; Gray, Worthy *et al.* 2012). While RVFV is primarily hepatotropic, it can be found in almost every tissue of the mouse and has been detected in the liver, brain, lung, spleen, kidney, heart and eyes (Flick and Bouloy 2005; Smith, Steele *et al.* 2010). There is large amount of necrosis in the liver via virally induced apoptosis of hepatocytes (Smith, Steele *et al.* 2010; Gray, Worthy *et al.* 2012). When the livers of sick mice are examined, the hepatocytes have eosinophilic intranuclear inclusions (Findlay 1931; Ishak, Walker *et al.* 1982; Smith, Steele *et al.* 2010; Gray, Worthy *et al.* 2012). These inclusion bodies are the result of the filamentous structures produced by the NSs protein (Struthers and Swanepoel 1982; Yadani, Kohl *et al.* 1999).

While most mice die within 4 days after RVFV infection due to visceral disease, a small percentage of mice will survive the initial stage of the disease and develop neurological disease during the second week of infection (Smith, Steele *et al.* 2010). Interestingly, Morrill *et al.* found that a subpopulation of RVFV is primarily neuroinvasive in mice (Morrill, Ikegami *et al.* 2010). This study identified two forms of ZH501 present in infected animals. The ZH501 M847-A strain (amino acid Glutamic acid at position 277) had a similar virulence as ZH501. The ZH501 M847-G strain (amino acid Glycine at position 277) had a reduced virulence. The two strains of the virus are identical with the exception of the one point mutation at nucleotide position 847 in the Gn gene. Animals that are infected with the attenuated ZH501 M847-G that succumb to infection will yield ZH501 with the single nucleotide substitution in the mRNA M847-A as the major population when virus is recovered from the brain during necropsy (Morrill, Ikegami *et al.* 2010). Recently, published studies have described a mouse strain that is more susceptible to RVFV infection than conventionally inbred laboratory strains and may provide a better model to evaluate the efficacy of vaccines and antiviral drug treatments (do Valle, Billecocq *et al.* 2010). The MBT/Pas mouse strain was created from wild trapped mice and shows that host genetic variation is important in RVFV infection. MBT/Pas mice were propagated by sibling-mating at the Institute Pasteur from recently (1980) caught *M. musculus* mice. The MBT/Pas mice had signs of disease similar to BALB/cByJ mice, but the MBT/Pas mice started to show clinical signs two days earlier. The authors suggest that the less efficient innate immunity of the MBT/Pas is the reason for the increase in viral titer and the decrease in time to death (do Valle, Billecocq *et al.* 2010).

As with mice, rats are also highly susceptible to RVFV infection. Following infection, RVFV is found in most tissues of Wistar-Furth and Brown Norway rats and in high titers (Peters and Slone 1982; Anderson and Smith 1987). Most of the pathology is seen in rats is in the liver as expected (Peters and Slone 1982). Rat species show

differential susceptibility to RVFV infection. ACL rats have a mortality rate of only 50% while Lewis (LEW) rats exhibit none of the classical clinical signs of disease when infected via the subcutaneous route (Peters and Slone 1982; Anderson and Smith 1987). Recently published data indicate that genetics (of both the virus and the host) may play a role in RVFV pathogenesis in rats (Anderson and Peters 1988; Ritter, Bouloy *et al.* 2000). Ritter *et al.* infected Wistar-Furth (WF) and Lewis rats from a European breeding colony and their results were contradictory to previously findings using mice bred in American colonies (Ritter, Bouloy *et al.* 2000). Ritter found that the European WF rats were resistant to RVFV infection while American bred WF rats were found to die due to hepatitis caused by RVFV infection (Anderson and Peters 1988; Ritter, Bouloy *et al.* 2000). While Ritter proposed that this difference was due to the genetic backgrounds of the rats, Anderson and Peters proposed that the RVFV strain could also determine the outcome of infection in the rat model. RVFV strains isolated from an outbreak in Egypt during the 1970s are a 1,000,000-fold more virulent in WF rats than strains isolated during outbreaks in sub-Saharan Africa (Anderson and Peters 1988).

Further, rodents have been found to be susceptible to infection with aerosolized RVFV (Anderson, Lee *et al.* 1991; Bales, Powell *et al.* 2012; Reed, Lin *et al.* 2013). WF rats and Swiss Webster mice ultimately succumb to hepatitis due to liver necrosis after aerosol exposure (Brown, Dominik *et al.* 1981; Bales, Powell *et al.* 2012; Reed, Lin *et al.* 2013). ACI (August-Copenhagen-Irish) and normally resistant LEW rats developed encephalitis after infection and virus was only recovered from the brain after aerosol infection. The LEW rats that did not develop encephalitis and survived the infection were not protected against subsequent challenge (Bales, Powell *et al.* 2012). Mice that are infected with ZH501 via the aerosol route have brain involvement that is more severe and seen earlier than mice that are infected via other routes (Reed, Lin *et al.* 2013). Even though RVFV does have the potential to cause disease through aerosol exposure, it is of

note that the liver necrosis still remains an important pathological feature and time to death increases by at least 2 days post aerosol infection (Ross, Bhardwaj *et al.* 2012).

Non-human primates (NHPs)

Rhesus macaques are susceptible to RVFV infection. The majority of rhesus macaques infected intravenously with 1×10^5 PFU of ZH501 become viremic but do not develop any signs of illness. Some infected animals may become febrile, and a small percentage may develop severe disease with hemorrhagic manifestations and subsequently succumb to the disease (Morrill, Jennings *et al.* 1989; Morrill, Jennings *et al.* 1990; Morrill, Czarniecki *et al.* 1991; Ross, Bhardwaj *et al.* 2012). Pathology reports from infected macaques have identified liver lesions similar to those described in humans and other animals (Findlay 1932; Easterday 1965; van Velden, Meyer *et al.* 1977). The liver lesions are caused by hepatic necrosis which leads to DIC and anemia (Davenport, Hennessy *et al.* 1953). Marmosets are more susceptible to RVFV than rhesus macaques, and the disease presentation closely resembles that in humans. Marmosets develop acute hepatitis following RVFV infection, with an increase in liver enzymes and hemorrhaging and late-onset encephalitis with all animals becoming viremic and 50% succumbing after subcutaneous infections (Smith, Bird *et al.* 2012). Even though disease pathogenesis in NHPs mimics human infections and they provide the most realistic model of RVFV in NHPs to date (Peters 1994; Smith, Bird *et al.* 2012), they are not a great model for human infection as only a small percentage began to hemorrhage and subsequently can be used to study the hemorrhagic manifestations of the disease. Due to this, pathogenesis studies in NHPs are not as readily available as those of other species of animals (Ross, Bhardwaj *et al.* 2012).

HOST RESPONSE TO RVFV

Cell signaling during RVFV infection

To better understand how RVFV enters a cell and affects the host immune response, the cellular pathways that are activated during infection need to be examined in depth. Pathways that are activated soon after infection are most likely associated with virus binding to a host cell receptor and entering the cell. Downstream signaling pathways may be the intracellular response to viral replication. Understanding the regulation of intracellular signaling following viral infection is essential to understanding how the host immune system responds to infection and replication of RVFV.

Several *in vitro* studies examining cell signaling events after RVFV infection have recently been published. The p53 protein is regulated by post-translational modifications and it acts as a transcription factor for many genes involved in apoptosis, DNA repair, and cell cycle arrest (Wu 2004; Olsson, Manzl *et al.* 2007). Many proteins involved in the DNA repair response have been found to be phosphorylated in response to RVFV infection, including p53 (Baer, Austin *et al.* 2012). Phosphorylation increases the stability of p53 and its ability to bind to DNA (Chehab, Malikzay *et al.* 2000; Wu 2004). The pro-apoptotic protein p53 is phosphorylated at Ser-12 and Ser-46 during RVFV infection by activation of ataxia-telanglectasia mutated protein (ATM) in response to DNA damage. ATM is activated after the viral protein NSs is synthesized. The filamentous structures that NSs forms in the cell nucleus cause DNA damage (Mansuroglu, Josse *et al.* 2010; Popova, Turell *et al.* 2010; Baer, Austin *et al.* 2012). While previous studies show that phosphorylation of p53, a pro-apoptotic protein, is increased during infection, it has been shown that RVFV NSm protein has anti-apoptotic properties through the inhibition of caspases 3, 8, and 9 (Won, Ikegami *et al.* 2007). The activation of p53 would be beneficial to the host as its activation would normally lead to cell death after viral infection. The death of the cell early in the course of infection

would lead the release of immature, presumably not infectious, virus particles. These particles would quickly be phagocytized by macrophage cells.

Increases in the levels of phosphorylated proteins within the MAPK cascade, including JNK, p38, and ERK1/2, have also been observed in recent studies. The phosphorylation profiles of these three proteins were similar after ZH501 infection. These changes in phosphorylation were seen where there was no significant change in the levels of total proteins after both MP-12 and ZH501 infection (Popova, Turell *et al.* 2010). These results indicate that the increases in phosphorylation seen were not due to an increase in the amount of the protein present. JNK is likely one of the major targets of RVFV as it had an initial increase in phosphorylation that was followed by a rapid dephosphorylation at higher MOIs (Popova, Turell *et al.* 2010). Phosphorylation of JNK is important in apoptosis and cell survival and happens in response to inflammatory cytokines, growth factors and cellular stress. JNK and p38 MAPK are similar in that they are both activated by cellular stress and are important in apoptosis/survival pathways. After MP-12 infection, p38 is upregulated and activates pro-survival pathways possibly in response to NSm (Narayanan, Popova *et al.* 2011).

Cytokine response during RVFV infection

Cytokines are used by cells to communicate with one another. If the cytokine response to infection can be understood, then treatments that exploit this response can be devised. At present, there is no approved treatment for patients infected with RVFV. Since ZH501 infection causes the release of large amounts of cytokines *in vivo*, if the response of key cytokines can be controlled during infection, the virus can be cleared and some of the pathogenesis caused by an overactive immune response can be avoided.

Type I IFNs are known as the antiviral cytokines as they responsible for the activation of various pathways that would help clear a viral infection. RVFV evades the host immune response through manipulation of the type I interferon response. The earlier

and stronger the type I interferon (IFN- α and - β) response after infection the easier the host clears virus (do Valle, Billecocq *et al.* 2010). Other than the potential role of type I IFN in limiting disease that was discussed earlier, little else is known about the host immune response to RVFV infection.

The importance of type I IFN has also been shown in MBT/Pas mice. Even though studies have shown that NSs blocks the transcription of type I IFN, it seems that wild type RVFV infection does lead to a small amount of interferon secretion in these animals (Le May, Mansuroglu *et al.* 2008; do Valle, Billecocq *et al.* 2010). As with other mice, MBT/Pas mice survive infection with RVFV lacking a functional NSs gene and succumb to infection with wild type virus. While mouse embryonic fibroblast (MEFs) taken from the MBT/Pas mice had higher viral titers throughout the experiment when compared to MEFs from BALB/cByJ mice, they also had a weaker IFN response than BALB/cByJ mice (do Valle, Billecocq *et al.* 2010).

This gives support to the concept that the slightly stronger IFN response in the BALB/cByJ mice, while still lower when compared to other viral infections, is what allows that mouse to survive longer after infection when compared to the MBT/Pas mice. Even though RVFV decreases transcription in infected cells, it appears that the basal level of IFN activation that is happening is important to the host response to the virus and allows animals to survive infection (Morrill, Jennings *et al.* 1989; Morrill, Jennings *et al.* 1990; Bouloy, Janzen *et al.* 2001; Le May, Mansuroglu *et al.* 2008).

The effect of type II interferon (IFN- γ) in response to RVFV infection has also been evaluated. It has been shown that even after IFN- γ increase there is no decrease in viral replication in mice infected with wild type RVFV (Jansen van Vuren, Tiemessen *et al.* 2011). On the other hand, IFN- γ was shown to be important in RVFV infection in rhesus macaques. Macaques given IFN- γ replacement therapy were able to control viral infection as demonstrated by a decrease in viremia and protection from fatal disease when compared to control macaques. Generally, approximately 20% of challenged

monkeys develop severe disease and exhibit hemorrhagic manifestations before they ultimately succumb to the infection (Morrill, Jennings *et al.* 1990; Morrill, Czarniecki *et al.* 1991).

TNF α is a cytokine with an important role in inflammation and helping to stimulate the acute phase reaction. Narayanan *et al.* shows that both MP-12 and ZH501 increase TNF α protein expression in human small airway lung epithelial cells (HSAECs) (Narayanan, Popova *et al.* 2011). McElroy and Nichol demonstrate that wild type RVFV inhibits the expression of TNF α in human monocyte derived macrophages (MDMs) (McElroy and Nichol 2012). This shows that RVFV can induce completely different responses to infection depending on the origin of the cells. IL-10 is an important anti-inflammatory and immunosuppressive cytokine that controls the expression of many other cytokines (Donnelly, Dickensheets *et al.* 1999). Jansen van Vuren *et al.* observed an increase in IL-10 gene expression in the livers of infected mice as RVFV replication increased (Jansen van Vuren, Tiemessen *et al.* 2011). It was suggested that the increase in IL-10 is a detriment to the host as IL-10 suppresses the immune response and leads to inefficient clearance of wild type RVFV. When viral replication was at its peak, the IL-10/IFN- γ response was skewed in favor of IL-10. An enhanced IL-10 response can lead to a decrease in inflammation while an IFN- γ -mediated response points to viral clearance. From these data it appears that the host is concentrating its efforts on limiting immunopathology by decreasing inflammation and not on efficient viral clearance (Jansen van Vuren, Tiemessen *et al.* 2011). This inefficient clearance leads to a vicious cycle where the virus overwhelms the host and, to compensate, the host produces more cytokines in an attempt to up-regulate the immune response. From what I have seen, it appears that the immune up-regulation contributes to the damage that has already been caused by replicating virus in the host cell and can cause much of the pathology that is attributed to an overactive immune response.

JUSTIFICATION OF STUDIES

In Africa, many people and countless animals have died from RVF since its discovery in the 1930s. The research discussed here is relevant to not only Africa and the Arabian Peninsula, but to the world as a whole. The ubiquitous nature of *Aedes* spp. mosquitoes poses a significant problem in the control of RVFV because many members of this genus are potential vectors for RVFV. The widespread nature of potential vectors provides for a possible worldwide spread of RVFV. RVFV is also stable at 4°C and has been shown to be transmitted by aerosol. If the virus were to spread into a new area either naturally or intentionally, it could become established in that area as the virus can be maintained in the mosquito population through vertical transmission (Linthicum, Davies *et al.* 1985).

Since very little is known about the cellular response after RVFV infections, a foundation needs to be laid that can be built upon for the development of antiviral treatment and vaccines. By evaluating the cytokine profile and cellular response to infection, it will be possible to identify specific mechanisms of viral propagation and interference with the host response early in infection. Once it is determined how the host reacts to infection, it will be possible to identify new targets to interfere with the RVFV infection. This could lead to the better design of vaccines or therapeutic strategies and result in protective immunity against RVFV.

The innate immune response is important in RVFV infection because the onset of symptoms is swift, and the animal host does not have time to make antibodies before they succumb to the hemorrhagic phase of the disease (Shoemaker, Boulianne *et al.* 2002). The majority of humans that survive the initial stages of disease and produce antibodies generally survive infection. While the host innate immune response to RVFV is not fully understood, it is known that vaccination and passive antibody transfer protect from lethal disease (Smithburn 1949; Randall, Gibbs *et al.* 1962; Niklasson, Meadors *et al.* 1984;

Caplen, Peters *et al.* 1985; Dingu, Louw *et al.* 2010). The problem is that no vaccine or treatment is currently approved for human use. In endemic areas, where animal vaccines are in use, these vaccines have adverse effects or animals need yearly boosters which is not economically feasible in the areas they are needed most.

In these studies, my focus was on the characterization of the host response to RVFV infection in the mouse model system. These studies examined the regulation of cytokine expression and the intracellular signaling associated with induction of the cytokine response following infection with a wild type or vaccine strain of RVFV *in vitro* and *in vivo*. While the increase of pro-inflammatory cytokines released in other hemorrhagic fevers such as Ebola and Crimean-Congo hemorrhagic fever (CCHF) shows a correlation to the increase in mortality (Villinger, Rollin *et al.* 1999; Gupta, Mahanty *et al.* 2001; Stroher, West *et al.* 2001; Ergonul, Tuncbilek *et al.* 2006; Papa, Bino *et al.* 2006; Hutchinson and Rollin 2007; Connolly-Andersen, Douagi *et al.* 2009), the cytokine response to RVFV has not been examined as closely. In the hopes of understanding where cytokines originate *in vivo*, *in vitro* studies involving murine macrophages and dendritic cells were performed. These cells, both primary and cell lines, were infected with ZH501, MP-12, irradiated MP-12, and rMP12-C13type virus and the cell signaling and cytokine response was examined using multiplex assays. The effect of RVFV on C57BL/6 mice was also examined by infecting these mice with ZH501 and MP-12. After infection cytokine secretion, blood counts, and pathology were examined.

These studies have provided a better understanding of the host response to RVFV infection in the organism as a whole. If I have a better understanding of the host response, therapies that utilize inhibition or activation of cell signaling pathways and/or cytokine secretion could potentially be developed.

SPECIFIC AIMS OF DISSERTATION

Specific Aim 1: Identify cell specific signaling responses associated with RVFV attachment and entry *in vitro*.

Hypothesis: After infection with ZH501, there will be a stronger increase in phosphorylation of pro-inflammatory proteins and a reduced phosphorylation of pro-apoptotic proteins compared to infection with MP-12. Previously, it has been shown that ZH501 has the ability to inhibit apoptosis, likely giving the virus the advantage to replicate to high titers in the infected host cell (Won, Ikegami *et al.* 2007).

Specific Aim 2: Identify IFNs and inflammatory cytokines whose secretion is affected following infection *in vitro* with RVFV wild type strain ZH501 or MP-12.

Hypothesis: While the IFN response to infection with either ZH501 or MP-12 will be similar, more pro-inflammatory cytokines will be released following ZH501 infection since the pathology that is seen after RVFV infection has been repeatedly attributed to an overactive immune response.

Specific Aim 3: Identify a panel of cytokines whose secretion is affected following infection *in vivo* with wild type RVFV or MP-12.

Hypothesis: ZH501 will induce a stronger anti-viral and pro-inflammatory response *in vivo* than MP-12.

Chapter 2 Materials and Methods

ESTABLISHED CELL LINES

Immortalized macrophage cells (RAW 264.7, ATCC# TIB-71) generated from the ascites fluid of adult male BALB/c mice were maintained in Dulbecco's Modified Eagle's Media (DMEM) supplemented with 10% BGS, 1% non-essential amino acids, and 1% sodium pyruvate, as recommended by ATCC. Immortalized dendritic cells (DC 2.4) that were generated from the bone marrow of adult male C57BL/6 mice were maintained in RPMI 1640 supplemented with 10% FBS, 1% non-essential amino acids, and 1% D-glucose as previously described (Shen, Reznikoff *et al.* 1997). DC 2.4 cells were provided by Dr. D. Mark Estes (University of Georgia, College of Veterinary Medicine). VERO C1008 (Vero 76, clone E6, Vero E6) cells (ATCC # CRL-1586) were maintained in MEM media supplemented with 10% BGS, 1% non-essential amino acids. All cells were passaged every 3-4 days depending on cell confluency. All cells were kept at 37°C and 5% CO₂.

PRIMARY CELLS

Adult (8-10 weeks old) female C57BL/6 mice were used for isolation of primary macrophages and dendritic cells.

Isolation of peritoneal macrophages: After CO₂ asphyxiation and cervical dislocation, mice were sprayed with 70% EtOH. The skin was nipped, with scissors to avoid cutting into the peritoneal cavity. The skin was then pulled back to expose the peritoneal cavity of the mouse. Using an 18-gauge needle, the peritoneal cavity was then injected with 8 ml of RPMI media (supplemented with 1% penicillin/streptomycin). With the needle still in place, the mouse's belly was then massaged for 3 minutes and the media was pulled out of the peritoneal cavity back in to the syringe. While the needle

was still in the mouse, contact with fat and the intestines was avoided to prevent contamination of the peritoneal macrophage cells. The cells from 5 mice were pooled in a 50 ml conical tube and pelleted by spinning at 300g for 7 min 4°C. The pellet was washed with RPMI media (with 1% penicillin/streptomycin), cells then resuspended in complete RPMI media (supplemented with 10% FBS and 1% penicillin/streptomycin; cRPMI) and counted. Cells were then seeded at 1×10^6 cells per well of a 12-well plate. After incubation for 2 hours at 37°C and 5% CO₂, to allow cells to adhere to the plate, the media was removed and cells washed with PBS to remove non-adherent cells. Fresh cRPMI media was added, and the cells were cultured 24-hours until use (Yang, Zhao *et al.* 2007).

Isolation of BMD macrophages and dendritic cells: After CO₂ asphyxiation and cervical dislocation, mice were sprayed with 70% EtOH. The skin was removed from the thigh of the mouse and the femurs were removed by carefully making two cuts; one below the knee joint and another above the hip. It was important to keep the bone intact to avoid killing cells when placing the bone in 70% EtOH. The muscle was then removed from the bone using sharp scissors and forceps. The exposed bone was washed in 70% EtOH and rinsed in a 35-mm petri dish containing RPMI media (with 1% penicillin/streptomycin). After the bones were rinsed, the ends of the femur were cut off just below the joints using sterile scissors and the bone marrow cells were flushed from the bone shafts into fresh cRPMI media using a 23-gauge needle attached to a 5 ml syringe. When the bones were completely white, almost transparent, they were discarded as all the bone marrow had been removed. The bone marrow was then broken up using two 23-gauge needles and the cell suspension transferred to a 50 ml conical tube. The petri dish was washed with 3 ml of media to remove any residual cells and added to the 50 ml conical tube.

Cells were pelleted by centrifuging at 300g for 7 minutes 4°C, supernatant was discarded and the pellet resuspended in 5 ml of RBC lysis buffer (eBioscience catalog #

00-4333-57). The solution was incubated for 5 minutes at room temperature with occasional rocking. Next, 10 ml of RPMI (with 1% penicillin/streptomycin) was added to the solution to stop the activity of the lysis buffer and cells were centrifuged at 300g for 7 minutes 4°C. The pellet was then washed twice with RPMI (with 1% penicillin/streptomycin) and resuspended in complete RPMI (with 10% FBS and 1% penicillin/streptomycin) and the cells counted using a hemocytometer. Cells were then plated in 150mm x 25mm petri dishes at a volume of 2×10^7 cells/dish in 60 ml of cRPMI media. For bone marrow cells that were to be differentiated into dendritic cells, cRPMI media was supplemented with 20 ng/ml of GM-CSF (eBioscience #14-8331). For bone marrow cells that were to be differentiated into macrophages, cRPMI media was supplemented with 20 ng/ml of M-CSF (eBioscience #14-8983).

To stimulate the dendritic cells to mature, every 48 hours half the volume of media was replaced with fresh cRPMI media complemented with 20 ng/ml GM-CSF. To do this, 40 ml of the cell supernatant was removed and placed in a 50 ml conical tube, media was left on the cells so that they did not dry out. The supernatant was then spun at 300g for 7 minutes at 4°C. After centrifugation, 30 ml of the supernatant was removed and discarded, 30 ml of fresh cRPMI media (supplemented with 20ng/ml of GM-CSF) added, and the pellet resuspended. The cell suspension was then re-added to the original petri dish. After 8 days, non-adherent cells were counted and plated for infection or stimulation.

To obtain macrophages, after 3 days half the volume of cRPMI media (supplemented with 20 ng/ml M-CSF) was replaced as stated above for the dendritic cells. After 4 additional days (on day 7 after primary cell isolation), the supernatant was removed, the cells were washed with PBS (without calcium and magnesium), and then 3 ml of non-enzymatic cell dissociation buffer (Sigma catalog # C5914) added to the plate. The plate was then incubated at 37°C and 5% CO₂ for 10 min. After the incubation, the

cells were removed from the plates, centrifuged at 300g for 7 minutes at 4°C, and then plated for infection or stimulation.

VIRUSES

RVFV wild type strain ZH501 (ZH501) and vaccine strain MP-12 (MP-12) were obtained from Dr. John Morrill (UTMB). Recombinant RVFV MP-12 Clone13 type (rMP12-C13type) virus was kindly provided by Dr. Testuro Ikegami (UTMB). All viruses were cultured and titrated on Vero E6 cells. Each virus went through one or two passages in Vero E6 cells to grow laboratory working stocks. After infection, the virus was allowed to grow on Vero E6 cells for three days. The virus was then harvested and frozen at -80°C in 500µl aliquots until use.

For experimental infection of cells, the virus was diluted in DMEM supplemented with 4% FBS. For virus challenge of mice, virus was diluted in serum-free DMEM prior to inoculation. All work involving handling of infectious ZH501, was performed in the Robert E. Shope or Galveston National Laboratory BSL-4 laboratories (UTMB). All samples removed from BSL-4 laboratory were γ -irradiated (5 Mrad) prior to analysis at BSL-2. Tissues were fixed with 10% buffered formalin and removed from the BSL-4 laboratory following BSL-4 SOPs.

VIRUS TITRATION

Vero E6 cells were infected with 100µl of sample through 10-fold serial dilutions. Plates were incubated for 1 hour in a 37°C incubator with 5% CO₂ and gentle rocking every 15 minutes. A 0.8% tragacanth/MEM overlay with 2% FBS and 1% penicillin/streptomycin was applied to the wells. After 4 days, the overlay was removed and the cells were stained with 0.2% crystal violet diluted in 10% neutral buffered formalin. The plaques were counted and the titers determined. Viral titers are reported as log₁₀ plaque forming unit (PFU).

For rMP12-C13type, Vero E6 cells were infected with 100µl of sample through 10-fold serial dilutions. Plates were incubated for 1 hour in a 37°C incubator with 5% CO₂ and gentle rocking every 15 minutes. Two milliliters of an overlay composed half of 1.2% noble agar (VWR, catalog #101170-362) and half of 2X MEM media (supplemented with 10% FBS, 1% penicillin/streptomycin and 10% tryptose phosphate broth (MP biomedical, catalog #168249) was put on the cells and they were incubated for three days in a 37°C incubator with 5% CO₂. After three days, another mixture of the half noble agar/half MEM media mixture was created and 500ul of 0.33% neutral red was added to the mixture before two milliliters of the overlay was added directly to the wells on top of the previous overlay. The plates were incubated an additional 24 hours. As above, the plaques were counted and the viral titers were reported as log₁₀ PFU.

CELL INFECTION

Virus was diluted with medium (DMEM or RPMI) and the cells were infected at either a multiplicity of infection (MOI) of 1 (for cytokine studies) or 4 (for phosphoprotein studies). Virus was placed on the cells and the plates were incubated at 37°C and 5% CO₂ for 1 hour with rocking every 15 minutes. After incubation, the cells were washed three times with sterile PBS and were then covered with complete DMEM media supplemented with either 4% FBS (for DCs) or 4% BGS (for macrophages). After infection the cells were placed back in the incubator for the remainder of the experiment. At each time point, 500 µl of supernatant and lysate was harvested and frozen at -80°C. Cell culture supernatants were used for ELISA and Bio-Plex analysis. Lysates were used for western blot and Bio-Plex analysis.

MOUSE CHALLENGE STUDIES

Adult (8-10 week old), female C57BL/6 mice (Harlan Sprague Dawley) were infected with 1,000 PFU via the subcutaneous (s.c.) route with ZH501, MP-12 or an

equivalent volume of diluent. The LD₅₀ for ZH501 is ~1 PFU (personal communication, J. Morrill). Each challenge group consisted of 5 animals. Three challenge groups (one group each: ZH501, MP-12 and mock infected) were sacrificed every 12 hours post-infection (HPI) by terminal cardiac bleed under deep isoflurane anesthesia. Mice from groups designated for sacrifice on the last day of the experiment were implanted with BioMedic Data Solutions (BMDS) (Seaford, DC) transponders 2 days prior to challenge and had their weight and body temperature measured daily throughout the course of the experiment.

At sacrifice, whole blood was collected for hematology and clinical chemistry and serum was isolated for analysis of the cytokine response profile and for virus titration. Approximately half of each organ examined (liver, spleen and brain) was harvested and homogenized in 0.5 ml PBS using a TissueLyser (Qiagen) to be used for virus titration and cytokine profile analysis. All animal studies were carried out with IACUC approval in an AAALAC accredited animal facility.

BIO-PLEX ASSAY

In vitro phosphoprotein assays: For these experiments, cells were plated in 12-well plates and infected with media, inactivated (γ -irradiated, 5 Mrad) MP-12, MP-12, or ZH501 at a MOI of 4 or mock infected. A high MOI was used in the phosphoprotein studies to ensure consistent activation of cell signaling pathways. At each time point the cell lysates from predetermined wells were collected. The cells were lysed using a cell lysis kit from Bio-Rad (Bio-Rad catalog #171-304011) that contained both wash buffer and lysis buffer and cell lysates were then frozen at -20°C in 500 μ l of lysis buffer from the kit containing 200 μ l of 500 mM phenylmethylsulfonyl fluoride (PMSF) (Sigma catalog #P7626) as a serine protease inhibitor. Before use, the cell lysates were thawed on ice. Lysates were then placed in 96-well plates and analyzed for phosphorylation of various different proteins using Bio-Plex custom designed assays. These multiplex

assays examined p-JNK, p-STAT2/3, p-ERK 1/2, p-p38 MAPK, p-c-jun, p-p53 and p-NF- κ B (Bio-Rad). The assay was performed following the manufacturer's instructions for incubations and washes. These plates were analyzed on a Bio-Plex 200 system (Bio-Rad). Fluorescence of the samples was compared to mock infected controls and naïve cells to determine a relative fold change. Irradiated virus was used to determine activated pathways in association with viral attachment as opposed to viral replication.

In vitro cytokine assays: For these experiments, cells were infected with either media only (mock), ZH501, rMP12-C13type, MP-12 or replication deficient MP-12 at a MOI of 1. A sample of the supernatant was taken at different time points and frozen at -80°C until use. The cytokines were coupled to cytokine-specific multiplex beads following the manufacturer's instructions (Bio-Rad catalog #M60-0060BEF) in pre-designed multiplex assays that included nine cytokines (IFN- γ , IL-1 α , IL-12(p70), IL-12(p40), MCP-1, MIP-1 α , MIP-1 β , RANTES and TNF- α). With the samples, a standard of known concentration was diluted and used to generate a standard curve. This standard curve was used to determine the concentration of each cytokine in the samples to pg/ml levels. The cytokine levels were reported in terms of fold-change relative to mock infected cells. This assay was used to provide information as to the concentration of cytokines that are released by macrophages and dendritic cells after infection with RVFV.

For tissues and serum collected in vivo: After mice were euthanized, one lobe of the liver, approximately half of the spleen and approximately half of the brain of each mouse were removed. The tissues were placed in 1.5 ml tissue lyses tubes with steel beads. The tubes were then placed into a TissueLyser (Qiagen) and shaken for 5 minutes. The homogenates were then centrifuged at 1,100rpm for 10 minutes at 4°C to remove tissue debris. The supernatant was transferred into new tubes and then frozen at -80°C until use.

Tissue homogenates and serum were processed according to manufacturer instructions (Bio-Rad #M60-009RDPD) and then analyzed using a Bio-Plex 200 system (Bio-Rad, Hercules, CA). Briefly, the samples were centrifuged for 10 minutes at 1,000 rpm at 4°C to remove cellular debris. The supernatants were collected and aliquoted into 96-well plates in pre-determined wells; this plate was centrifuged at 1,250 rpm to remove any remaining debris. The supernatant was transferred to a 96-well flat bottom plate and processed for use on the Bio-Plex system. The cytokines were coupled to cytokine specific multiplex beads (Bio-Rad) following the manufacturer's instructions using pre-designed assays that measured the concentration of a panel of cytokines including IL-1 α / β , IL-2, IL-3, IL-4, IL-5, IL-6, IL-9, IL-10, IL-12 (p40, p70), IL-13, IL-17, eotaxin, IFN- γ , KC (CXCL1), monocyte chemoattractant protein (MCP)-1 (CCL2), granulocyte colony-stimulating factor (G-CSF), granulocyte macrophage colony-stimulating factor (GM-CSF), macrophage inflammatory protein (MIP)1 α / β (CCL3/CCL4), tumor necrosis factor (TNF)- α and RANTES (CCL5).

ELISA

Assays for IFN- β were performed by ELISA following the manufacturer's instructions (PBL Biomedical Laboratories, Piscataway, NJ). *In vitro*, cell culture supernatant was collected at each time point. *In vivo* samples were prepared similarly to the Bio-Plex samples. All samples were centrifuged for 10 minutes at 1,000 rpm at 4°C to remove cellular debris. The supernatant was transferred to ELISA strips processed for use on the plate reader (Bio-Rad microplate reader model #680) at 560 nm. The IFN- β in the sample adhered to the wells pre-coated with IFN- β antibodies during incubation. After washing, the plates were incubated with HRP-conjugated secondary antibody, with a washing step between incubations. The strips were then incubated with a TMB solution for 15 minutes and 100 μ l of stop solution was added. These strips were read at 450 nm within 5 minutes of addition of stop solution.

CLINICAL EVALUATION OF INFECTED MICE

Complete blood counts (CBC) were evaluated on a Hemavet hematology analyzer (Drew Scientific, Dallas, TX) in the BSL-4 laboratory. Analysis included total white (WBC) and red blood cell (RBC) counts, platelet counts, hemoglobin concentration, hemocrit, and the counts of white blood cell subpopulations (lymphocytes, monocytes, eosinophils, neutrophils and basophils). Clinical chemistry analysis was performed on a VetScan2 Chemistry Analyzer (Abaxis, Union City, CA) in the BSL-4 laboratory. Fourteen analytes were examined including the liver enzyme alanine transferase (ALT), serum glucose, amylase, plasma electrolytes (calcium, phosphorus, sodium, and potassium), globulin, albumin, total bilirubin, blood urea nitrogen, creatinine, and total protein. Mice were micro chipped with BMDS (Seaford, DE) transponders and temperature readings at each time point. Weights were taken from groups of five mice each.

IMMUNOHISTOCHEMISTRY (IHC) ON MOUSE TISSUES

Formalin-fixed tissues were processed in a Shandon VIP Processor, and were mounted in paraffin blocks. Staining of RVFV antigen was prepared using mouse on mouse polymer technology and the Sequenza cover plate system. Briefly, the steps were: 1) Antigen retrieved using DIVA solution in a steamer (20 min); 2) Peroxide block using peroxidase (5 Min); 3) Blocking step using Rodent Block M (30 min); 4) RVFV mouse hyper-immune ascitic fluid (Dr. Robert Tesh, World Reference Collection for Emerging Viruses and Arboviruses at UTMB), used at 1:100 dilution (60 min); 6) Secondary antibody using Biocare MM HRP Polymer (30 min); 7) Chromagen was DAB (5 min); 8) Counterstained with hematoxylin for 5 minutes.

STATISTICAL ANALYSIS

Initially (in the studies involving only MP-12) a paired Student's t test ($P > 0.05$ for a 95% confidence interval) was used to compare the data from virus infected and mock infected cells. In experiments where MP-12 and ZH501 viruses were used a one-way analysis of variance (ANOVA) was used to test for difference among the wild type infected, MP-12 infected or mock infected cells. A T-test correction ($P > 0.05$ for a 95% confidence interval) was used to determine statistical significance between the two different infected groups.

As the test groups are small, a Fisher's exact test was used to determine the significance between ZH501, MP-12 and mock infected groups of animals in clinical and cytokine analyses. A Kaplan-Meier test was applied to the weight and temperature measurements that were taken daily post infection from the group of mice that was designated to be sacrificed 6 days post infection (DPI).

Chapter 3 The response of immunomodulatory cells to RVFV infection

Specific Aim 1: *Identify cell specific signaling responses associated with RVFV attachment and entry in vitro.*

Hypothesis: After infection with ZH501, there will be a stronger increase in phosphorylation of pro-inflammatory proteins and a reduced phosphorylation of pro-apoptotic proteins compared to infection with MP-12. Previously, it has been shown that ZH501 has the ability to inhibit apoptosis, likely giving the virus the advantage to replicate to high titers in the infected host cell (Won, Ikegami *et al.* 2007).

Rationale: Understanding the cell signaling response after viral infection will lead to a better understanding of how a virus manipulates the host's immune response. Once this process is better understood and specific cellular targets have been identified, antiviral treatments and vaccines could be developed. RVFV NSs protein has been shown to prevent the activation of the IFN- β promoter and to down-regulate general host transcription (Le May, Dubaele *et al.* 2004; Le May, Mansuroglu *et al.* 2008). Even though NSs blocks the transcription of type I IFNs, studies with MBT/Pas and BALB/cByJ mice show that ZH501 does induce low activation of IFN-signaling (Le May, Mansuroglu *et al.* 2008; do Valle, Billecocq *et al.* 2010). Pas mice have in general a lower activation level of IFN-signaling and succumb to RVFV infection on average 4.5 days sooner when compared to BALB/cByJ mice after i.p. infection with 100 PFU of RVFV strain ZH548. The weaker IFN response likely contributes to the increased pathogenicity of RVFV in Pas mice. Even though RVFV decreases general transcription levels in infected cells, it appears that the still occurring transcription involves cellular defense genes, important to the host response to the virus (Le May, Mansuroglu *et al.* 2008). Recently, Popova and colleagues characterized the phosphorylation of p53, p38

MAPK, JNK, and ERK among other proteins in ZH501-and MP-12-infected human small airway epithelial cells (HSAECs) and found that phosphorylation of these proteins was up regulated after infection with ZH501 but not MP-12-infected cells (Popova, Turell *et al.* 2010). These proteins are important in apoptotic signal transduction and cell growth and differentiation.

In my studies, the goal was to determine if differences in the early host response could be detected that are a direct response to RVFV attachment, entry, and replication. I hypothesize that a difference in cytokine response and cell signaling in immunomodulatory cells can be shown as a result between infection with MP-12 and ZH501. To test this hypothesis, both macrophage and dendritic cell lines and primary cells were used. While cell lines are expected to yield homogeneous results, primary cell responses will likely more accurately reflect results observed in *in vivo* studies. Immortalized mouse macrophages (RAW 264.7), immortalized mouse dendritic cells (DC 2.4), primary mouse BMD macrophages, and primary mouse BMD dendritic cells were used and the results are discussed by cell type.

RESULTS

Cell-signaling response in immortalized mouse macrophage cells (RAW 264.7)

Cells were infected with MP-12 and the induction of phosphorylation was measured for several key signaling proteins including STAT2, JNK, p38 MAPK, and p53 (Figure 3.1) by multiplex analysis. Only MP-12 was used in this part of the study as the Bio-plex equipment that was used to measure phosphorylation was not available for use in the BSL-4 (therefore preventing analysis of ZH501-infected cell samples) and preliminary studies showed that the irradiation process performed to remove the samples for the BSL-4 changed the concentrations of phosphoprotein that was detected (data not shown). When examining the MP-12 and ZH501 surface glycoproteins, Gn and Gc, there are four nucleotide substitutions of which three result in amino acid changes at

nucleotide positions 715 (Leucine in MP-12 to Glutamine in ZH501), 1824 (Isoleucine in MP-12 to Valine in ZH501), and 2981 (Glutamic acid in MP-12 to Aspartic acid in ZH501). These amino acid substitutions do not change the charges on the surface proteins and the receptor usage does not appear to be affected by these mutations (Lokugamage, Freiberg *et al.* 2012).

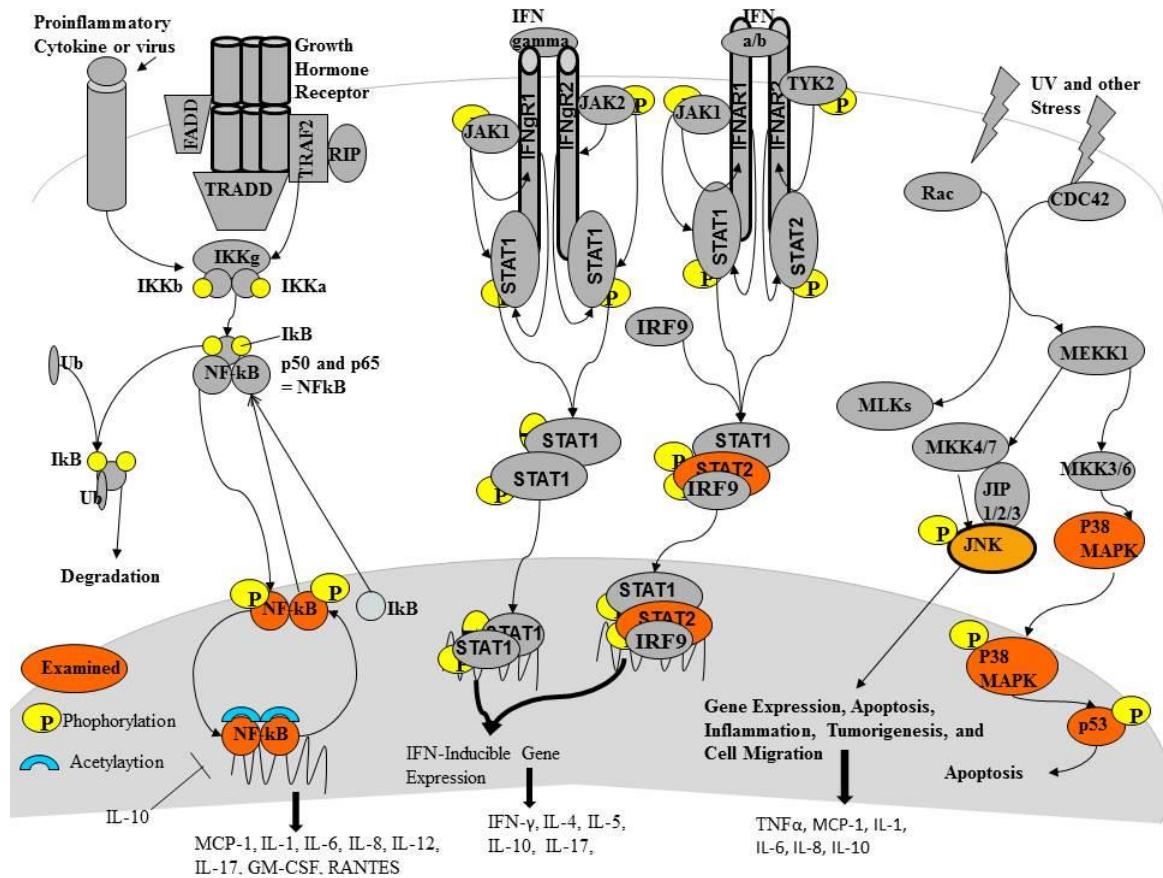


Figure 3.1. Schematic of signaling pathways examined

Schematic of signaling pathways that are to be examined in this chapter. The orange tiles highlight the proteins that will be specifically discussed in this chapter. The yellow circles represent phosphorylation and the blue arcs represent acetylation. The bold arrows show the cytokines that are activated by the various pathways.

A high MOI (MOI=8) was used to ensure that multiple virus particles would bind to the cellular receptor(s) and subsequently activate cellular pathways. I found that at a lower (1) or higher (8) MOI, RVFV grew to at least 5 logs in RAW 264.7 cells within 18

hours of infection (Figure 3.2). Following virus attachment, as the signal is transduced it will be amplified and result in the phosphorylation of downstream effector proteins. I infected the cells with either replication-competent MP-12 or –incompetent (γ -irradiated) MP-12. The early signaling for both of these viruses should be similar since they should bind to and activate the same receptor. The early signaling results could give insight as to the pathways activated in response to viral attachment and entry. The signaling response within the first 2 hours of infection was examined and no significant difference between infections with MP-12 and irradiated MP-12 was detected. This was expected as irradiation does not likely affect the morphology of the viral surface glycoproteins.

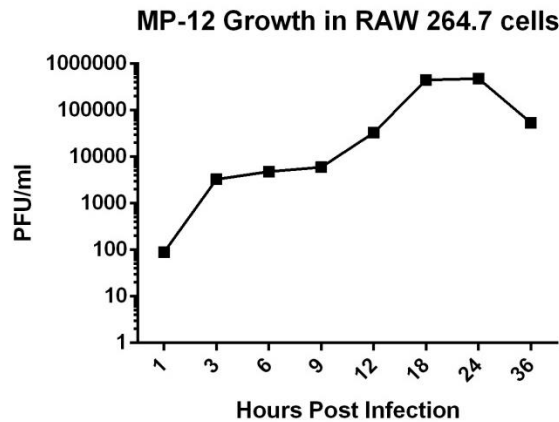


Figure 3.2. MP-12 growth in RAW 264.7 cells

The growth of MP-12 in RAW 267.7 cells through the course of infection (1-36 HPI). One replication cycle of RVFV is approximately 6-8 hours.

Initially, total amounts of various proteins (JNK, c-Jun, NF-kB, ERK, p38 MAPK, and p53) were examined after infection of RAW 264.7 cells (Figure 3.3). For 24 hours after infection, the concentration of total proteins did not show a significant change for any of the proteins examined from mock and irradiated MP-12-infected cells (Figure 3.3). Beginning at around 9 HPI, the amount of total protein decreased significantly for cells infected with live MP-12, indicative of decreased protein levels that could be due to reduced cellular transcription caused by the NSs protein.

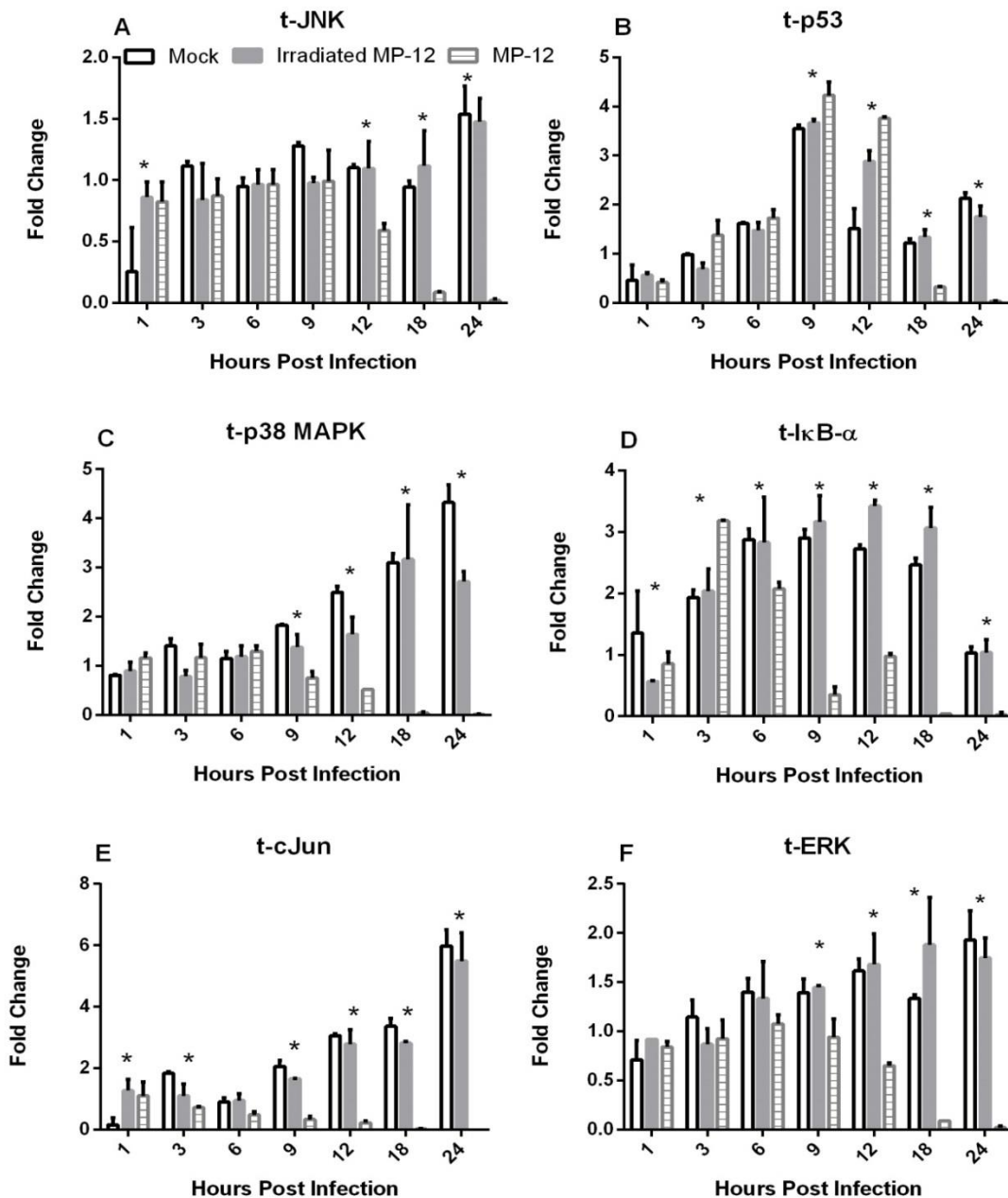


Figure 3.3. Total protein levels in RAW 264.7 cells

Total protein levels in RAW 264.7 cells after infection with irradiated MP-12 and live MP-12. Changes in protein levels are represented as a fold change over uninfected samples at 0 HPI. Cells were plated, allowed to rest for 24 hours and then infected. Open bars represent mock-infected cells, gray bars represent cells infected with irradiated MP-12 and striped bars represent cells infected with MP-12. Error bars are + standard deviation and * indicates $p < 0.05$ between mock- and MP-12-infected groups. Cells were infected with a MOI of 8.

Next, the amount of phosphorylated protein before and after infection was measured (Table 3.1 shows the phosphorylation sites of the proteins examined). The amount of signal transducer and activator of transcription (STAT) proteins phosphorylated after MP-12 infection was increased when compared to mock-infected cells and was significantly decreased in comparison to cells infected with irradiated MP-12 from 1-24 HPI. While the concentration of p-STAT2 increased significantly after infection with irradiated MP-12 over mock beginning at 3 HPI and remained elevated for the duration of the experiment, p-STAT2 protein showed a significant increase only between 3 and 9 HPI with MP-12 over mock-infected cells (Figure 3.4A). At 9 HPI there was an increase in the amount of p-STAT3 after infection with irradiated MP-12 that was not significant. Beginning at 12 HPI and lasting until the completion of the experiment at 24 HPI, the amount of p-STAT3 was significantly higher in cells that were infected with irradiated MP-12 than in mock-infected cells (Figure 3.4B). The levels of p-STAT3 appear to decrease beginning at 12 HPI after MP-12 infection. This reduction correlates with the decrease observed in total protein levels and is thought to be contingent upon the levels of total protein.

Protein	Phosphorylation Site
c-Jun	Ser-63
ERK 1/2	Thr-202/Tyr-204, Thr-185/Tyr-187
JNK	Thr-183/Tyr-185
NF-κB	Ser-536
p38 MAPK	Thr-180/Tyr-182
p53	Ser-15
STAT2	Tyr-689
STAT3	Tyr-705

Table 3.1: Phosphorylation Sites

Proteins that are phosphorylated and the phosphorylation site for the proteins that are examined using the Bio-plex assay.

Various proteins involved in the late phases of MAP kinase cascades were also examined. MAP kinases are involved in many different processes in the cell, such as cell growth and development, differentiation, inflammation and apoptosis. JNK proteins are activated in response to many different cytokines, and bind and phosphorylate c-Jun. JNK also regulates the synthesis of cytokines, such as RANTES, IL-8, and GM-CSF. While there was a significant increase in p-JNK 1 hour after live MP-12 infection, a stronger increase in phosphorylation could be detected after infection with irradiated MP-12 in the early stages of infection (Figure 3.5A). The amount of p-JNK increased more than 5-fold at 9 hours after infection with irradiated MP-12 in RAW 264.7 cells. The concentration of p-JNK increased at 1 and 6 hours after live MP-12 infection and remained elevated until 18 HPI (Figure 3.5A and C). At 9 HPI, the amount of p-JNK peaked at over a 55-fold increase in the amount of phosphorylated protein detected when compared to uninfected mock control. I also examined the phosphorylation of JNK in the early stages of infection (≤ 90 minutes post infection (MPI)). The concentration of p-JNK increased as soon as 45 MPI with irradiated MP-12, decreased at 60 MPI and elevated again at 90 and 120 MPI (Figure 3.5C). The increase of pJNK concentration at 60 MPI, which is also observed after infection with irradiated MP-12, could possibly be due to receptor binding and the later increases (≥ 6 HPI) could be due to the involvement of JNK during viral replication.

The protein p53 is a tumor suppressor protein, which plays a crucial role in regulation of the cell cycle, genomic stability, and can initiate apoptosis. It is activated in response to the activity of kinases that belong to the MAPK family (JNK, ERK1/2 and p38 MAPK). No change in the concentration of p-p53 was detected within the first 3 HPI for cells infected with irradiated and live MP-12. Cells infected with irradiated MP-12 showed only a decrease in the amount of p-p53 at 12 HPI. While there was a decrease in p-p53 at 6 HPI for live MP-12-infected cells, this trend was reversed and increased levels were observed starting at 12 HPI and lasted throughout the entire time course

(Figure 3.6A). The amount of p53 detected at 18 and 24 HPI was not different between the two MP-12 infection groups (Figure 3.6A). The phosphorylation of p38 MAPK, an upstream effector of p53, was only significantly higher than mock-infected cells at 1 HPI with irradiated MP-12 (Figure 3.6C). The phosphorylation of p38 MAPK was significantly increased between 6 and 12 hours after live MP-12 infection, after which the signals decreased to levels equivalent to mock. For p-ERK 1/2, signals in all samples were below detection limits (data not shown).

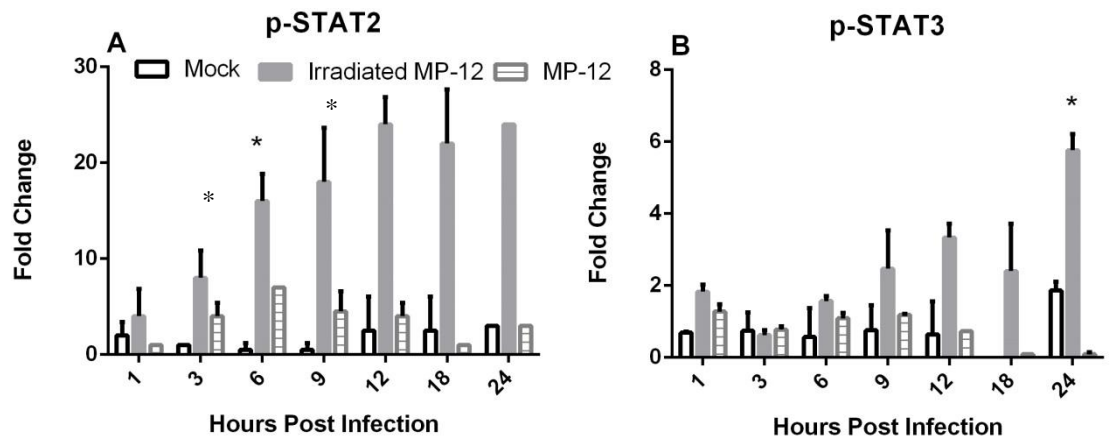


Figure 3.4. Protein levels of STAT proteins in RAW 264.7 cells

Protein levels in RAW 264.7 cells of p-STAT2 (A) and p-STAT3 (B) after infection with irradiated MP-12 and live MP-12. Changes in phosphorylation levels are represented as a fold change over uninfected samples at 0 HPI. Cells were plated, allowed to rest for 24 hours and then infected. Open bars represent mock-infected cells, gray bars represent cells infected with irradiated MP-12 and striped bars represent cells infected with MP-12. Error bars are + standard deviation and * indicates $p < 0.05$ between mock- and MP-12-infected groups. Cells were infected with a MOI of 8.

The transcription factor NF- κ B is responsible for the regulation of the genes of many different pro-inflammatory cytokines (e.g. IL-6 and IL-2) and chemokines (e.g. RANTES, IL-8, and MCP) (Olajide, Bhatia *et al.* 2013). With the exception of 18 HPI, there was no significant change in the phosphorylation of NF- κ B (Figure 3.6C). At 18

HPI, there was a large increase in p-NF- κ B detected after infection with irradiated MP-12, however. There was also a decrease in the concentration of NF- κ B 24 hours after MP-12 infection. This decrease correlated with the decrease that was seen in the concentration of total protein.

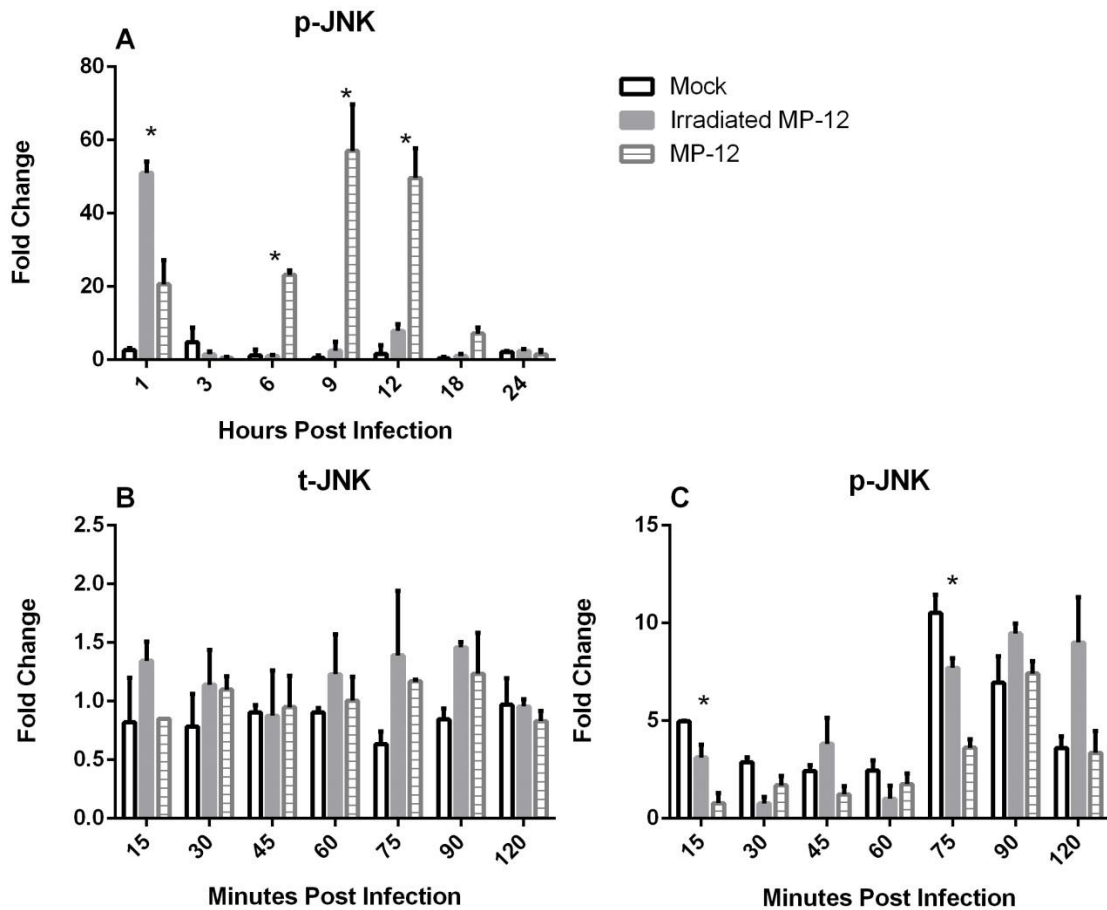


Figure 3.5. Protein levels in RAW 264.7 cell of JNK

Protein levels in RAW 264.7 cells of p-JNK and t-JNK after infection with irradiated MP-12 and live MP-12. Changes in phosphorylation levels are represented as a fold change over uninfected samples at 0 HPI. Cells were plated, allowed to rest for 24 hours and then infected. Open bars represent mock-infected cells, gray bars represent cells infected with irradiated MP-12 and striped bars represent cells infected with MP-12. Error bars are + standard deviation and * indicates $p < 0.05$ between mock- and MP-12-infected groups. Cells were infected with a MOI of 8.

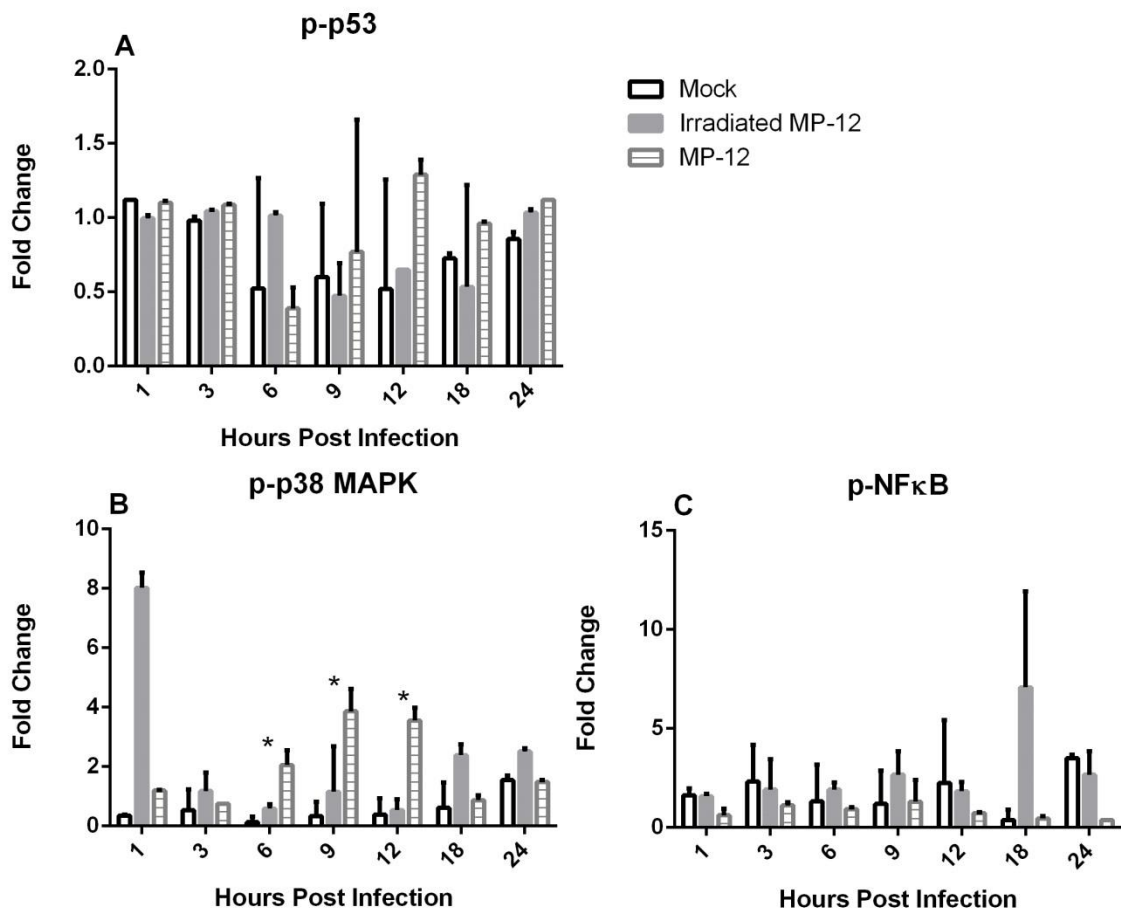


Figure 3.6. Phosphoprotein levels in RAW 264.7 cells of p53, p38 MAPK, and NF-κB
 Protein levels in RAW 264.7 cells of p-p53 (A), p-p38 MAPK (B), and p-NF-κB (C) after infection with irradiated MP-12 and live MP-12. Changes in phosphorylation levels are represented as a fold change over uninfected samples at 0 HPI. Cells were plated, allowed to rest for 24 hours and then infected. Open bars represent mock-infected cells, gray bars represent cells infected with irradiated MP-12 and striped bars represent cells infected with MP-12. Error bars are + standard deviation and * indicates $p < 0.05$ between mock- and MP-12-infected groups. Cells were infected with a MOI of 8.

Cell-signaling response in immortalized mouse dendritic cells (DC 2.4)

The same infection experiments that were described in the macrophage cell line, RAW 264.7, were also performed in the dendritic cell line, DC 2.4. After infection with an MOI of 8, the virus grew to 5 logs (Figure 3.7) in the same amount of time it needed to

reach maximum titers of 5.5 logs in the RAW 264.7 cell line (Figure 3.2). The phosphorylation of various different proteins involved in pathways from cell growth to apoptosis was examined to determine how viral entry and replication affect the phosphorylation pattern of these proteins. Total protein levels of DC 2.4 cells were similar after mock, irradiated MP-12, and live MP-12 infection until 18 HPI (data not shown). After that time, the level of total proteins dropped drastically in the live MP-12- and mock-infected samples. The drop in total protein amounts in DC 2.4 cells that were infected with live MP-12 can be attributed to the observed cytopathic effects. By 18 HPI there was approximately 75% CPE in the cells and at 36 HPI there were no cells alive on the plate. The drop seen in the mock-infected cells could possibly be due to the cells becoming overgrown and starting to die during the experiment. While the plates were all seeded with the same number of cells, the mock-infected cells grew faster than the cells infected with irradiated MP-12 and this over confluency could be why there was a drop in total protein levels.

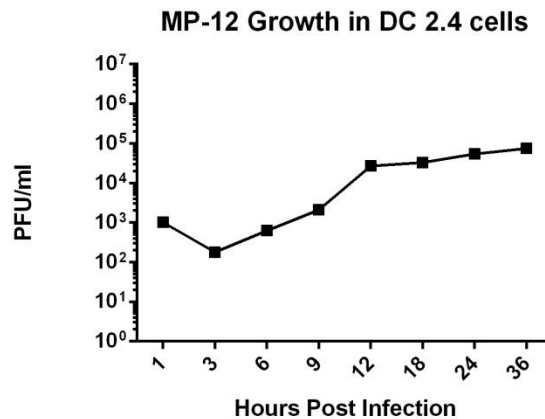


Figure 3.7. MP-12 growth in the DC 2.4 cell line

The growth of MP-12 in DC 2.4 cells through the course of infection (1-36 HPI).

As with the RAW 264.7 cells, there was no significant change in the phosphorylation of the examined proteins immediately following virus attachment and

binding (between 15 MPI and 2 HPI) after live and irradiated MP-12 infection (data not shown).

Phosphorylation of STAT2 in DC 2.4 cells began to show significant increases 6 HPI with irradiated MP-12 and live MP-12 (Figure 3.8A). This increase was transient as p-STAT2 levels were not significantly higher during the course of infection. The drastic decrease that is seen at 24 hours after live MP-12 infection correlates with the decrease in cell numbers and total protein levels, due to increased cytopathic effects. The trend observed in pSTAT3 was similar to one that was observed in total protein levels (Figure 3.8B). No significant change was detected until 18HPI, when suddenly the levels of p-STAT3 in mock and live MP-12-infected cells dropped. Since this trend was similar to one observed for total protein, these results suggest that no change in the amount of STAT3 phosphorylation occurred due to MP-12 infection compared to mock-infected samples.

The phosphorylation of JNK increased slightly, although not significantly, within the first hours after infection with live and irradiated MP-12 and might be related to virus attachment and entry. This temporal increase in phosphorylation vanished by 3HPI. A significant increase in phosphorylation of JNK was detected (up to 8-fold increase) after live MP-12 infection between 6 and 12 HPI, which then decreased to near mock levels at 18 HPI. However, a significant (3-fold) elevated phosphorylation level was still detectable (Figure 3.8C). No significant change in p-JNK levels could be detected in cells infected with irradiated MP-12.

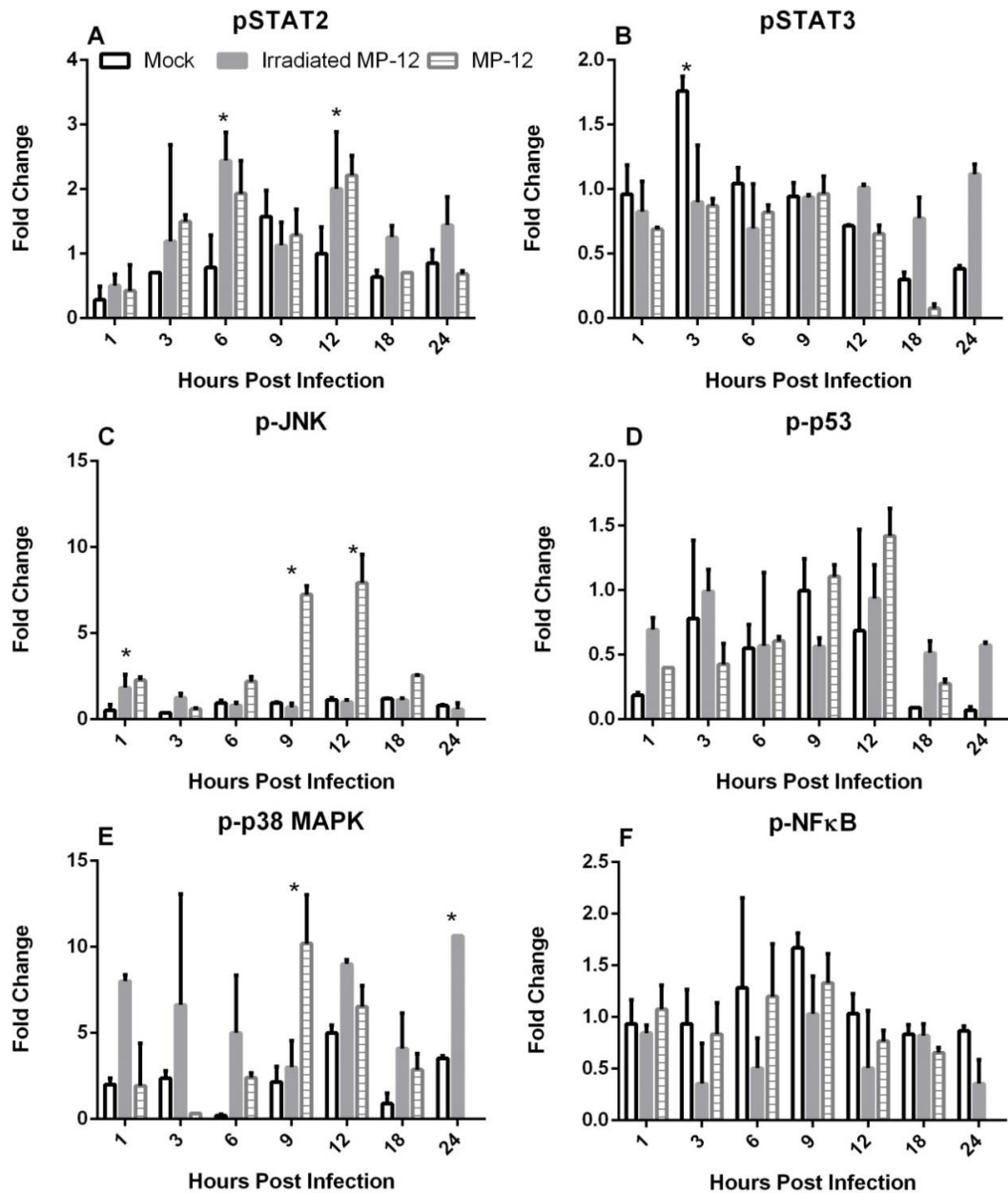


Figure 3.8. Phosphoprotein levels in DC 2.4 cells

Protein levels in DC 2.4 cells of p-STAT2 (A), p-STAT3 (B), p-JNK (C), p-p53 (D), p-p38 MAPK (E), and p-NF- κ B (F) after infection with irradiated MP-12 and live MP-12. Changes in phosphorylation levels are represented as a fold change over uninfected samples at 0 HPI. Cells were plated, allowed to rest for 24 hours and then infected. Open bars represent mock-infected cells, gray bars represent cells infected with irradiated MP-12 and striped bars represent cells infected with MP-12. Error bars are + standard deviation and * indicates $p < 0.05$ between mock- and MP-12-infected groups. Cells were infected with a MOI of 8.

While there was no significant change in the phosphorylation of p53, certain inconsistent fluctuations in all three samples occurred over the entire time course of the experiment and no apparent trend in the phosphorylation levels could be detected (Figure 3.8D). As with p-p53, changes in p-p38 MAPK were inconsistent (Figure 3.8E). However, there were significant increases after irradiated MP-12 infection at 1, 12, and 24 HPI, as well as a significant increase 9 hours after live MP-12 infection. Similar to the p-p53 results, the phosphorylation of NF- κ B was inconsistent during this experiment and no significant change occurred between the mock and MP-12-infected cells (Figure 3.8F). This inconsistency could be due to the fact that both NF- κ B and p53 need to be in the nucleus to perform their desired functions. It is possible that the total amount of p-p53 and p-NF- κ B in total cell lysates is not as important as the amount of phosphorylated protein that has translocated to the nucleus. As previously determined in the RAW 264.7 cells, ERK 1/2 amounts were below the detection limit (data not shown).

To compare the results gained from experiments performed in immortalized mouse macrophage and dendritic cells, infections in primary mouse peritoneal macrophage and bone-marrow derived dendritic cells were performed.

Cell-signaling response in primary mouse macrophage cells

For experiments utilizing primary cells, in addition to MP-12 and irradiated MP-12, ZH501 and rMP12-C13 type virus were included to characterize phosphorylation events. During initial experiments performed in cell lines, the required equipment (Bio-Plex) necessary to measure phosphorylation profiles was not available inside the BSL-4 laboratory. Samples from cell lines could previously not be removed from the BSL-4 laboratory for analysis at BSL-2, due to the fact that gamma-irradiation affected the phosphorylation of the proteins to be analyzed.

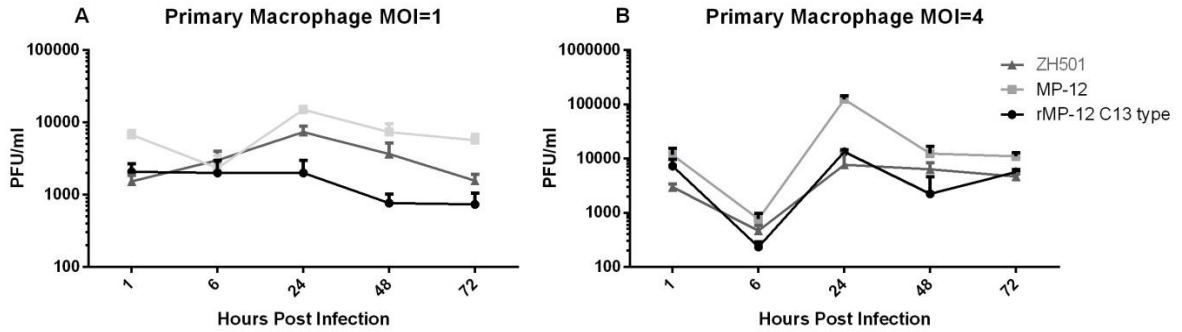


Figure 3.9. Viral titers in BMD macrophages after infection

Viral titers in BMD macrophage cells after infection with MP-12, rMP12-C13type, and ZH501. The line with closed diamonds is viral growth after cells were infected with ZH501, the line with closed squares represents cells were infected with MP-12, and the line with closed triangles represents cells were infected with rMP12-C13type virus. Error bars are \pm standard deviation.

Initially, growth kinetics of pathogenic ZH501, attenuated MP-12 and MP-12-clone13type (rMP12-C13type) were performed in primary mouse cells. Overall, only limited replication of RVFV could be detected in primary macrophages after infection. Over the first 24 hours post infection, the amount of infectious virus in the supernatant increased in rMP12-C13type-, MP-12-, and ZH501-infected cells by at least one log. Two separate MOIs were tested as to determine if the higher MOI would result in higher viral titers and a different phosphorylation profile. No further increase in viral titer could be detected throughout the remaining time course and virus titer plateaued (Figure 3.9). The viral titer appear to only slightly increase early after infection and the low level of CPE observed until ≤ 24 HPI reflects the low viral replication. There was approximately 70% cell death at 72 hours after infection with ZH501 and approximately 20% cell death 72 hours after infection with MP-12 (Figure 3.10).

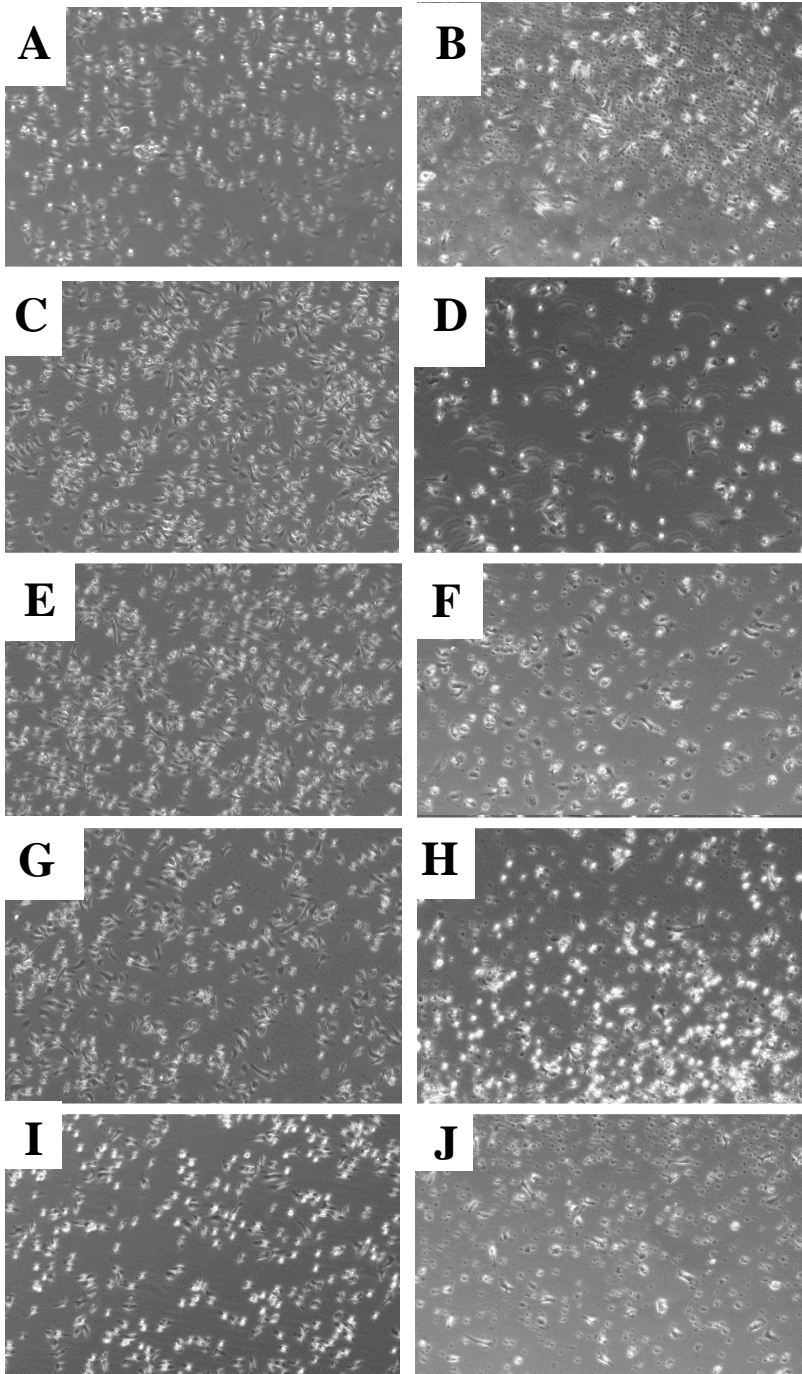


Figure 3.10. Primary BMD macrophages 1 or 72 HPI

Primary BMD macrophage cells 1 or 72 hours after infection. (A) Mock-infected cells, 1 HPI, (B) Mock-infected cells, 72 HPI, (C) cells infected with irradiated MP-12, 1 HPI, (D) cells infected with irradiated MP-12, 72 HPI, (E) cells infected with MP-12, 1 HPI, (F) cells infected with MP-12, 72 HPI, (G) cells infected with rMP12-C13type, 1HPI, (H) cells infected with rMP12-C13type, 72HPI, (I) cells infected with ZH501, 1HPI, (J) cells infected with ZH501, 72HPI. MOI=4

Next, the concentration of the phosphorylation states of eight different proteins was measured in whole cell lysates to gain an understanding as to which pathways are activated after RVFV infection. To ensure that the primary cells were capable of responding to stimulus and phosphorylation of these proteins, LPS-stimulated cells were included as a positive control. JNK phosphorylation did not change in primary macrophages after infection with a low MOI of 1 (data not shown). When the MOI was increased (from 1 to 4), there was an almost 4-fold increase in the phosphorylation of JNK 72 hours after infection with live MP-12 only (Figure 3.11A). None of the other infections resulted in a significant change in p-JNK. Since p-JNK phosphorylates c-Jun, a similar profile was expected to be observed between phosphorylation states of the two proteins. The protein c-Jun has anti-apoptotic properties and is required for the cell to progress through the cell cycle. The amount of c-Jun increased 18-fold starting at 6 hours after rMP12-C13type infection at the lower MOI (MOI = 1) (data not shown). After infection with a MOI of 4, the increase in phosphorylation was already detectable as early as 1 hour after infection (Figure 3.11B). A similar pattern of phosphorylation increase was observed after infection with irradiated MP-12 (3-fold increase), but the increase was not as high as the increase seen after infection with rMP12-C13type (12-fold increase). As with p-JNK, there was no significant change in the phosphorylation of c-Jun after irradiated MP-12 or ZH501 infection.

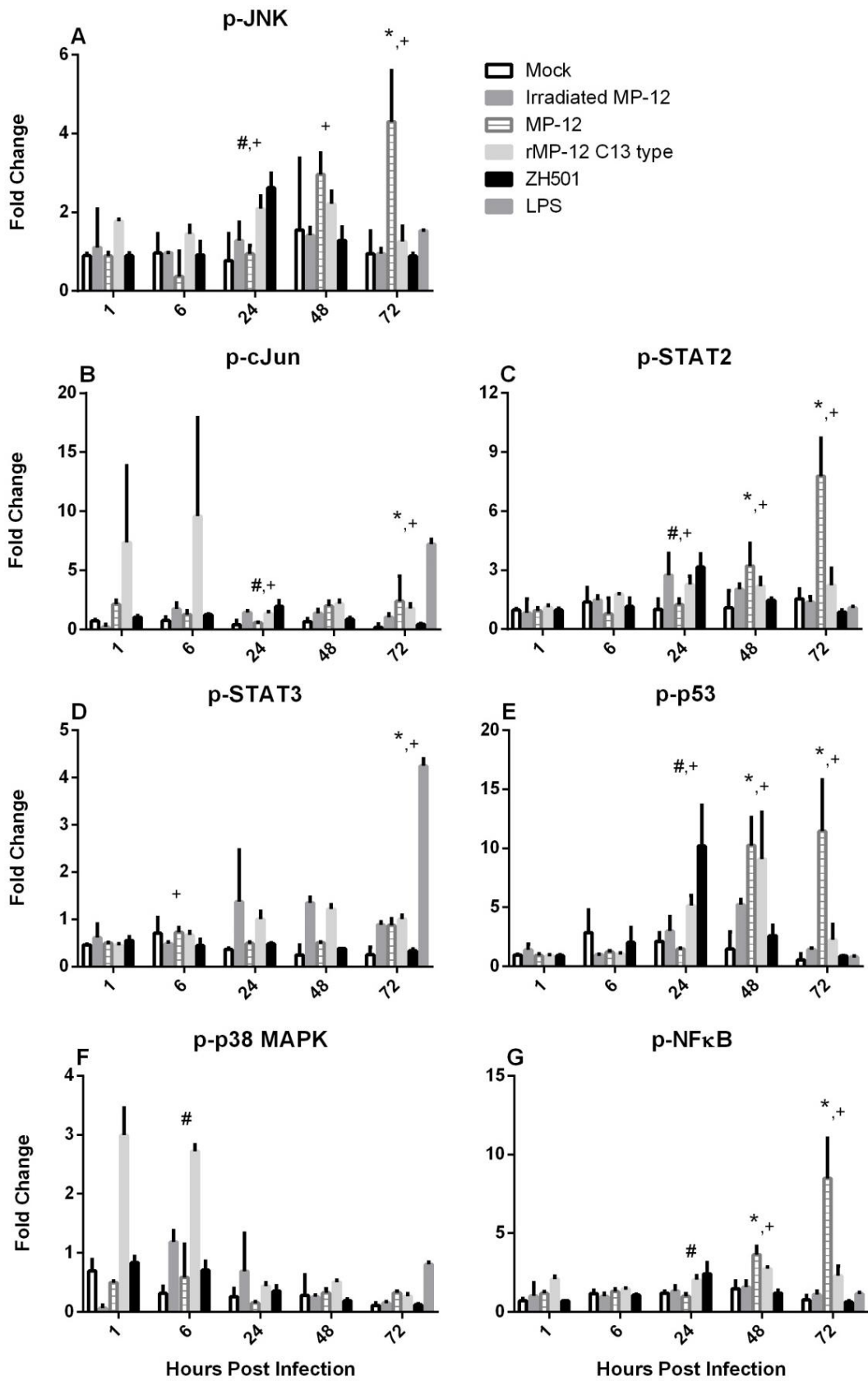


Figure 3.11. Phosphoprotein levels in primary macrophage cells

Protein levels in primary BMD macrophage cells of p-JNK (A), p-c-Jun (B), p-STAT2 (C), p-STAT3 (D), p-p53 (E), p-p38 MAPK (F), and p-NF- κ B (G) after infection with irradiated MP-12, live MP-12, rMP12-C13type, or ZH501 or stimulated with LPS. Changes in phosphorylation levels are represented as a fold change over cells at 0 HPI. Cells were plated, allowed to rest and then infected after 24 hours. Open bars represent mock-infected cells, dark gray bars represent cells infected with irradiated MP-12, striped gray bars represent cells infected with MP-12, light gray bars are cells infected with rMP12-C13type virus and black bars are representative of ZH501-infected cells. LPS stimulated samples were only taken after 72 hours and are represented by the last bar on the graph. Error bars are \pm standard deviation and *, #, and + indicates $p < 0.05$ between mock/MP-12, mock/ZH501, and MP-12/ZH501, respectively. MOI = 8

STAT proteins are important in the cell signaling response to IFN binding to its receptors. In primary macrophages, STAT2 phosphorylation increased but not significantly during the course of rMP12-C13type virus infection and 48 hours after infection with irradiated MP-12 (Figure 3.11C). There was also an increase in STAT2 phosphorylation after MP-12 infection, at 48HPI (4-fold) and 72 HPI (3-fold), respectively. STAT3 phosphorylation only exhibited a slight increase after infection with rMP12-C13type and irradiated MP-12 infection (Figure 3.11D). This was expected as the rMP12-C13type is missing a large section of the NSs gene, the virulence factor for RVFV, and irradiated MP-12 is replication deficient. MP-12 infection did not lead to any increase in pSTAT3 and infection with ZH501 did not result in any increase in the concentration of p-STAT2 or p-STAT3 with the exception of a 3-fold transient and significant increase of p-STAT2 at 24 HPI (Figure 3.11C and D).

The levels of phosphorylated pro-apoptotic protein p53 increased significantly after rMP12-C13type, MP-12 and irradiated MP-12 infection beginning at 48 HPI (Figure 3.11E). By 72 HPI, the increase in p-p53 after rMP12-C13type and irradiated MP-12 infection was gone but a significant increase after MP-12 infection was seen. Furthermore, there was also a 10-fold increase in p53 phosphorylation 24 hours after ZH501 infection (MOI=4). Directly upstream of p53 in its signaling cascade, is p38 MAPK. P38 MAPK is also an upstream effector of IL-1 and TNF α . This protein

increased in phosphorylation beginning 1 hour after rMP12-C13type infection with a 6-fold increase over mock-infected cells at the same time and 6 hours after infection with irradiated MP-12 with a 4-fold increase (MOI = 4) (Figure 3.11F). The concentration of p-p38 MAPK remained significantly elevated 6 hours after rMP12-C13type infection. Since there was approximately 36 hours between the increase in p38 MAPK phosphorylation and p53 phosphorylation, it appears that the detected p53 phosphorylation was not a direct result of the phosphorylation of p38 MAPK.

NF- κ B, which plays a key role in regulation of the immune response and in vascular inflammation (Brasier 2006), only demonstrated an increase in phosphorylation at 48 and 72 hours post MP-12 and rMP12-C13type infection (Figure 3.11G). It is possible that at these time points, the cells were trying to regulate the immune response to control and ultimately survive RVFV infection. In conjunction with the other cell signaling data gained from the performed analyses, it appeared that at 48 and 72 HPI the macrophage cells were at a critical time point where they will either control and survive the infection or undergo apoptosis. Only two of the proteins examined showed an increase in phosphorylation after ZH501 infection and only after infection with the high MOI. The observed increases in phosphorylation appeared to be a random occurrence after RVFV infection and might indicate that ZH501 interrupts the macrophage intracellular signaling response to viral infection (Figure 3.11).

Cell-signaling response in primary mouse dendritic cells

Data from growth kinetics performed in primary BMD dendritic cells, indicated that these cells appeared to be refractory to RVFV infection or that active viral replication failed in these cells (Figure 3.12). The initial increase in viral titer at 6 hours post infection might be a possible result from cell-bound virions that could have detached from the dendritic cells instead of entering the cells. This is contrary to what generally happens as viral titers in cell culture supernatants will generally decrease as virus

particles will bind and ultimately enter target cells (Lozach, Kuhbacher *et al.* 2011). Over the entire time course of 72 hours, no obvious visual change in infected primary DCs was observed (Figure 3.13).

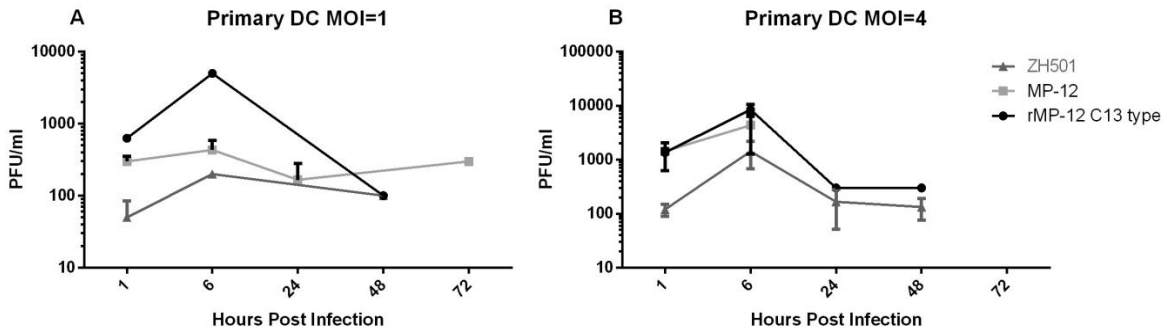


Figure 3.12. Viral titers in BMD dendritic cells after infection

Viral titers in BMD dendritic cells after infection with MP-12, rMP12-C13type, and ZH501. The line with closed diamonds is viral growth after cells were infected with ZH501, the line with closed squares represents cells were infected with MP-12, and the line with closed triangles represents cells were infected with rMP12-C13type virus. Error bars are \pm standard deviation.

Of the examined eight proteins, three (JNK (Figure 3.14A), STAT3 (Figure 3.14D), and Erk (data not shown)) showed no change in the level of its phosphorylated counterpart. The other proteins demonstrated sporadic changes that exhibited no continuity. While there was no change in p-JNK concentration, one of its downstream effector proteins did have an increase in phosphorylation. The concentration of p-c-Jun increased significantly 6 hours after infection with rMP12-C13type and 48 hours after infection with live MP-12 (Figure 3.14B). As with p-JNK and p-c-Jun, two proteins that are sequentially activated, p53 and p38 MAPK phosphorylation did not show any correlation in response (Figure 3.14E and F). No change in p38 MAPK phosphorylation during the experiment was detected until 6 hours after infection with rMP12-C13type. After rMP12-C13type infection, there was no significant change detectable in p53 phosphorylation. The only time point at which p53 phosphorylation increased was late in the experiment, 72 hours after MP-12 infection. Both STAT2 and NF-kB (Figure 3.14C

and G) experienced only a sporadic increase in phosphorylation at 48 and 72 hours after MP-12 infection.

DISCUSSION

After a virus binds to its host cellular receptor, it initiates the activation of specific signaling pathways. Once a virus has entered the cell and begins to replicate, the cell initiates secretion of cytokines and can stimulate pathways within itself (autocrine signaling) or in nearby cells (paracrine signaling). A virus can manipulate the host signaling response to its benefit and by gaining an understanding of these manipulations, it will be possible to design treatments that counteract the virus' activities in the host. Initially, total levels of JNK, ERK1/2, I κ B, c-Jun, p38 MAPK, and p53 were examined and no significant change in the amounts of total protein between mock, irradiated MP-12, and live MP-12-infected samples were detected for the cell types examined. This has also previously been observed in HSAEC cells after MP-12 and ZH501 infection (Popova, Turell *et al.* 2010). Since no significant change in total protein concentration was detected in mouse macrophage and dendritic cells, changes that were observed in the phosphorylation status of these proteins are likely due to phosphorylation of the proteins already present in the cell, as opposed to new protein being synthesized.

Although not definitive, it appears that while RVFV can infect and replicate in BMD macrophages, it cannot replicate in BMD DCs. No increase in viral titer was detectable over 72 hours after RVFV infection of BMDCs. The viral growth kinetics might indicate that initially after infection (within 1 HPI) cell-bound virus is dissociating, subsequently resulting in an increase of infectious virus in the cell supernatant of the primary DCs. In most infections, the titer generally decreases within the first 6 HPI as the virus enters the cell and begins to replicate, generating new infectious virions.

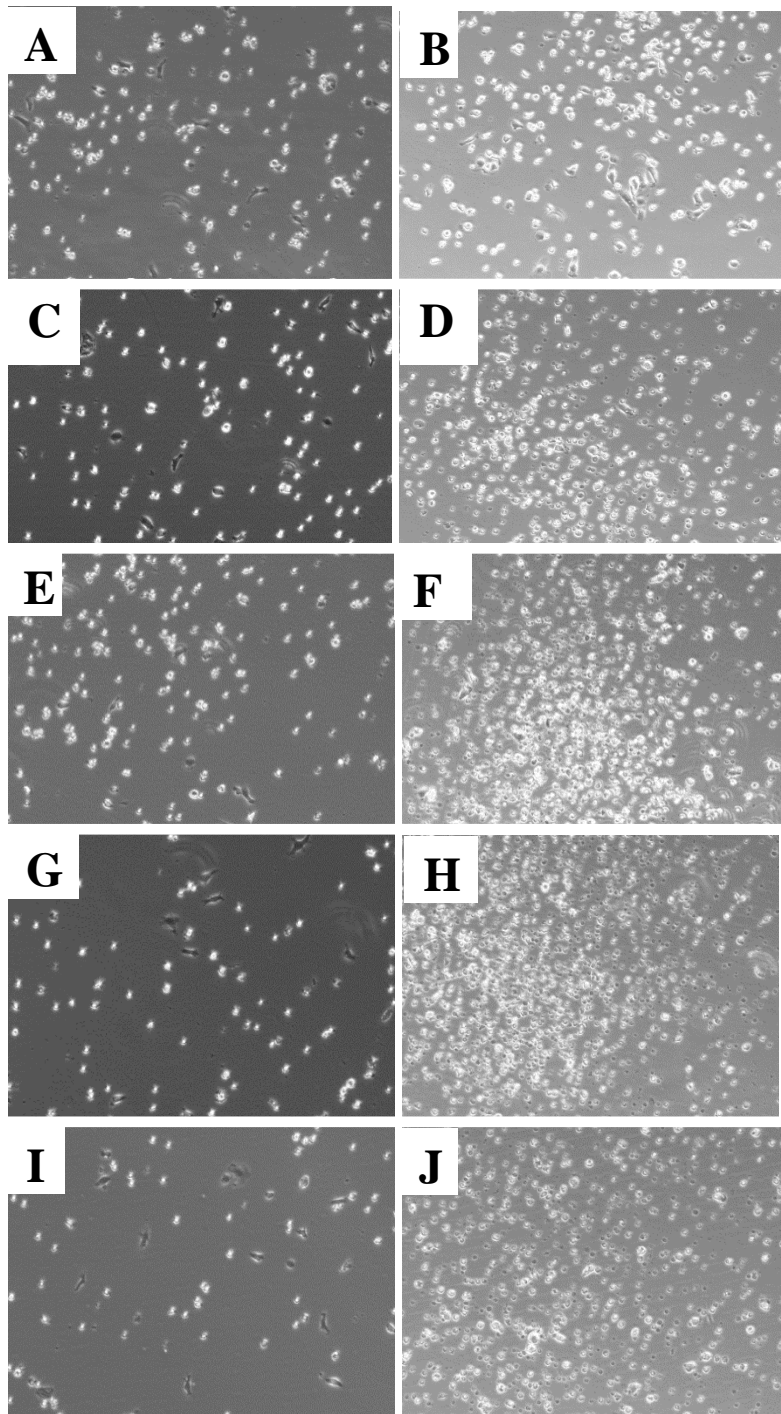


Figure 3.13. Photographs of primary dendritic cells 1 or 72 HPI

Primary BMD dendritic cells 1 or 72 hours after infection. (A) Mock-infected cells, 1 HPI, (B) Mock-infected cells, 72 HPI, (C) cells infected with irradiated MP-12, 1 HPI, (D) cells infected with irradiated MP-12, 72 HPI, (E) cells infected with MP-12, 1 HPI, (F) cells infected with MP-12, 72 HPI, (G) cells infected with rMP12-C13type, 1HPI, (H) cells infected with rMP12-C13type, 72HPI, (I) cells infected with ZH501, 1HPI, (J) cells infected with ZH501, 72HPI. MOI=4

Cell signaling data indicate that similar pathways (in relation to the proteins examined in this study) were activated early in infection with irradiated and live MP-12 virus. This was expected as irradiation used to inactivate the virus, results in degradation of viral RNA and should have minimal impact on viral surface glycoproteins. While the purpose of using these live and inactivated viruses was to differentiate between signaling cascades activated by viral attachment and viral replication, none of the proteins examined showed a significant difference between mock, irradiated MP-12, MP-12, or ZH501 infections in primary macrophages. These data lead to the conclusion that they are possibly not involved in the entry of RVFV and that alternative proteins are being used for viral entry.

My first main observation was the increase in the phosphorylation of proteins that are generally involved in pro-apoptotic pathways (JNK, p53 and p38 MAPK) after rMP12-C13type and MP-12 infections. JNK is important in cellular proliferation and cell survival and apoptosis. It represents a link between apoptotic pathways and gene expression in cells (Wu 2004). JNK is involved in the release of various cytokines including RANTES, IL-8 and GM-CSF. The increase in p-JNK could be a precursor to cell migration and the release of pro-inflammatory cytokines. Generally, p53 is phosphorylated in response to IFN stimulation and is used as a transcription factor to activate the cellular apoptotic process. It is also important in DNA repair and cell cycle arrest (Olsson, Manzl *et al.* 2007). In response to DNA damage, the cell cycle is halted at the end of the G1 stage. If the DNA can be repaired, the cell cycle continues, if the damage cannot be repaired, then the cell begins to undergo apoptosis. The activation of these DNA damage signaling pathways has been attributed to the NSs virulence factor of RVFV (Baer, Austin *et al.* 2012).

The NSm protein has been shown to be targeted to the mitochondria via its C terminus. NSm prevents apoptosis through the inactivation of various caspases by

unknown mechanisms (Won, Ikegami *et al.* 2007; Terasaki, Won *et al.* 2012). While p-p53 concentration increases, the downstream effectors (caspases) are possibly not being activated due to the decrease in cleavage that accompanies NSm.

P38 MAPK is an upstream regulator of p53, which is known to be a pro-apoptotic cell signaling molecule (Wu 2004). Since the damage in the liver is believed to be caused by apoptosis (Smith, Steele *et al.* 2010), the increases observed in p-JNK and p-p38 MAPK concentrations could indicate the initiation of apoptosis after MP-12 infection. Popova *et al.* and Narayanan *et al.* detected a significant increase in p-p53 and p-p38 MAPK, respectively, in HSAECs (Popova, Turell *et al.* 2010; Narayanan, Popova *et al.* 2011; Austin, Baer *et al.* 2012).

Overall, the pro-apoptotic MAPK pathways that were examined showed an increase in the phosphorylation of key proteins after infection with MP-12 or rMP12-C13type. Even though there was no increase in these proteins after ZH501 infection, there was more cell death observed after ZH501 infection than after MP-12 infection. From the data shown, ZH501-infected cells appear not to go through apoptosis, but possibly die due to the fact that cellular processes have been re-programmed to synthesize new virus particles. Since the viruses grow to similar titers in the macrophage cells, these data suggest that ZH501 affects components of the host response that MP-12 does not. While NSs has been shown to decrease transcription in host cells (Le May, Dubaele *et al.* 2004) and both viruses (MP-12 and ZH501) have an intact NSs protein, it has been shown that the NSs protein of wild type RVFV strain ZH548 and MP-12 functions differently in host animals (Bouloy, Janzen *et al.* 2001). This might indicate that alternative pathways exist through which ZH501 can manipulate the host response in macrophage cells.

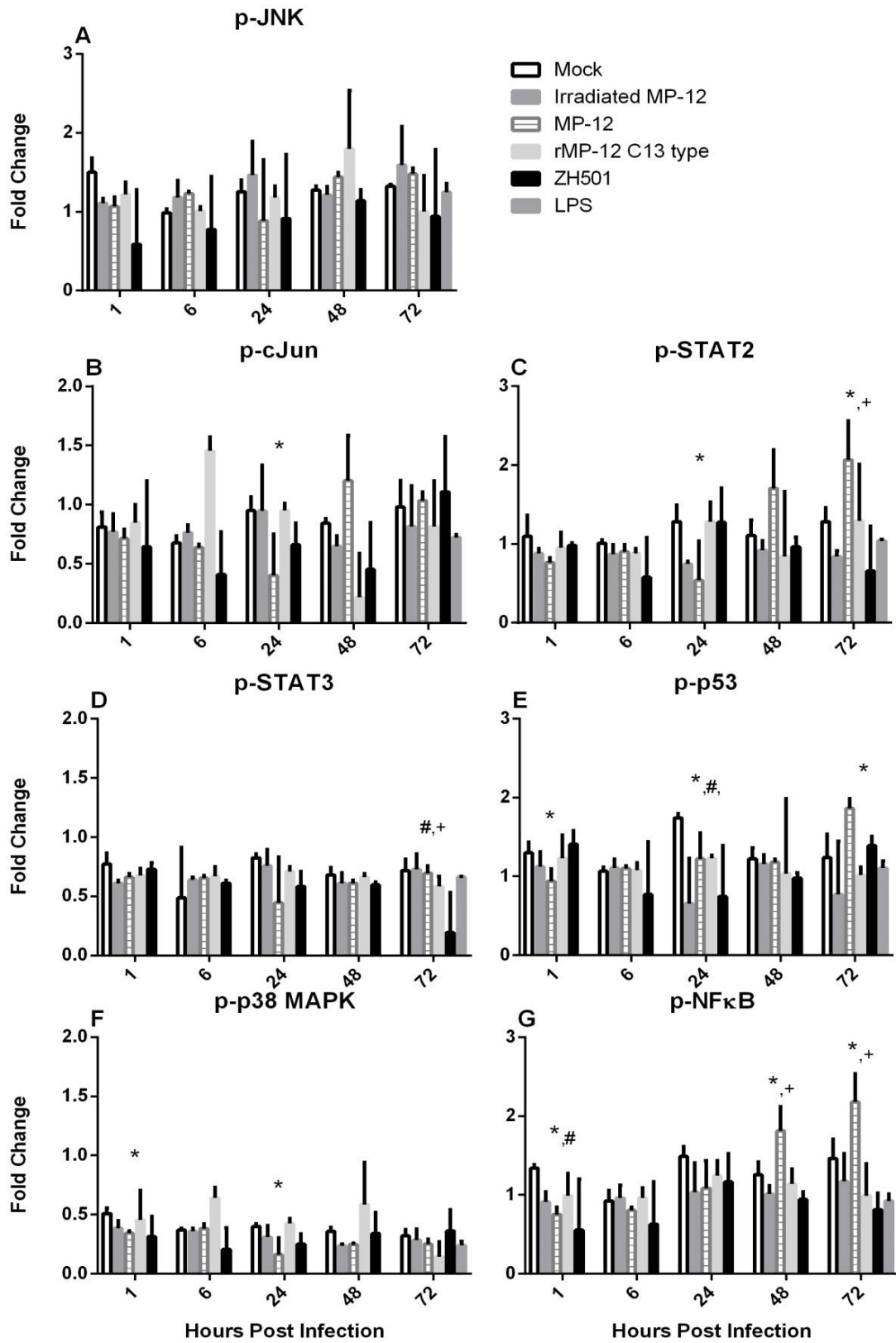


Figure 3.14. Protein levels in primary BMD dendritic cells

The fold change of p-JNK (A), p-c-Jun (B), p-STAT2 (C), p-STAT3 (D), p-p53 (E), p-p38 MAPK (F), and p-NF- κ B (G) after infection with irradiated MP-12, live MP-12, rMP12-C13type, or ZH501 or stimulated with LPS. Changes in phosphorylation levels are represented as a fold change over cells at 0 HPI. Cells were plated, allowed to rest and then infected after 24 hours. Open bars represent mock-infected cells, dark gray bars represent cells infected with irradiated MP-12, striped gray bars represent cells infected with MP-12, light gray bars are cells infected with rMP12-C13type virus and black bars are representative of ZH501-infected cells. LPS stimulated samples were only taken after 72 hours and are represented by the last bar on the graph. Error bars are \pm standard deviation and *, #, and + indicates $p < 0.05$ between mock/MP-12, mock/ZH501, and MP-12/ZH501, respectively. MOI = 8

Viral infection generally causes infected cells to release IFN- γ resulting in JAK/STAT pathway activation in bystander cells through paracrine signaling. STAT proteins regulate a spectrum of cellular functions downstream of activated cytokine receptors. They stimulate proliferation, differentiation, and survival of cells as well as host resistance to pathogens. The JAK/STAT pathway appears to be activated after infection with MP-12 as there is a large increase in p-STAT2 72 hours after infection in primary macrophage cells. The JAK/STAT pathway terminates with the activation of IFN- γ activated sequence (GAS) or IFN-stimulated response elements (type I IFN) such as IL-6, chemokine (C-C) receptors, RANTES, and MCP. The increase of p-STAT2 is seen at the very end of the time course after MP-12 infection (at least in my experiments) and may be a possible attempt at repair since the STAT proteins are important components of cellular growth and survival. This activation after infection could be in response to the various cytokines that are released after MP-12 infection.

While recent published studies indicate that there is no change in levels of p-STAT3 after MP-12 and ZH501 infection (Popova, Turell *et al.* 2010), I observed a 2-fold increase in pSTAT3 48 hours after infection with rMP12-C13type when compared to mock-infected cells. This could be due to the use of different cell types (primary mouse immuno-modulatory cells used here versus HSAECs used in the other studies), the lack of the NSs protein in rMP12-C13 type virus, or since this increase is only transient, it

could have been missed in other studies. I have found that STAT3 phosphorylation was unchanged after live MP-12 infection, while p-STAT2 showed increases starting at 48 HPI. The late increase in p-STAT2 after viral infection in cells could be due to an antiviral response that is initiated when the virus initially enters the cells.

Early in the course of infection (≤ 24 HPI), p-NF- κ B concentration does not differ between the infection groups. Beginning at 48 HPI there is a 2-fold increase in NF- κ B concentration which increases to 10-fold at 72HPI. Since NF- κ B is important in the mediation of vascular inflammation (Han, Runge *et al.* 1999; Brasier, Recinos *et al.* 2002) through the regulation of various pro-inflammatory cytokines (RANTES, MCP-1, MIP-1, and IL-6), it is possible that this increase could facilitate an increase in the pro-inflammatory cytokines. Further studies need to be done to examine the amount of NF- κ B in the nuclear fraction of the cell since NF- κ B is active after it translocates to the nucleus and binds to DNA (Shirakawa and Mizel 1989).

My data suggest that pro-inflammatory pathways that respond to NF- κ B are down-regulated since NF- κ B expression does not increase until 48 and 72 HPI and only after MP-12 infection. NF- κ B also inhibits apoptosis, and since the levels of pro-apoptotic proteins phosphorylated after MP-12 infection increases, it is not surprising that the anti-apoptotic protein NF- κ B does not show an increase. The cells infected with MP-12 appear to undergo apoptosis. As seen with the other proteins examined, there is no increase in NF- κ B after ZH501 infection which is probably due to viral inhibition of cellular transcription.

I have found that proteins that are involved in pro-apoptotic and survival pathways are phosphorylated after MP-12 infection in primary BMD macrophage cells. This phosphorylation, with the exception of p-p38 MAPK, is late in the course of infection. It appears that the delicate balance in the cell is disrupted by RVFV infection. After entering host cells, RVFV shuts down cellular transcription approximately 8 hours post infection with the MOI used, (Billecocq, Spiegel *et al.* 2004). A better

understanding of the overall host immune response to RVFV infection will not only contribute to increase my knowledge on RVFV pathogenicity but also to the development of antiviral strategies. The goal of this aim was to examine and characterize the early host cell signaling response after infection with RVFV. Many recent studies have examined the cell signaling response to RVFV infection and have begun to piece together modulation of general pathways to viral replication (Popova, Turell *et al.* 2010; Narayanan, Popova *et al.* 2011; Austin, Baer *et al.* 2012).

Chapter 4 Cytokine secretion that is affected following RVFV infection

Specific Aim 2: Identify IFNs and inflammatory cytokines whose secretion is affected following infection *in vitro* with RVFV wild type strain ZH501 or MP-12.

Hypothesis: While the IFN response to infection with either ZH501 or MP-12 will be similar, more pro-inflammatory cytokines will be released following ZH501 infection since the pathology that is seen after RVFV infection has been repeatedly attributed to an overactive immune response.

Rationale: For this study, the goal was to determine the host immune response to RVFV infection in cell culture systems. In an effort to characterize the host response to RVFV infection, the overall cytokine response was examined in primary murine immune-modulatory cells (macrophages and bone-marrow derived dendritic cells) and immune-modulatory cell lines (RAW 264.7 macrophage and DC 2.4 dendritic cells) with the expectation that the response would be similar and provide data to support the use of murine cell lines in studies characterizing the host response to RVFV infection. Furthermore, if a similar response can be detected between human (data from published studies) and mouse immune-modulatory cells, this would provide additional support for the use of murine cells to study infection. If the host cytokine response can be deduced, efficient treatment therapies could be devised.

McElroy and Nichol examined TNF α and IFN levels in peripheral blood mononuclear cells obtained from four individual healthy human donors (McElroy and Nichol 2012). They found that human primary monocyte derived macrophages were susceptible to RVFV infection, and developed CPE at 12 hours post infection (HPI). Furthermore, they determined that infection with ZH501 did not cause an increase in type I IFN (IFN- α 2 and IFN- β) or TNF α at 24 HPI, but that infection with irradiated ZH501

led to an increase in TNF α and IFN- α 2 levels in three out of the four donors. Cells that were infected with a recombinant RVFV lacking NSs showed an exponential increase in IFN- α 2, IFN- β , and TNF α in all four donors when compared to mock and ZH501-infected cells (McElroy and Nichol 2012).

Similar to the described results from McElroy and Nichol, I detected an increase of multiple different pro-inflammatory cytokines in murine primary macrophages after infection with a recombinant RVFV lacking the NSs protein (rMP12-C13type) (Ikegami, Won *et al.* 2006). No difference in cytokine response was detected between mock and ZH501-infected primary macrophage cells and only a slight increase in cytokine concentration after infection with γ -irradiated virus. The response by MP-12-infected primary macrophage cells seemed to be delayed and less intense when compared to the response by rMP12-C13type-infected primary macrophage cells.

RESULTS

Cytokine response in RAW 264.7 cells

Mouse-derived RAW 264.7 cells were infected with MP-12 or ZH501 at a MOI of 1. One hour after infection, cell culture supernatant aliquots were taken at multiple time points (over a course of 36 hrs) and the concentration of a panel of Th1 associated cytokines (IFN- γ , IL-12(p70), and IL-12(p40)) and chemokines (MCP-1, MIP-1 α , MIP-1 β , and RANTES) was examined. IFN- γ is considered an antiviral cytokine and is thought to directly inhibit viral replication (Milstone and Waksman 1970; Hayashi and Koike 1989; Shirazi and Pitha 1992; Lin, Kwong *et al.* 2004; Dash, Prabhu *et al.* 2005; Konishi, Okamoto *et al.* 2012). In ZH501-infected RAW 264.7 cells, no significant change in IFN- γ concentration was detected until 36 HPI, after which the concentration increased to 2.5 times higher than observed in mock-infected RAW cells (Figure 4.1A). At 36 HPI, the ZH501 viral titer was 6.5 log and the number of surviving cells was less than 10% (data not shown). With such high titers and low number of surviving cells, it

appears that the cellular response is inefficient at controlling viral replication and subsequently clearing RVFV. Although macrophages are not the primary producers of IFN- γ (natural killer and natural killer T-cells are the principal source of IFN- γ *in vivo*), IFN- γ is needed for activation of macrophages and it may serve in an autocrine manner to self-activate the cells. The release of IFN- γ by macrophages is important in this context to examine the effect of RVFV on the functionality of these cells. However, IFN- γ secretion does not change significantly through the course of the experiment after MP-12 or irradiated MP-12 infection. IFN- γ secretion only increased toward the end of infection with ZH501.

IL-12(p70) (Figure 4.1B) and IL-12(p40) (Figure 4.1C) were both examined after RVFV infection. IL-12(p70) is a heterodimer and is considered the active form of the protein. Th1 cells stimulated by IL-12(p70) proliferate and produce IFN- γ (Hsieh, Macatonia *et al.* 1993). IL-12(p40) is a homodimer and is an IL-12 antagonist. While IL-12(p70) exhibited no significant change in concentration throughout the course of infection with ZH501, at 12 HPI, there was approximately a 5-fold decrease in the concentration of IL-12(p70) after MP-12 infection compared to mock-infected cells. Even though the amount of secreted IL-12(p70) increased throughout the course of infection, after infection with irradiated MP-12 the concentration was lower compared to mock-infected cells. No change in the concentration of IL-12(p40) was detected after infection with either MP-12 or ZH501 when compared to mock-infected cells (Figure 4.1C). At 9 and 12 HPI, MP-12 and ZH501-infected cells secreted amounts of IL-12(p40) that were significantly different from one another.

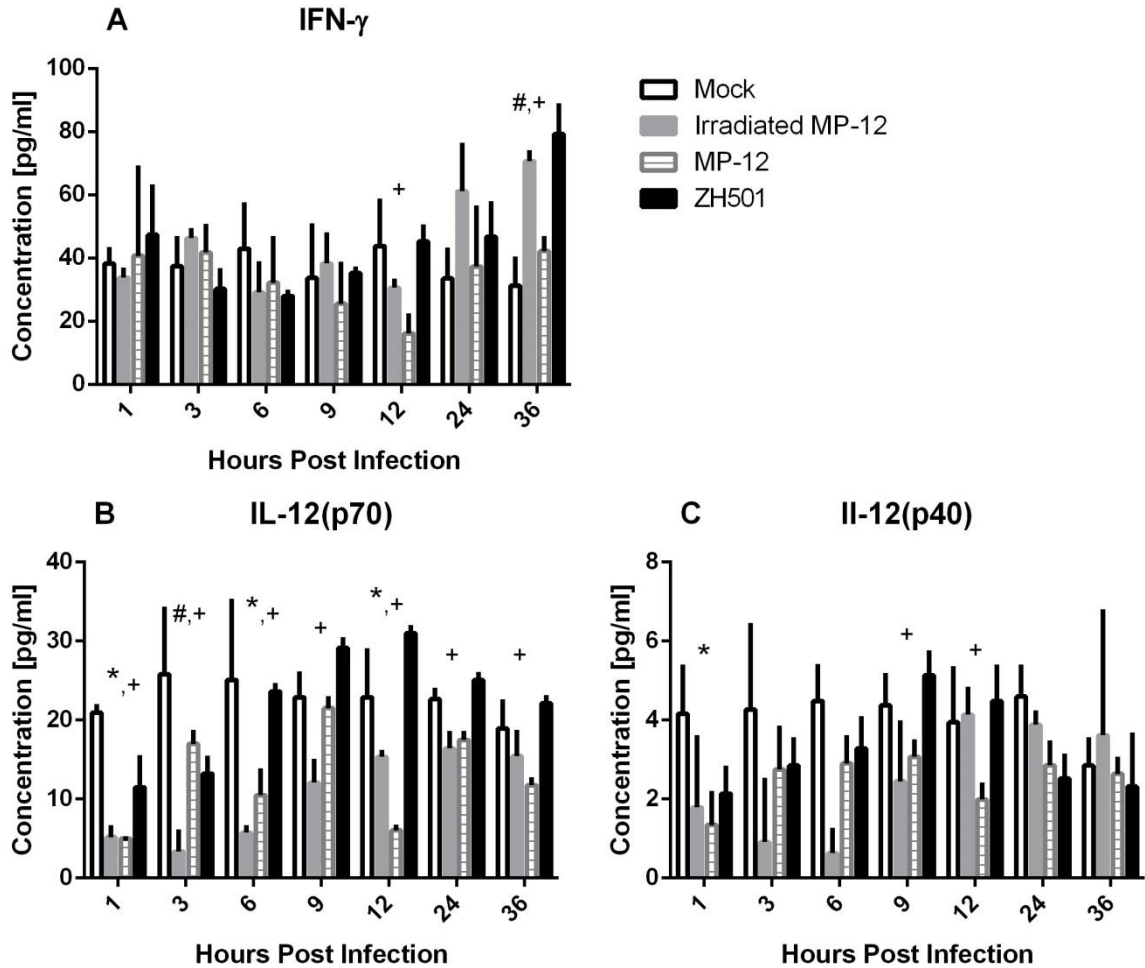


Figure 4.1. Th1 cytokines secreted by RAW 264.7 cells

Th1 cytokines secreted by RAW 264.7 cells after infection with irradiated MP-12, live MP-12, or ZH501. Cells were plated, allowed to rest and then infected after 24 hours. Open bars represent mock infected cells, gray bars represent cells infected with irradiated MP-12, gray striped bars represent cells infected with MP-12, and black bars represent cells infected with ZH501. Error bars are \pm standard deviation and *, #, and + indicate $p < 0.05$ between mock/MP-12, mock/ZH501 or MP-12/ZH501, respectively. Cells were infected with a MOI of 1.

A significant increase in the amount of secreted TNF α was detected at 12 HPI after irradiated MP-12 infection compared to both MP-12- (4-fold increase) and mock-infected cells (45-fold increase) (Figure 4.2). While MP-12 caused a 4-fold increase in the secretion of TNF α early in the course of infection (1-3 HPI), no difference could be detected between TNF α concentrations in mock and MP-12-infected samples during the end stages of the experiment (24-36 HPI). The concentration of TNF α after ZH501

infection increased by a factor of three when compared to mock-infected controls early in infection (1-3 HPI) and then began to gradually decline until 36 HPI. By 24 HPI, the concentration of TNF α secreted after MP-12 and ZH501 infections decreased to levels below that of mock-infected cells, while concentrations after infection with irradiated MP-12 gradually increased throughout the time course (Figure 4.2). These data suggest that replicating RVFV might inhibit TNF α expression.

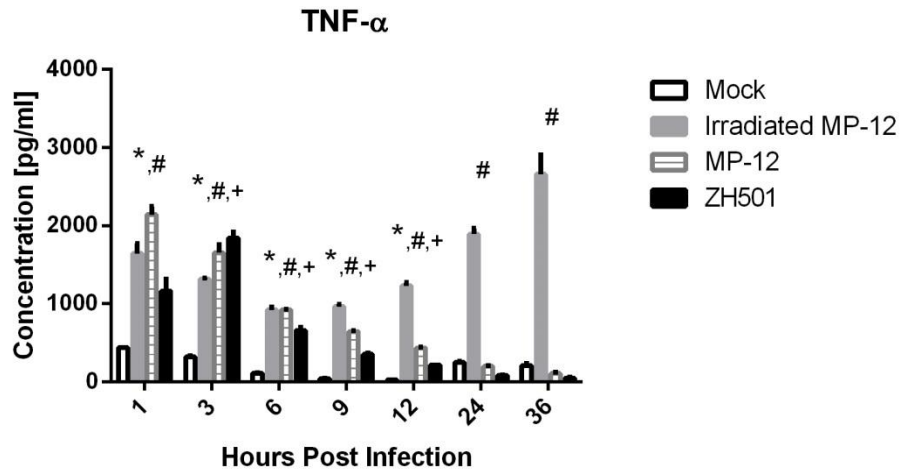


Figure 4.2. TNF α secreted by RAW 264.7 cells

TNF α secreted by RAW 264.7 cells after infection with irradiated MP-12, live MP-12, and ZH501. Cells were plated, allowed to rest and then infected after 24 hours. Open bars represent mock-infected cells, gray bars represent cells infected with irradiated MP-12, gray striped bars represent cells infected with MP-12, and black bars represent cells infected with ZH501. Error bars are \pm standard deviation and *, #, and + indicate $p < 0.05$ between mock/MP-12, mock/ZH501 or MP-12/ZH501, respectively. Cells were infected with a MOI of 1.

The chemokines RANTES, MCP-1, MIP1 α and MIP1 β play an important role during the host response to infection, due to their chemotactic properties and recruiting activity of immune cells, such as macrophages, to the sites of viral replication. While there was no detectable change in RANTES concentration between mock- and ZH501-infected samples, a large gradual increase was observed after infection with irradiated MP-12 that lasted throughout the entire course of the experiment (Figure 4.3A). This

change became apparent at 6 HPI (a 3-fold increase) and steadily increased until 36 HPI (a 40-fold increase). A decrease in RANTES secretion after MP-12 infection could be detected when compared to all other treatments. The decrease was first observed at 3 HPI when there was approximately a 40% decrease in the concentration of RANTES released after MP-12 infection. The decrease was greatest at 36 HPI with a 75% reduction in the concentration of RANTES in the cell supernatants. MCP-1 concentration in both MP-12- and ZH501-infected cells was decreased when compared to mock-infected samples throughout the entire time course (Figure 4.3B). During the course of the experiment, it appeared that MCP-1 was naturally secreted from RAW 264.7 cells and the active replication of RVFV hindered this secretion by compromising the functionality of the macrophage cells. MIP-1 α concentration followed a similar pattern as MCP-1 after RVFV infection (Figure 4.3C). There were significant decreases in both MP-12- and ZH501-infected samples after infection when compared to mock. ZH501-infected samples (even though secreting less MIP-1 α than mock-infected cells) secreted significantly more MIP-1 α than observed for MP-12-infected cells. IL-1 α concentration did not change after infection with RVFV (data not shown).

Cytokine response in DC 2.4 cells

As observed in the RAW 264.7 cells after RVFV infection, there was no increase in the concentration of IFN- γ in the DC 2.4 cells with the exception of 12 HPI, when both MP-12- and ZH501-infected cells secreted higher amounts of IFN- γ than mock cells (Figure 4.4A). This increase was only significant between mock- and MP-12-infected cells. At early time points after infection (between 1 and 9 HPI), a 60% (at 1 HPI) and 30% decrease (at 9 HPI) in the concentration of IFN- γ could be detected after infection with ZH501 compared to MP-12- and mock-infected cells (Figure 4.4A). Cells infected with irradiated MP-12 showed no significant difference in induction of IFN- γ at the translational level when compared to mock samples. IL-12(p70) exhibited no significant

change in concentration throughout the course of infection with RVFV MP-12 or ZH501, but was consistently lower in irradiated MP-12 infected DC 2.4 cells when compared to uninfected controls (Figure 4.4B). While IL-12(p70) concentration did not change when comparing mock- to MP-12-infected cells, the concentration of this cytokine showed a significant decrease at 6, 9, and 12 HPI after infection with ZH501 when compared to MP-12-infected cells. As with the RAW 264.7 cells, there was no detectable change in IL-12(p40) (data not shown).

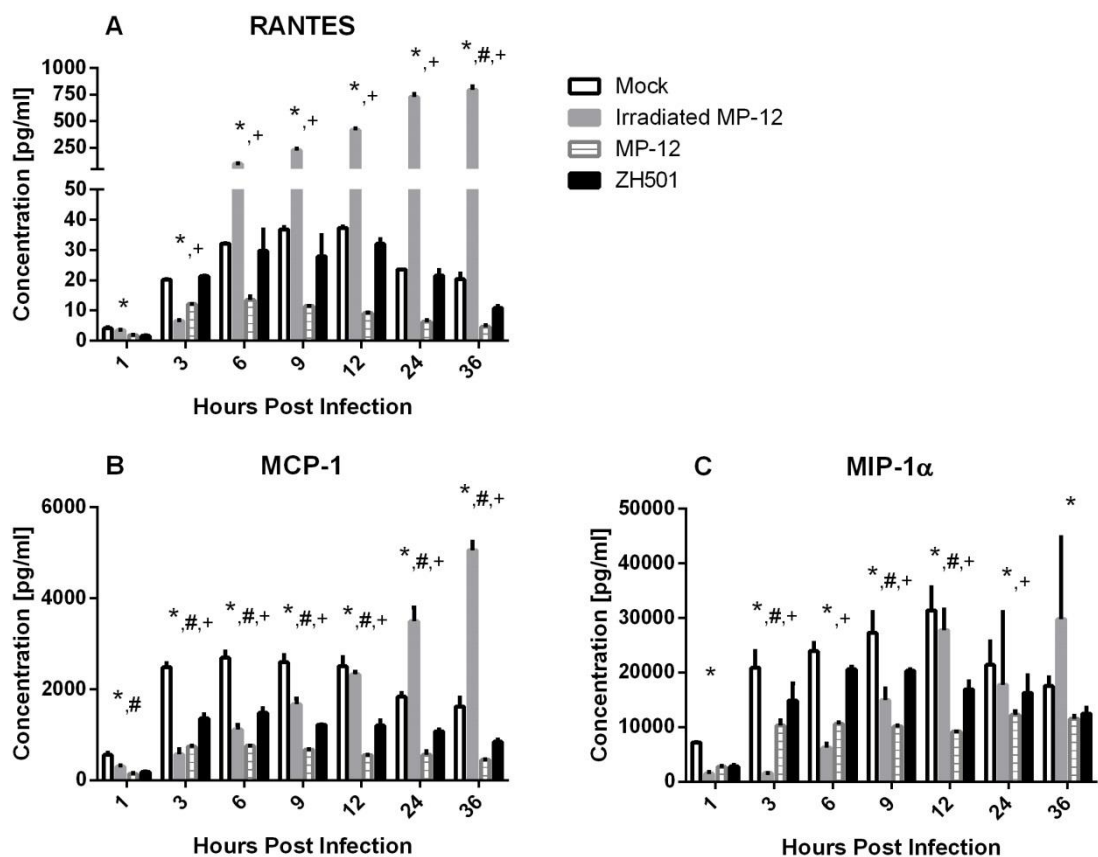


Figure 4.3. Chemokines secreted by RAW 264.7 cells

Chemokines secreted by RAW 264.7 cells after infection with irradiated MP-12, live MP-12, and ZH501. Cells were plated, allowed to rest and then infected after 24 hours. Open bars represent mock-infected cells, gray bars represent cells infected with irradiated MP-12, gray striped bars represent cells infected with MP-12, and black bars represent cells infected with ZH501. Error bars are \pm standard deviation and *, #, and + indicate $p < 0.05$ for mock/MP-12, mock/ZH501 or MP-12/ZH501, respectively. Cells were infected with a MOI of 1.

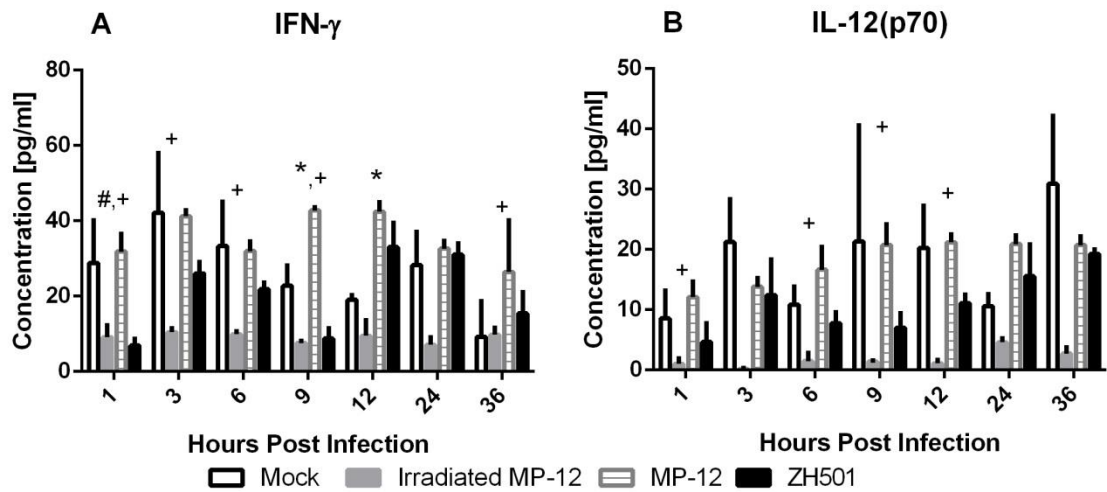


Figure 4.4. Th1 cytokines secreted by DC 2.4 cells

Th1 cytokines secreted by DC 2.4 cells after infection with irradiated MP-12, live MP-12, and ZH501. Cells were plated, allowed to rest and then infected after 24 hours. Open bars represent mock-infected cells, gray bars represent cells infected with irradiated MP-12, gray striped bars represent cells infected with MP-12, and black bars represent cells infected with ZH501. Error bars are \pm standard deviation and *, #, and + indicate $p < 0.05$ between mock/MP-12, mock/ZH501 or MP-12/ZH501, respectively. Cells were infected with a MOI of 1.

At 1 hour post ZH501 infection, there was a significant 2.5-fold increase in the amount of secreted TNF α . TNF α secretion peaked at 6 HPI and remained elevated until 9 HPI after ZH501 infection. From 12 to 24 HPI, the concentration of TNF α was not different among DC2.4 cells infected with MP-12 or ZH501 but TNF α concentration did increase after infection with irradiated MP-12 (Figure 4.5).

The concentrations of the chemokines RANTES, MCP-1, MIP-1 α and MIP-1 β were evaluated next in the supernatant of DC 2.4 cells. Unlike observations made in RAW 264.7 cells, there was an increase in RANTES in DC 2.4 cells after MP-12 infection (Figure 4.6A). At 1 HPI, there was a 2-fold increase, which lasted from 3 to 6 HPI, when the concentration of TNF α released after MP-12 infection was significantly higher than the concentration of TNF α released from the mock-infected samples. The ZH501-infected DC 2.4 cells showed no difference from mock-infected cells until 24 HPI

when there was a 2-fold decrease in the concentration of secreted RANTES. MCP-1 concentration was constantly lower in ZH501-infected DC 2.4 cells when compared to MP-12-infected cells. While the RANTES concentration in all three viral infections steadily increased over the course of the experiment, at 24 HPI the concentrations of MCP-1 in MP-12- and ZH501-infected cells dropped as the levels in mock-infected samples continued to increase (Figure 4.6 B). MIP-1 α and MIP-1 β concentrations were unchanged or decreased in both MP-12- and ZH501-infected samples when compared to mock (Figure 4.6C; data not shown for MIP-1 β).

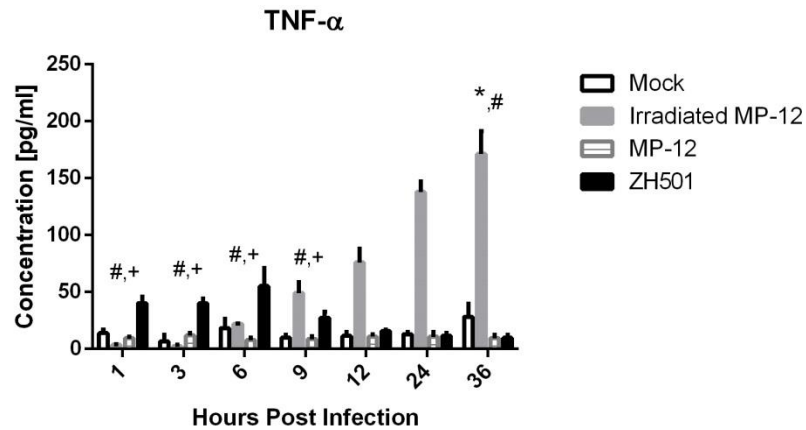


Figure 4.5. TNF α secreted by DC 2.4 cells

TNF α secreted by DC 2.4 cells after infection with irradiated MP-12, live MP-12, and ZH501. Cells were plated, allowed to rest and then infected after 24 hours. Open bars represent mock-infected cells, gray bars represent cells infected with irradiated MP-12, gray striped bars represent cells infected with MP-12, and black bars represent cells infected with ZH501. Error bars are \pm standard deviation and *, #, and + indicate $p < 0.05$ between mock/MP-12, mock/ZH501 or MP-12/ZH501, respectively. Cells were infected with a MOI of 1.

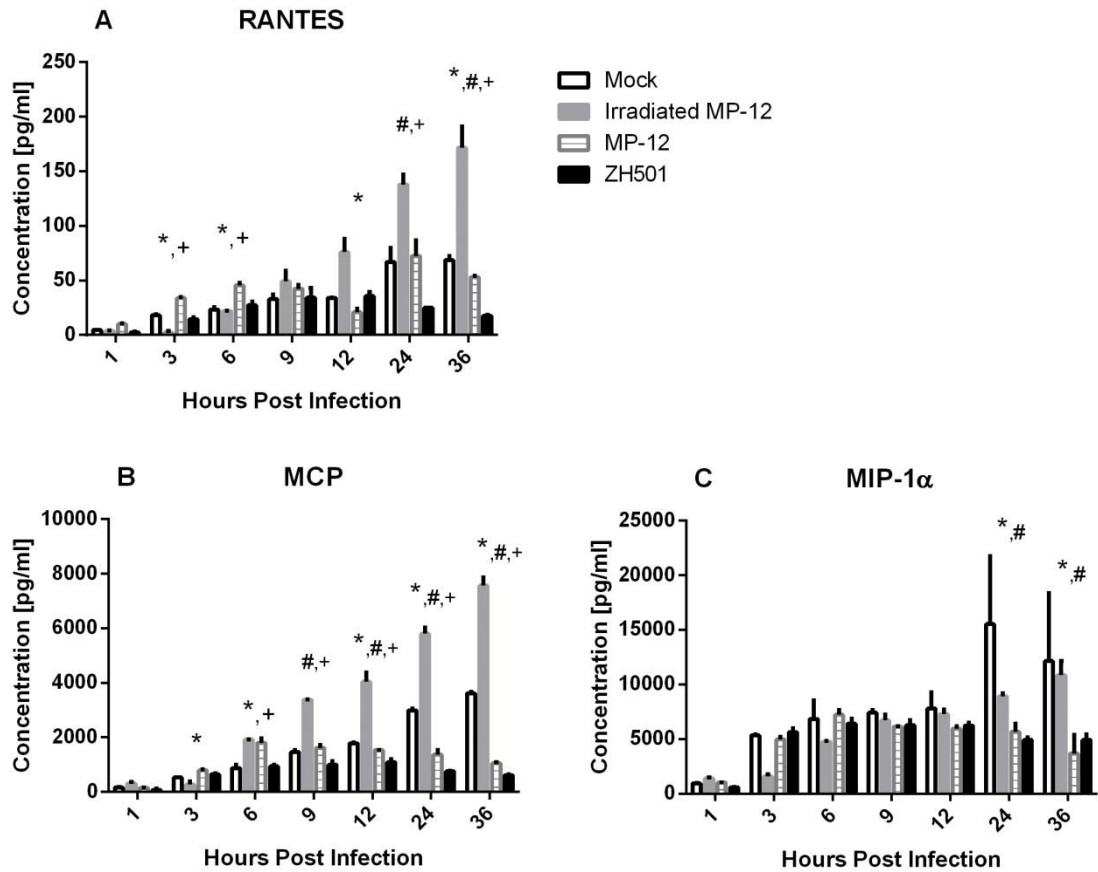


Figure 4.6. Chemokines secreted by DC 2.4 cells after infection

Chemokines secreted by DC 2.4 cells after infection with irradiated MP-12, live MP-12, and ZH501. Cells were plated, allowed to rest and then infected after 24 hours. Open bars represent mock-infected cells, gray bars represent cells infected with irradiated MP-12, gray striped bars represent cells infected with MP-12, and black bars represent cells infected with ZH501. Error bars are \pm standard deviation and *, #, and + indicate $p < 0.05$ between mock/MP-12, mock/ZH501 or MP-12/ZH501, respectively. Cells were infected with a MOI of 1.

Cytokine response in primary macrophage cells

Current *in vitro* experiments have been performed in immortalized mouse macrophage and dendritic cells, due to their availability, ease of handling, and low cost. To determine if the cell lines are a suitable surrogate for primary immune-modulatory cells and if the host cell immune response displays similarities between the two cell

systems, experiments were also performed in mouse primary macrophage and dendritic cells. Immortalized cell lines potentially have an altered response when compared to the primary cells. LPS was used as a positive control to ensure that the primary cells were secreting the cytokine of interest, and cells responded strongly to LPS stimulation and secreted large amounts of the cytokines examined (Chia, Pollack *et al.* 1989; Pan, Kim *et al.* 2008; Yi, Bi *et al.* 2013).

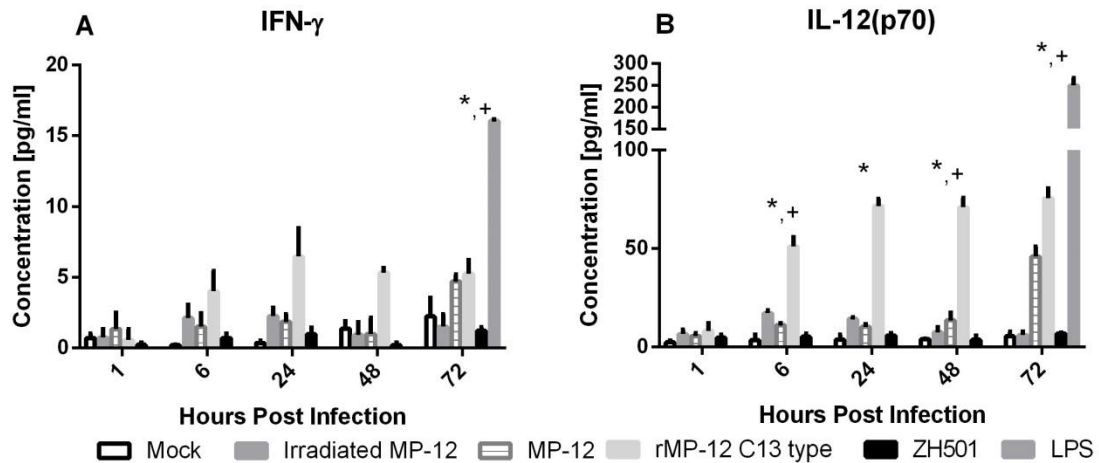


Figure 4.7. Th1 cytokines secreted by primary macrophages

Th1 cytokines secreted by primary BMD macrophage cells after infection with irradiated MP-12, live MP-12, rMP12-C13type and ZH501, or LPS stimulated. Cells were plated, allowed to rest for 24 hours, moved into the BSL-4, infected, and then harvested at the time point indicated. The LPS stimulated cells were only harvested at 72 HPI. Open bars represent mock-infected cells, medium gray bars represent cells infected with irradiated MP-12, gray striped bars represent cells infected with MP-12, light gray bars represent cells infected with rMP12-C13type, black bars represent cells infected with ZH501. Error bars are \pm standard deviation and *, #, and + indicate $p < 0.05$ between mock/MP-12, mock/ZH501 or MP-12/ZH501, respectively. Cells were infected with a MOI of 4.

Primary bone marrow-derived macrophages were infected with irradiated MP-12, and replication-competent MP-12, rMP12-C13type or ZH501 at two different MOIs (1 and 4). While the overall response was similar, cells infected with the higher MOI secreted cytokines sooner than those infected with the lower MOI. The cytokine panel used to evaluate RAW 264.7 and DC 2.4 cells to infection with RVFV was also used to

evaluate responses to infection in primary cells with the addition of interleukins (IL) -2, -3, -4, -5, -6, -7, -8, -9, and -10, eotaxin, G-CSF, and GM-CSF to better correlate the *in vitro* primary cell data with *in vivo* analysis performed in Specific Aim 3 (Chapter 5).

Results from infections with RVFV (MOI=1) in primary macrophages was not consistent with observations made in the macrophage cell line, RAW 264.7. While macrophages are not a typical source of IFN- γ *in vivo*, there were changes in the concentration of IFN- γ in the culture supernatant of infected BMD macrophages (Figure 4.7A). Similar to observations made with RAW 264.7 cells, there was no change in the concentration of secreted IFN- γ after infection with ZH501 except a decrease observed at 72 HPI. After infection with MP-12, IFN- γ levels increased to levels significantly higher (a 2-fold increase) than mock- and ZH501-infected cells at 72 HPI. There was also an increase in IFN- γ concentration after infection with rMP12-C13type virus that was detectable as early as 6 HPI. After infection with this naturally attenuated avirulent RVFV isolate, which is lacking 70% of the NSs gene, IFN- γ gradually began to increase and was significantly higher than other treatment groups beginning at 24 HPI. This is not surprising because the NSs gene has been shown to be the virulence factor for RVFV and is known to interfere with the host innate immune response by blocking the production of type I IFNs (Bouloy, Janzen *et al.* 2001; Billecocq, Spiegel *et al.* 2004; Ikegami, Narayanan *et al.* 2009; Ikegami, Narayanan *et al.* 2009; Kalveram, Lihoradova *et al.* 2011; Kalveram, Lihoradova *et al.* 2013). It is possible that NSs also has functions in blocking IFN- γ that have yet to be elucidated. Therefore, the lack of NSs in the rMP12-C13type virus would explain the increase in IFN- γ .

Changes in IL-12(p70) (Figure 4.7B) and IL-12(p40) (data not shown) concentration mirrored those observed for IFN- γ . While there was no change in concentration of IL-12 after ZH501 infection when compared to mock-infected cells, there was a significant decrease in IL-12 secretion after ZH501 infection when compared to MP-12-infected cells. There was also an 8.5-fold increase in the amount of IL-12

detected 72 hours after MP-12 infection. As expected, since rMP-12-C13type infection caused an increase in the secretion of IFN- γ , IL-12(p70) increased rapidly after rMP12-C13type infection. There were significantly higher amounts of IL-12(p70) and IL-12(p40) being detected beginning at 6 HPI and 24 HPI, respectively, and lasting throughout the remainder of the experiment.

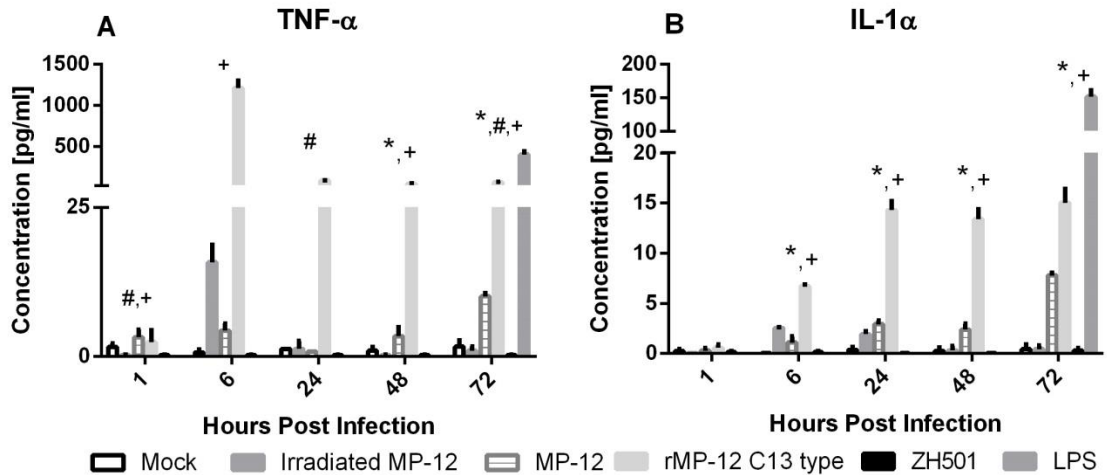


Figure 4.8. TNF α secreted by primary macrophages

TNF α secreted by primary BMD macrophage cells after infection with irradiated MP-12, live MP-12, rMP12-C13type and ZH501, or LPS stimulated. Cells were plated, allowed to rest for 24 hours, moved into the BSL-4, infected, and then harvested at the time point indicated. The LPS stimulated cells were only harvested at 72 HPI. Open bars represent mock-infected cells, medium gray bars represent cells infected with irradiated MP-12, gray striped bars represent cells infected with MP-12, light gray bars represent cells infected with rMP12-C13type, black bars represent cells infected with ZH501. Error bars are \pm standard deviation and *, #, and + indicate $p < 0.05$ between mock/MP-12, mock/ZH501 or MP-12/ZH501, respectively. Cells were infected with a MOI of 4.

TNF α concentration in primary macrophage cells seemed to increase slightly at 6 HPI following stimulation with irradiated MP-12 (Figure 4.8A). No additional changes in the concentration of TNF α after infection with irradiated MP-12 or ZH501 were observed. After rMP12-C13type infection, TNF α increased during infection beginning at 6 HPI, when the concentration of secreted TNF α peaked, and remained elevated

throughout the course of the experiment. TNF α was only significantly elevated 72 hours after MP-12 infection.

The concentration of IL-1 α did not change in the macrophages after infection with ZH501 (Figure 4.8B). Similar to what was observed in regards to the concentration of TNF α , there is only a change in IL-1 α concentration at 6 HPI with irradiated MP-12. After infection with rMP12-C13type, the amount of IL-1 α detected in the culture supernatant of macrophage cells increased sharply at 6 HPI (>100 fold increase when compared to mock-infected cells) and remained elevated until the termination of the experiment at 72 HPI (a 35-fold increase above mock is seen). MP-12 did cause a significant increase in IL-1 α secretion during all time points examined except 1 HPI.

The chemokines KC (IL-8), RANTES, MIP-1 α , MIP-1 β , and MCP-1 all increased after infection with rMP12-C13type (Figure 4.9A-D). The concentration of the chemokines examined was significantly higher after rMP12-C13type infection when compared to other infection groups beginning as early as 6 HPI. The concentration of RANTES (Figure 4.9A) and MCP-1 (Figure 4.9B) increased significantly once the macrophages were infected with rMP12-C13type when compared to mock-infected samples. Of interest is the lack of increase of RANTES and MCP-1 early during the course of MP-12 infection, but elevated levels of RANTES and MCP-1 could be detected at 24, 48, and 72 HPI. At 24 hours after infection with irradiated MP-12, even more of these chemokines were secreted when compared to MP-12 infection. RANTES levels were three times higher and MCP-1 levels were two times higher after infection with irradiated MP-12. The same amount of RANTES that secreted into the supernatant at 72 hours after MP-12 infection was also secreted after infection with irradiated MP-12. The increase in both RANTES and MCP-1 secreted after irradiated MP-12 or MP-12 infection (MOI=4) was significant when compared to mock-infected cells. MIP1 α (Figure 4.9C) and MIP1 β (data not shown) did not increase until 72 hours after MP-12 infection. KC (IL-8) values began to increase early after MP-12 infection (6 HPI) and were higher

compared to mock-infected samples throughout the course of the experiment but the values were not significantly elevated in comparison to irradiated MP-12 until 48 HPI (Figure 4.9D).

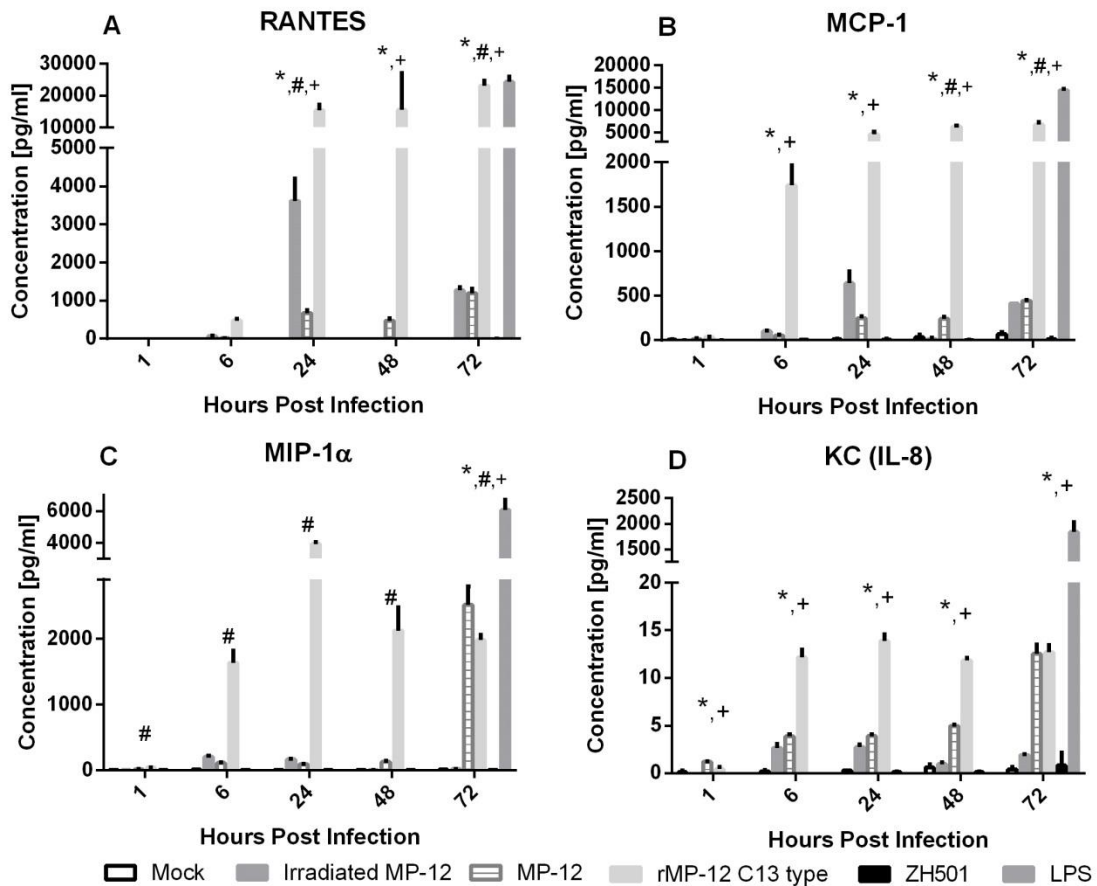


Figure 4.9. Cytokines secreted by primary macrophages

Chemokines secreted by primary BMD macrophage cells after infection with irradiated MP-12, live MP-12, rMP12-C13type and ZH501, or LPS stimulated. Cells were plated, allowed to rest for 24 hours, moved into the BSL-4, infected, and then harvested at the time point indicated. The LPS stimulated cells were only harvested at 72 HPI. Open bars represent mock-infected cells, medium gray bars represent cells infected with irradiated MP-12, gray striped bars represent cells infected with MP-12, light gray bars represent cells infected with rMP12-C13type, black bars represent cells infected with ZH501. Error bars are \pm standard deviation and *, #, and + indicate $p < 0.05$ between mock/MP-12, mock/ZH501 or MP-12/ZH501, respectively. Cells were infected with a MOI of 4.

Both G-CSF (Figure 4.10A) and GM-CSF (Figure 4.10B) levels increased after infection with rMP12-C13type at the later stages of infection (≥ 6 HPI). These levels were significantly higher than all other infection groups with the exception of samples taken after infection with MP-12 at 72 HPI. At that time, the cells that were infected with MP-12 resulted in increased amounts of released G-CSF and GM-CSF.

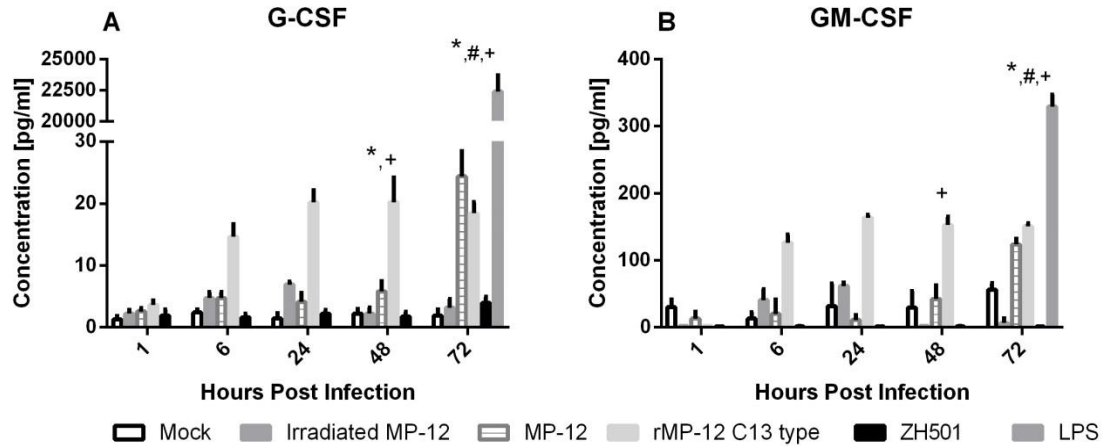


Figure 4.10. G-CSF and GM-CSF secreted by primary macrophages

G-CSF and GM-CSF secreted by primary BMD macrophage cells after infection with irradiated MP-12, live MP-12, rMP12-C13type and ZH501, or LPS stimulated. Cells were plated, allowed to rest for 24 hours, moved into the BSL-4, infected, and then harvested at the time point indicated. The LPS stimulated cells were only harvested at 72 HPI. Open bars represent mock-infected cells, medium gray bars represent cells infected with irradiated MP-12, gray striped bars represent cells infected with MP-12, light gray bars represent cells infected with rMP12-C13type, black bars represent cells infected with ZH501. Error bars are \pm standard deviation and *, #, and + indicate $p < 0.05$ between mock/MP-12, mock/ZH501 or MP-12/ZH501, respectively. Cells were infected with a MOI of 4.

The concentration changes of IL-6 (Figure 4.11A) and IL-10 (Figure 4.11B) after infection with RVFV were similar to each other. While IL-6 concentration increased significantly after infection with rMP12-C13type when compared to all other infection groups, IL-10 concentration was significantly elevated after rMP12-C13type infection compared to the other infection groups until 72 HPI. At 72 HPI, the concentration of IL-10 drastically increased after MP-12 infection and was significantly higher than all other

groups at the same time point after infection, including rMP12-C13type. IL-6 concentration after infection with irradiated MP-12 and MP-12 was higher than mock- and ZH501-infected samples starting at 6 HPI.

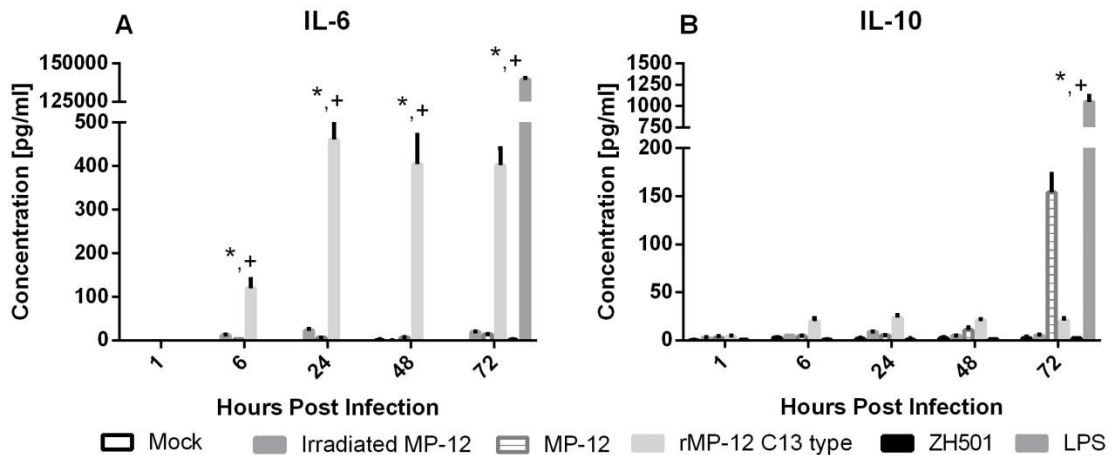


Figure 4.11. Pro/Anti-inflammatory cytokines secreted by primary macrophages

Pro/Anti-inflammatory cytokines secreted by primary BMD macrophage cells after infection with irradiated MP-12, live MP-12, rMP12-C13type and ZH501, or LPS stimulated. Cells were plated, allowed to rest for 24 hours, moved into the BSL-4, infected, and then harvested at the time point indicated. The LPS stimulated cells were only harvested at 72 HPI. Open bars represent mock-infected cells, medium gray bars represent cells infected with irradiated MP-12, gray striped bars represent cells infected with MP-12, light gray bars represent cells infected with rMP12-C13type, black bars represent cells infected with ZH501. Error bars are \pm standard deviation and *, #, and + indicate $p < 0.05$ between mock/MP-12, mock/ZH501 or MP-12/ZH501, respectively. Cells were infected with a MOI of 4.

Various other interleukins (IL-2, -3, -4, -5, and -9) were examined as well. The profiles of IL-2 and IL-9 showed no specific trend and values were not sufficiently consistent to predict any specific type of host response (data not shown). The concentrations of IL-3 (Figure 4.12A), IL-4 (Figure 4.12B), and IL-5 (Figure 4.12C) all had similar profiles. Starting 6 hours after rMP12-C13type infection, the concentrations of these 3 cytokines were significantly elevated and remained elevated throughout the course of the infection. While the concentrations after MP-12 infection were slightly higher, they were not as significantly increased until 6 HPI with IL-3 and IL-4. ZH501-

infected samples did not show any change in concentration after infection, but cells infected with irradiated MP-12 did secrete more of these cytokines compared to mock-infected cells even though the values were not significant.

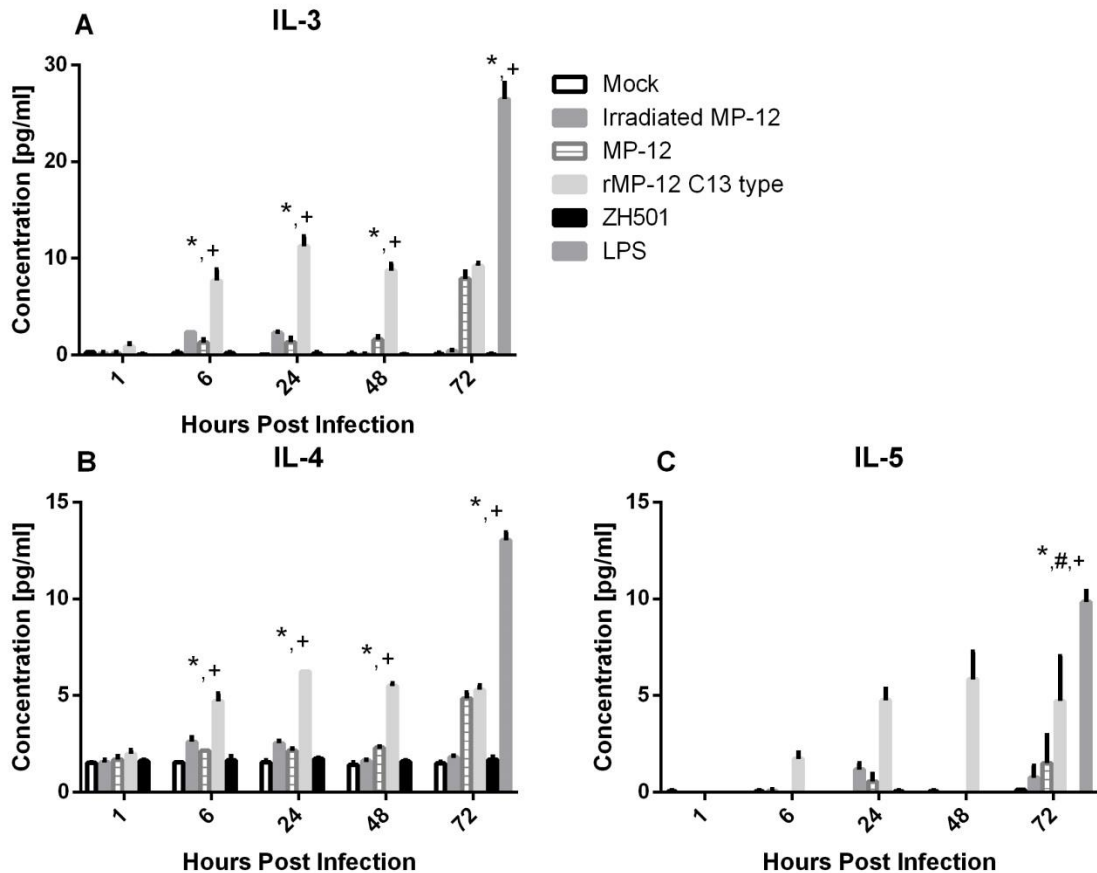


Figure 4.12. Interleukins secreted by primary macrophage cells

Interleukins secreted by primary BMD macrophage cells after infection with irradiated MP-12, MP-12, rMP12-C13type, or ZH501 or stimulated with LPS. Cells were plated, allowed to rest for 24 hours, moved into the BSL-4, infected, and then harvested at the time point indicated. The LPS stimulated cells were only harvested at 72 HPI. Open bars represent mock-infected cells, medium gray bars represent cells infected with irradiated MP-12, gray striped bars represent cells infected with MP-12, light gray bars represent cells infected with rMP12-C13type, black bars represent cells infected with ZH501. Error bars are \pm standard deviation and *, #, and + indicate $p < 0.05$ between mock/MP-12, mock/ZH501 or MP-12/ZH501, respectively. Cells were infected with a MOI of 4.

Cytokine response in primary BMD DCs

The Murine BMD DCs that I obtained did not appear to support productive infection by RVFV. Several attempts were made to infect DCs, but no attempt resulted in detection of active viral replication. The lack of viral replication was indicated by a constant and not increasing virus titer over the course of the experiment (Chapter 3; Figure 4.8), no apparent CPE present after infection (Chapter 3; Figure 4.9) and no obvious signaling pathway activation. Since there seemed to be no productive infection, the cytokine response in primary BMD dendritic cells was not examined further.

DISCUSSION

Currently, only a few studies have been published describing the detailed characterization of the cytokine and chemokine secretion after RVFV infection. None of these recently published studies have examined more than a few cytokines and their specific interactions with other cytokines and proteins (McElroy and Nichol 2012; Smith, Bird *et al.* 2012). The objective of this study was to achieve a more detailed overview of the general host immune response from immunomodulatory cells following RVFV infection by examining a comprehensive panel of cytokines and chemokines. In attempts of identifying a difference in the host response to virulent and non-virulent strains of the virus, cells were infected with a live and replicating vaccine strain of RVFV (MP-12), a replication-deficient vaccine strain (γ -irradiated MP-12), a recombinant MP-12 that resembled a naturally occurring attenuated avirulent isolate (rMP12-C13type), or with pathogenic ZH501.

IFNs are considered the antiviral cytokines because their activity leads to inhibition of viral replication and they induce a number of antiviral proteins, such as PKR, RNaseL, MxA, OAS-1, OAS-2, IL-6, MCP-1, and RANTES which could lead to resistance to viral infection (Milstone and Waksman 1970; Hayashi and Koike 1989; Shirazi and Pitha 1992; Lin, Kwong *et al.* 2004; Dash, Prabhu *et al.* 2005; Konishi,

Okamoto *et al.* 2012). IFNs bind to their receptors and then cause self-phosphorylation of STAT proteins inside the cell. The STAT proteins move into the nucleus and then bind to DNA to activate the transcription of antiviral genes. If an organism cannot produce and utilize IFN properly, it is generally very susceptible to viral infection. The secretion of the Th1 cytokines IFN- γ and IL-12 is inhibited during infection with MP-12 or ZH501 in RAW 264.7 and DC 2.4 cells, but this inhibition is not observed in primary BMD macrophage cells that are infected with rMP12-C13type or MP-12. Analyzed data collected from experiments performed in cell lines, indicate that RVFV vaccine strain MP-12 and ZH501 down regulate the immune response. However, in primary cells, the picture seems to be a little different. It appears that there is a delayed IFN- γ response after MP-12 infection in primary BMD macrophages that is important in viral clearance. IFN- γ has a synergistic response with IL-12(p70) to promote the proliferation of Th1 cells. The IFN- γ response in murine cells points towards a decrease in the Th1 cell response that would occur after ZH501 infection. The decrease in proliferation is seen soon after infection with MP-12, but it appears that the cells recover and begin to produce Th1 cytokines (IFN- γ and IL-12(p70)). These cytokines drive the cells toward a Th1 response starting at 72 HPI.

These two cytokines (IFN- γ and IL-12(p70)) could be the key in understanding the differences that are observed when these viruses infect living organisms. No difference could be detected in the cytokine response between mock and MP-12-infected primary macrophage cells until 72 HPI. The data suggest that there is a delay in the IFN response after MP-12 infection in comparison to rMP12-C13type-infection, while no response can be detected after infection with ZH501 infection. The small amount of IFN- γ produced by the primary macrophage cells after MP-12 and rMP12-C13 type viral infection could be the determining factor between viral attenuation and fatal infection. This could be what is needed to begin an immune response that will clear the virus.

I observed that TNF α , which works synergistically with IFN- γ (Feduchi, Alonso *et al.* 1989), increases in concentration 72 hours after infection with MP-12 in primary macrophage cells. TNF α mediates inflammatory and immune functions by manipulation of JNK, p38 MAPK, and NF- κ B pathways and IFN synthesis (Karin and Gallagher 2005; Karin and Greten 2005; Kant, Swat *et al.* 2011). Just as others have observed (McElroy and Nichol 2012), I detected an increase in TNF α secretion 24 HPI with virus that is lacking the NSs protein in primary macrophage cells. The increase of TNF α after rMP12-C13type infection seems to indicate that pro-inflammatory and pro-apoptotic pathways are activated after infection. The lack of TNF α secretion after ZH501 infection can likely be due to, at least partially, the activity of NSs since there was no TNF α response after MP-12 (which has an intact NSs protein) infection until very late time points, but an increased TNF α response could be detected after infection with rMP12-C13type. This decrease in TNF α secretion could also be due to the decrease in cell signaling that is seen after ZH501 infection. It has been shown that TNF α stimulation of cells with suppressed transcription or translation suppresses apoptosis (Aggarwal, Kohr *et al.* 1985; Sugarman, Aggarwal *et al.* 1985). While NSm has been shown to suppress apoptosis by suppressing the cleavage and thereby activation of caspase-3 and caspase-8 (Won, Ikegami *et al.* 2007), an inhibition of TNF α secretion early in infection by NSs could have a synergistic effect with NSm on blocking apoptosis since TNF α induces apoptosis through the caspase cascade.

The majority of newly assembled infectious MP-12 virions is released within the first 24 hours after infection (at MOI 1 or higher) (Ikegami, Won *et al.* 2006; Won, Ikegami *et al.* 2006; Won, Ikegami *et al.* 2007), and apparently occurs before the appearance of the first wave of cytokines. Only the cells infected with rMP12-C13type are secreting cytokines (IFN- γ , TNF α , IL-1 α , IL-8, IL-4, IL-5, IL-6, IL-10, IL-12, MCP-1, MIP-1 α , G-CSF, and GM-CSF) at less than 24 hours after infection in primary macrophage cells. The responses seen in other cytokines can be a reflection of the many

pathways that are activated by TNF α . My data suggest that the cytokine response in macrophages is significantly delayed or even suppressed at the translational level due to presence of the RVFV virulence factor NSs.

The chemokines IL-1 α , RANTES, MCP-1, and MIP-1 α all play important roles in cellular recruitment and trafficking. My data suggest that the recruitment of immune cells such as macrophages and T-cells may be severely restricted by ZH501-infected macrophages; however, without further investigation, it is not clear that recruitment is limited in DCs as they did not appear to be infected. It is possible that RVFV utilizes DCs as a means of transport, similarly to what has been observed in other viral infections in regards to macrophages (Koenig, Gendelman *et al.* 1986; Medeot, Contigiani *et al.* 1995; Miagostovich, Ramos *et al.* 1997; Gras and Kaul 2010; Mathieu, Pohl *et al.* 2011). It is also possible that the expression level of the homologue of the phlebovirus cellular receptor DC-SIGN (DC-SIGNR3) is lower in mouse bone marrow-derived DCs due to the activation status (mature versus immature) of the DC (Lozach, Kuhbacher *et al.* 2011) and needs to be evaluated in future studies. The presentation to naïve T-cells by DCs appears not to be inhibited by RVFV, because the DCs are not infected. It appears that the recruitment of activated macrophages to sites of infection is restricted due to the lack of chemokines released after MP-12 and ZH501 infection. Chemokines examined to date do not exhibit an increased expression in primary macrophage cells after ZH501 infection and these chemokines have a severely delayed release in cells infected with MP-12.

In summary, *in vitro* infection studies performed in mouse primary macrophages indicate that both, MP-12 and ZH501, inhibit chemokine secretion, and that ZH501 does so more efficiently. The cytokine response to rMP12-C13 type infection is elevated quickly after infection and remains that way throughout the experiment. Since studies have shown that virus lacking NSs provides protection in mice (Gowen, Bailey *et al.* 2013), the increase in cytokines I saw in primary macrophages, may be beneficial to the host. Activated macrophages are important in combating infection. Both MP-12 and

rMP12-C13 type viruses appear that they would be viable vaccine candidates. Furthermore, it appears that immortalized mouse dendritic cells and macrophages are not a sufficient cell culture system to study host cellular cytokine secretion after RVFV infection, since gained data are in stark contrast to the data collected from primary cell experiments.

Chapter 5 Chemotactic and Inflammatory Responses in the Liver and Brain are associated with Pathogenesis of Rift Valley Fever Virus Infection in the Mouse⁴

Specific Aim 3: Identify a panel of cytokines whose secretion is affected following infection *in vivo* with wild type RVFV or MP-12.

Hypothesis: ZH501 will induce a stronger anti-viral and pro-inflammatory response *in vivo* than MP-12.

Mice that were infected with ZH501 displayed higher levels of cytokines (Gray, Worthy *et al.* 2012) and pathology (primarily hepatitis, in a small percentage secondary encephalitis) that is typical of RVFV infection (Mims 1956; Flick and Bouloy 2005; Ikegami and Makino 2009; Bhardwaj, Heise *et al.* 2010; Mandell, Koukuntla *et al.* 2010; Smith, Steele *et al.* 2010; Ross, Bhardwaj *et al.* 2012). These mice indicate that there is a delicate balance between the immune response and viral clearance. The more subtle immune response seen after MP-12 infection apparently controlled viral replication and therefore cleared the virus without causing any fatal outcome.

Rationale: While some studies have analyzed only selected cytokines after RVFV infection and others examined the pathology after infection, no study has been performed characterizing both in the same animal model after RVFV infection. Here the goal was to describe the cytokine response and to correlate that response to the clinical and pathological finding following RVFV infection in the C57BL/6 mouse model.

RVFV is virulent in many different animal species, with mice being highly susceptible to infection (Ross, Bhardwaj *et al.* 2012). Currently, there is no detailed

⁴ The majority of this chapter, including figures, has been previously published. K. K. Gray, M. N. Worthy, *et al.* (2012). "Chemotactic and inflammatory responses in the liver and brain are associated with pathogenesis of Rift Valley fever virus infection in the mouse." *PLoS Negl Trop Dis* 6(2): e1529

understanding of the host immune response and how it relates to pathogenesis. While infection with MP-12 does not cause lethal disease in immune-competent mice, wild type RVFV generally results in up to 100% mortality in BALB/c, C57BL/6, and CD-1 mice within 3-5 days of infection (LD50 <10 PFU) (Bouloy, Janzen *et al.* 2001; Morrill, Ikegami *et al.* 2010; Smith, Bird *et al.* 2012). A study by Smith *et al.* examined pathogenesis in BALB/c mice following subcutaneous challenge with 1,000 PFU of wild type ZH501, focusing on viral titers in tissues, types of infected cells and histopathological changes during infection (Smith, Steele *et al.* 2010; Reed, Steele *et al.* 2012). While this study examined clinical parameters, it did not analyze the host immune response and relate that response to the in-depth discussion of the pathogenesis that was observed in the BALB/c mouse model. Recently, MBT/Pas inbred mice were shown to be more susceptible to RVFV than the traditionally used inbred laboratory strains BALB/cByJ and C57BL/6J. It is believed that this higher susceptibility is because the mice do not mount a proper innate immune response (do Valle, Billecocq *et al.* 2010). I chose to study C57BL/6 mice as this strain is biased toward a Th-1, or cell-mediated, immune response which is more typical in limiting viral infection (Heinzel, Sadick *et al.* 1989; Locksley, Heinzel *et al.* 1991; von Stebut, Belkaid *et al.* 2000; Gemmell, Winning *et al.* 2003; Pinto, de Mello Cortezia *et al.* 2003; Ritchie, Yam *et al.* 2003; Misslitz, Bonhagen *et al.* 2004).

As anticipated, I found that there was a marked difference between the host response to infection with wild type RVFV and the attenuated MP-12 vaccine strain. While neither virus caused overt changes in body weight or temperature, changes in the clinical parameters measured were more profound in animals infected with wild type virus than with the vaccine strain. Histopathologic lesions from animals infected with the wild type virus were more severe than MP-12-infected animals, including a large amount of necrosis in the liver which correlated with the presence of viral antigen. Furthermore, there was a significant cytokine response in wild type virus-infected animals in all organs

examined [liver, spleen, and the brain]; whereas the only significant changes detected in MP-12-infected animals were, surprisingly, in the brain. An increased cytokine response could also be correlated to histological changes observed in the organs of ZH501-infected animals versus those infected with MP-12. These studies suggest that the pathogenicity caused by RVFV infections in the mouse model is driven primarily by an unregulated host inflammatory response, which results in significant loss of liver function and development of neurologic disease.

RESULTS

Clinical observations

To assess the onset of illness with the host response, serum, liver, spleen, and brain were harvested from groups of 5 mice every 12 hours after virus inoculation and various different parameters were measured. As anticipated, MP-12-infected mice showed no signs of clinical disease and all survived until sacrificed. ZH501-infected mice began to develop signs of illness (i.e. ruffled fur and hunched posture) as early as 36 HPI and all infected mice showed signs of clinical illness and succumbed to disease. Of the subset of ZH501-infected animals monitored daily for their weight and body temperature, 85% were alive on day 2, while 30% survived to day 3, and all were dead at day 4 post infection (Figure 5.1). All animals in the monitored MP-12-infected group survived through completion of the study or sacrifice. Even though human disease is characterized by fever, during the course of the experiment, none of the mice became febrile or lost a significant amount of weight (Figure 5.2 A and B). While in some studies, mice lose weight, the studies I have seen did not examine fever in the mouse model.

Complete Blood Counts (CBCs)

CBCs are an important diagnostic and prognostic tool for determining overall clinical health and a reliable measure of multiple indices of whole blood components. CBCs were performed in this study to determine the utility of the parameters measured in assessing the health of mice during RVFV infections. Whole blood from animals that were either MP-12-, ZH501-, or mock-infected was collected by terminal cardiac puncture. Overall, no significant difference in the total white blood cell (WBC) count between mock- and MP-12-infected mice was observed for any of the measured parameters (Figure 5.3A and Table 1). The CBCs of ZH501-infected animals were not remarkably different from MP-12- or mock- infected animals until 60 HPI. A two-fold drop in total WBC count after ZH501 infection was observed at 60 and 72 HPI, but recovered to levels of uninfected controls 84 and 96 HPI. The only time point where the decrease of WBC was statistically significant relative to mock was at 72 HPI when there was a three-fold drop in ZH501-infected mice. A similar trend was observed for lymphocytes and monocytes (Figure 5.3B and Table 1). No significant difference was detected between the three challenge groups at any point of infection except at 72 HPI where the number of cells was lower in ZH501-infected animals than in the other two groups. Lymphocytes in ZH501-infected mice were almost 15- and 10-fold lower when compared to mock and MP-12-infected animals, respectively. At 96 HPI the concentration of monocytes in ZH501-infected animals was elevated relative to both mock and MP-12-infected animals, but the difference was not significant. Eosinophils only showed a change at 96 HPI after ZH501 infection where there were five times as many eosinophils circulating in the blood. The neutrophil population did not deviate significantly between the three treatments during the course of the experiment (Table 1).

Red blood cell (RBC) populations were largely the same between all three challenge groups (Figure 5.3C and Table 1). However, at 24 HPI the RBC concentration

in MP-12-infected animals was 1.5 times higher than in mock or ZH501-infected mice while at 72 HPI, ZH501-infected animals had a decreased RBC count (Figure 5.3C). Interestingly, the platelet count was within normal ranges (592-2,972 K/ul) for all groups until 72 HPI where the platelet concentration in ZH501-infected mice dropped well below normal and was 4 times lower than in mock or MP-12-infected mice (Figure 5.3D). There was a short temporal recovery to normal levels at 84 HPI, but then the level dropped to below normal values again at 96 HPI when mock and MP-12-infected mice displayed twice as many platelets as ZH501-infected mice.

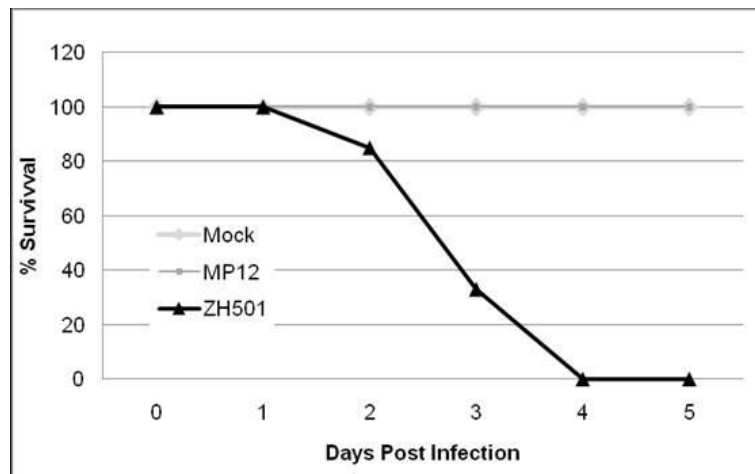


Figure 5.1. Mouse survival after RVFV infection

Percent survival of mice that were infected with 1000 PFU of vaccine strain MP-12 (square), wild type strain ZH501 (triangle) or were mock-infected (diamond). Of all animals included in this study, only three ZH501-infected animals survived to 96 HPI. All mock and MP-12-infected animals survived until euthanized for tissue collection.

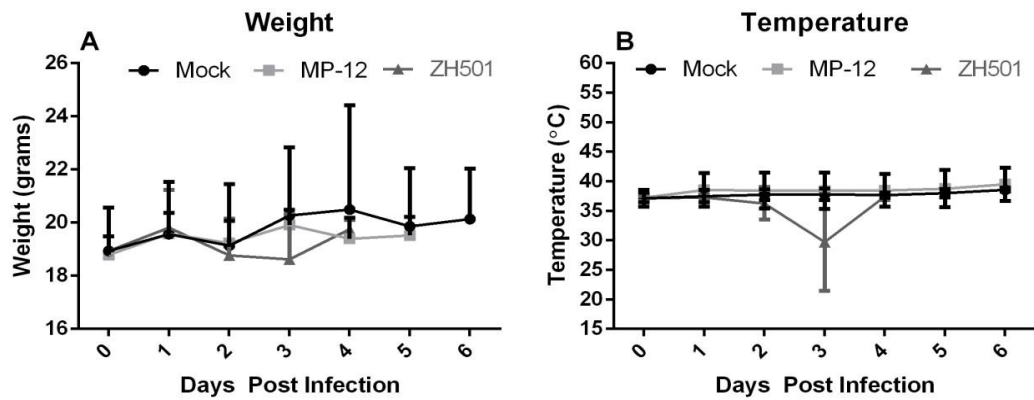


Figure 5.2. Mouse daily weight and temperature

(A) Daily weight (g) and (B) temperature (°C) of mock- (diamond), MP-12- (square) or ZH501-infected (triangle) C57BL/6.

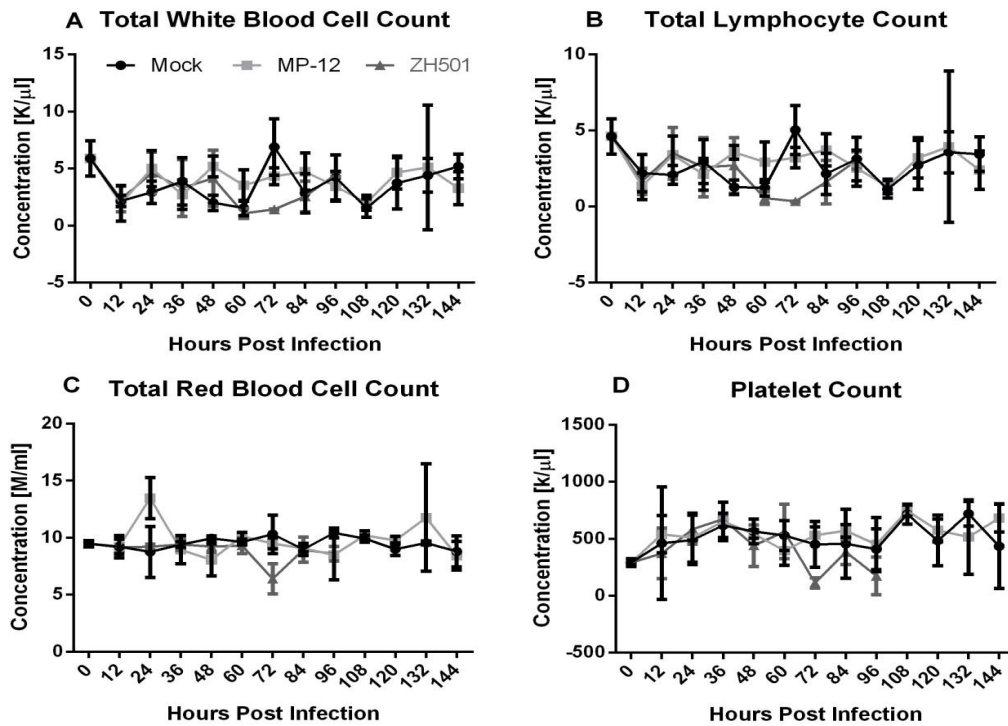


Figure 5.3. Hematology results

(A) Total white blood cell, (B) lymphocyte, (B) red blood cell and (C) platelet counts over the course of disease in mock- (closed diamond), MP-12- (closed square) or ZH501-infected (closed triangle) animals. Each data point represents the mean of 5 animals per group except at 96 HPI in the ZH501 group where only 3 animals remained.

Parameter	Normal Values	Hours Post Infection													
		0	12	24	36	48	60	72	84	96	108	120	132	144	
Mock (N=5)															
WBC (K/ μ l)	1.8 - 10.7	5.89 (1.5)	2.16 (0.5)	2.93 (0.9)	3.88 (2.1)	2.00 (0.7)	1.55 (0.7)	6.90 (2.4)	2.84 (1.7)	4.22 (1.9)	1.54 (0.8)	3.72 (2.3)	4.41 (1.5)	5.20 (1.1)	
LY (K/ μ l)	0.9 - 9.3	4.62 (1.2)	2.21 (1.2)	2.08 (0.6)	2.95 (1.5)	1.28 (0.5)	1.24 (0.6)	5.04 (1.6)	2.16 (1.4)	3.13 (1.4)	1.15 (0.6)	2.74 (1.6)	3.60 (1.4)	3.44 (1.1)	
MO (K/ μ l)	0.0 - 0.4	0.22 (0.07)	0.14 (0.02)	0.15 (0.1)	0.25 (0.2)	0.1 (0.07)	0.07 (0.02)	0.47 (0.4)	0.17 (0.1)	0.22 (0.1)	0.10 (0.07)	0.21 (0.2)	0.14 (0.02)	0.57 (0.4)	
EO (K/ μ l)	0.0 - 0.2	0.04 (0.03)	0.03 (0.04)	0.06 (0.1)	0.08 (0.07)	0.07 (0.06)	0.01 (0.01)	0.11 (0.04)	0.07 (0.06)	0.03 (0.02)	0.04 (0.03)	0.04 (0.04)	0.02 (0.01)	0.11 (0.05)	
NE (K/ μ l)	0.1 - 2.4	0.99 (0.4)	0.42 (0.1)	0.64 (0.3)	0.58 (0.4)	0.55 (0.1)	0.23 (0.1)	1.25 (0.5)	0.43 (0.3)	0.83 (0.4)	0.24 (0.1)	0.72 (0.6)	0.67 (0.1)	1.06 (0.3)	
RBC (M/ μ l)	6.36 - 9.42	9.47 (0.3)	9.22 (1.0)	8.76 (2.2)	9.39 (0.2)	9.95 (0.2)	9.62 (0.3)	10.3 (1.7)	8.97 (0.5)	10.43 (0.4)	9.92 (0.3)	8.99 (0.6)	9.55 (0.2)	8.79 (1.4)	
PLT (K/ μ l)	592 - 2972	291.33 (34.56)	460.50 (392.85)	488.75 (216.64)	618.00 (105.82)	564.75 (109.43)	529.60 (129.85)	452.25 (200.82)	455.20 (301.84)	408.60 (178.0)	716.20 (87.15)	484.20 (221.24)	719.00 (107.75)	434.20 (371.66)	
MP-12 (N=5)															
WBC (K/ μ l)			5.01 (1.6)	2.70 (1.3)	2.70 (1.3)	5.19 (0.9)	3.52# (1.4)	4.33 (0.7)	4.72 (1.6)	3.45 (1.3)	2.00 (0.7)	4.66 (1.5)	5.10 (5.5)	3.27 (1.4)	
LY (K/ μ l)			3.41 (1.2)	2.12 (1.1)	3.57 (0.5)	3.57 (0.5)	2.93 (1.3)	3.22 (0.7)	3.73 (1.1)	2.53 (1.2)	1.32 (0.5)	3.21 (1.3)	3.93 (4.9)	2.40 (1.3)	
MO (K/ μ l)			0.15 (0.13)	0.37 (0.21)	0.33 (0.3)	0.21 (0.04)	0.13# (0.04)	0.13 (0.04)	0.16 (0.06)	0.26 (0.1)	0.25 (0.1)	0.26 (0.1)	0.30 (0.2)	0.18 (0.1)	
EO (K/ μ l)			0.04 (0.07)	0.02 (0.07)	0.02 (0.03)	0.09 (0.07)	0.04 (0.05)	0.02# (0.01)	0.08 (0.04)	0.03 (0.04)	0.08 (0.07)	0.03 (0.02)	0.04 (0.03)	0.02 (0.03)	
NE (K/ μ l)			0.43 (0.4)	1.03 (0.2)	0.42 (0.2)	1.12 (0.4)	0.47# (0.1)	0.93 (0.3)	0.66 (0.5)	0.63 (0.2)	0.43 (0.2)	1.14 (0.3)	0.82 (0.6)	0.65 (0.1)	
RBC (M/ μ l)			9.24 (0.65)	13.48# (1.8)	8.94 (1.23)	8.05 (1.4)	10.13# (0.3)	9.50 (0.5)	9.07 (0.3)	8.50 (2.2)	10.21 (0.4)	9.76# (0.4)	11.76 (4.7)	8.41 (1.3)	
PLT (K/ μ l)			539.50 (164.1)	509.00 (215.0)	652.80 (170.3)	542.67 (37.3)	395.20 (129.5)	530.20 (76.4)	570.00 (55.8)	449.50 (238.4)	746.40 (50.82)	574.00 (100.4)	644.00 (178.3)	681.3 (121.9)	
ZH501 (N=5)*															
WBC (K/ μ l)			1.95 (1.6)	4.62# (1.8)	3.29 (2.5)	4.16 (2.5)	1.07 (0.4)	1.42 (0.1)	2.55 (1.3)	4.47 (0.2)					
LY (K/ μ l)			1.33 (0.9)	3.50# (1.7)	2.59 (1.9)	2.70 (1.8)	0.56# (0.4)	0.34 (0.03)	1.62 (1.4)	3.04 (0.6)					

MO	0.15	0.19	0.18	0.18	0.06	0.02	0.18	0.60
(K/ μ l)	(0.1)	(0.07)	(0.16)	(0.1)	(0.04)	(0.03)	(0.1)	(0.3)
EO	0.04	0.05	0.05	0.09	0.01	0.02	0.06	0.15
(K/ μ l)	(0.07)	(0.04)	(0.05)	(0.07)	(0.02)	(0.01)	(0.03)	(0.04)
NE	0.43	0.86	0.46	1.18	0.44	1.04	0.69	0.64
(K/ μ l)	(0.4)	(0.2)	(0.3)	(0.7)	(0.2)	(0.1)	(0.3)	(0.3)
RBC	9.24	9.21	9.41	9.22	9.31	6.39	8.95	8.59#
(M/ μ l)	(0.7)	(0.2)	(0.5)	(0.5)	(0.7)	(1.33)	(1.1)	(0.6)
PLT	539.50	584.40	672.75	440.20	563.20	112.00	383.80	174.00
(K/ μ l)	(164.1)	(132.0)	(37.0)	(183.0)	(239.4)	(43.8)	(109.8)	(165.8)

Table 5.1. Complete blood counts

Total white blood cell concentration (WBC), lymphocyte concentration (LY), monocyte concentration (MO), eosinophil concentration (EO), neutrophil concentration (NE), total red blood cell concentration (RBD) and platelet concentration (PLT) after mock, MP-12 or ZH501 infection. Each value is the average of 5 mice with the standard deviation (SD) below, except 96 HPI in the ZH501-infected mice which represent the average of the three surviving mice (SD). K/ μ l = 10³ cells/ μ l; M/ μ l = 10⁶ cells/ μ l. # indicates p<0.05 for that viral infection (MP-12 or ZH501) compared to mock-infected samples. *Note: n = 5 for all time points except 96 hours post ZH501 infection where n = 3

Plasma Chemistry

RVFV is known to be hepatotropic (McGavran and Easterday 1963) and to cause the release of liver specific enzymes from necrotic hepatocytes which can serve as clinical markers of hepatic dysfunction. Glucose and total bilirubin are also markers of liver function. Glucose production is one of the last functions of the liver to be lost as hepatocytes die and bilirubin increases with progressing degree of liver necrosis. In this study, serum liver enzyme concentrations became elevated in ZH501-infected mice as the disease progressed. Alanine aminotransferase (ALT) began to increase at 36 HPI and peaked in concentration at 60 HPI in ZH501-infected animals (Figure 5.4A). While normal values of ALT are between 17-77 U/L, at 36 HPI one mouse infected with ZH501 had ALT serum levels over 500 U/L, at 48 HPI one animal had levels of 1,300 U/L, and at 60 HPI two mice had over 1,500 U/L of ALT in their serum. No animals in the mock or MP-12-infected groups had an ALT concentration above 150 U/L (Figure 5.4A). Serum glucose levels dropped drastically in the ZH501-infected mice at 72 HPI (Figure 5.4B). Glucose levels in ZH501-infected mice began to increase at 84 HPI and were at higher than normal levels at 96 HPI. Total bilirubin was also elevated in ZH501-infected animals (Figure 5.4C). At 72 and 84 HPI, there was one mouse each in the ZH501-infected group that had elevated total bilirubin concentrations. Blood urea nitrogen (BUN) and creatinine levels are expected to increase in the serum with progressing kidney damage. BUN and creatinine levels were both elevated at 72 hours after ZH501 infection (data not shown). Creatinine levels in ZH501-infected mice dropped to similar levels as mock at 84 HPI and subsequently rose at 96 HPI. Analyzed plasma electrolytes (calcium, phosphorous, sodium, and potassium) did not show a significant deviation from normal concentrations (data not shown).

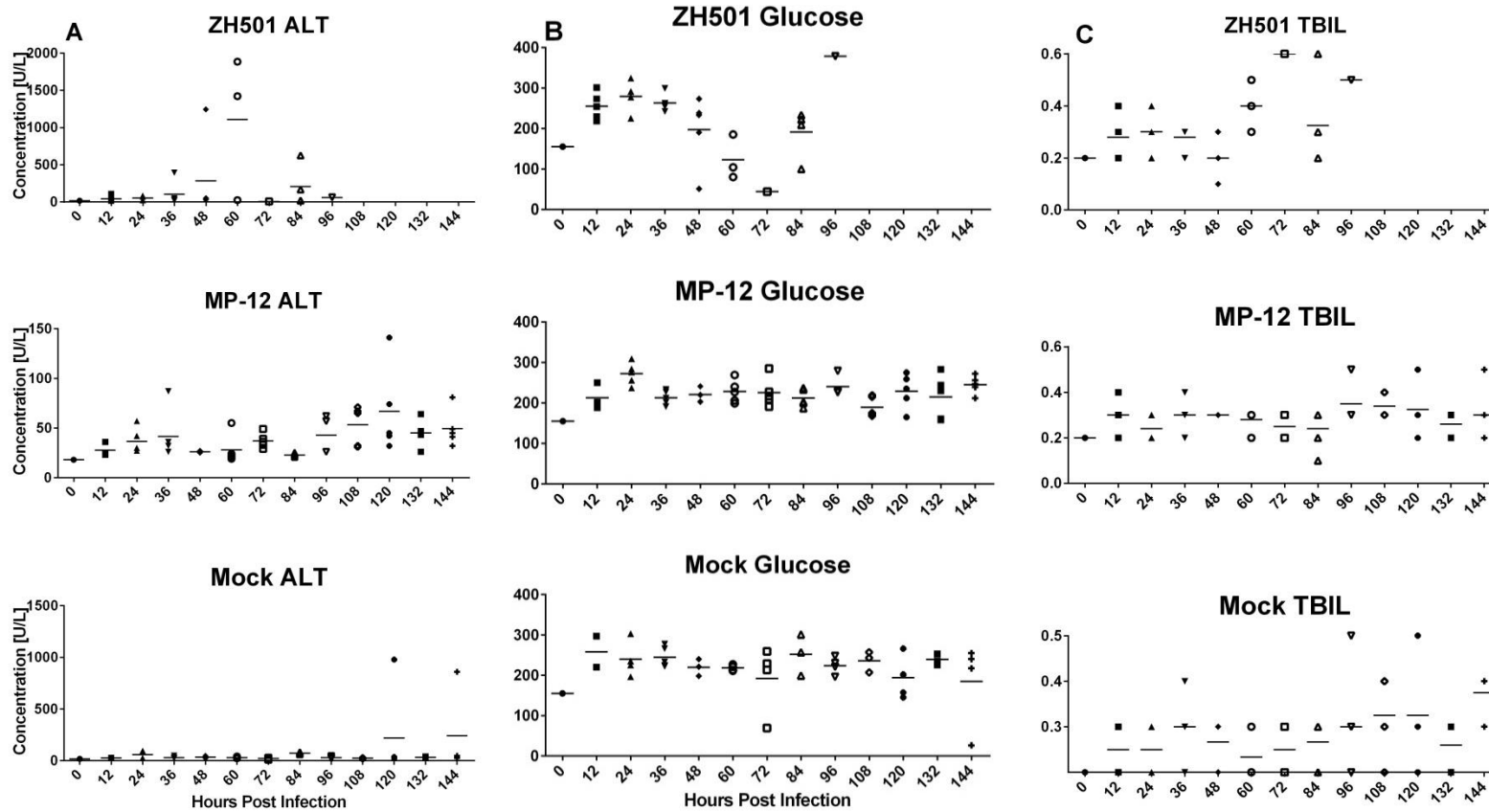


Figure 5.4. Liver function enzymes

Alanine aminotransferase (ALT) (A), glucose (B), and total bilirubin (TBIL) (C) concentrations in the serum of mock, MP-12, and ZH501-infected mice. Each symbol represents an individual mouse. There were five mice in each group, except at 96 HPI where only three animals had survived until this point of the study. The horizontal bar represents the average of the mice for that group.

Virus Distribution

To correlate the onset of illness with virus replication in different organs, tissues were harvested from groups of 5 mice every 12 hours and virus titers determined by plaque assay. ZH501 was detected at 24 HPI in the serum at 5 log₁₀ PFU/ml and peaked at 84 HPI with over 7 log₁₀ PFU/ml in the liver (Figure 5.5A). The points on the graph for serum and the liver represent at least 4 mice per time point, excluding 84 HPI where only 3 mice had positive ZH501 titers in the serum. In the spleen the peak viral titer was seen at 48 HPI where over 6 log₁₀ PFU/ml of virus was present. This is representative of only 1 mouse that had a positive viral titer. At all other time points, only 3 mice had ZH501 present in their spleens. While virus titers in the spleen drastically decreased, the titers in serum, liver, and brain remained elevated at 72 HPI. At each of the time points taken in the brain, only one mouse had positive viral titers. ZH501 titers peaked at 60 HPI in the brain and serum at 5 log₁₀ PFU/ml and 6 log₁₀ PFU/ml, respectively.

As observed in other animals, virus titers declined to undetectable levels after the initial phase of the disease (Smith, Steele *et al.* 2010; Kortekaas, Antonis *et al.* 2012; Nfon, Marszal *et al.* 2012; Smith, Bird *et al.* 2012) and plaque assay analysis of the serum, liver and brain in the three remaining animals sacrificed at 96 HPI showed no virus present (Figure 5.5A). MP-12-infected animals did not have any detectable virus in any tissue until they became viremic at 72 HPI with a peak titer of 2.5 log₁₀ PFU/ml. This peak in viremia was representative of 2 mice that had positive viral titers at this time point. The viremia was below detectable limits (~ 200 PFU) by 84 HPI. In the liver, virus appeared at 96 HPI when the viral load was just under 4 log₁₀ PFU/ml with a slight decrease in tissue titer at 108 HPI and was no longer detectable at 120 HPI. Each point of the graph that shows positive titers in the liver is representative of one mouse that had positive viral titers. MP-12 was not detected in the spleens or brains of infected mice at any point during the study (Figure 5.5B).

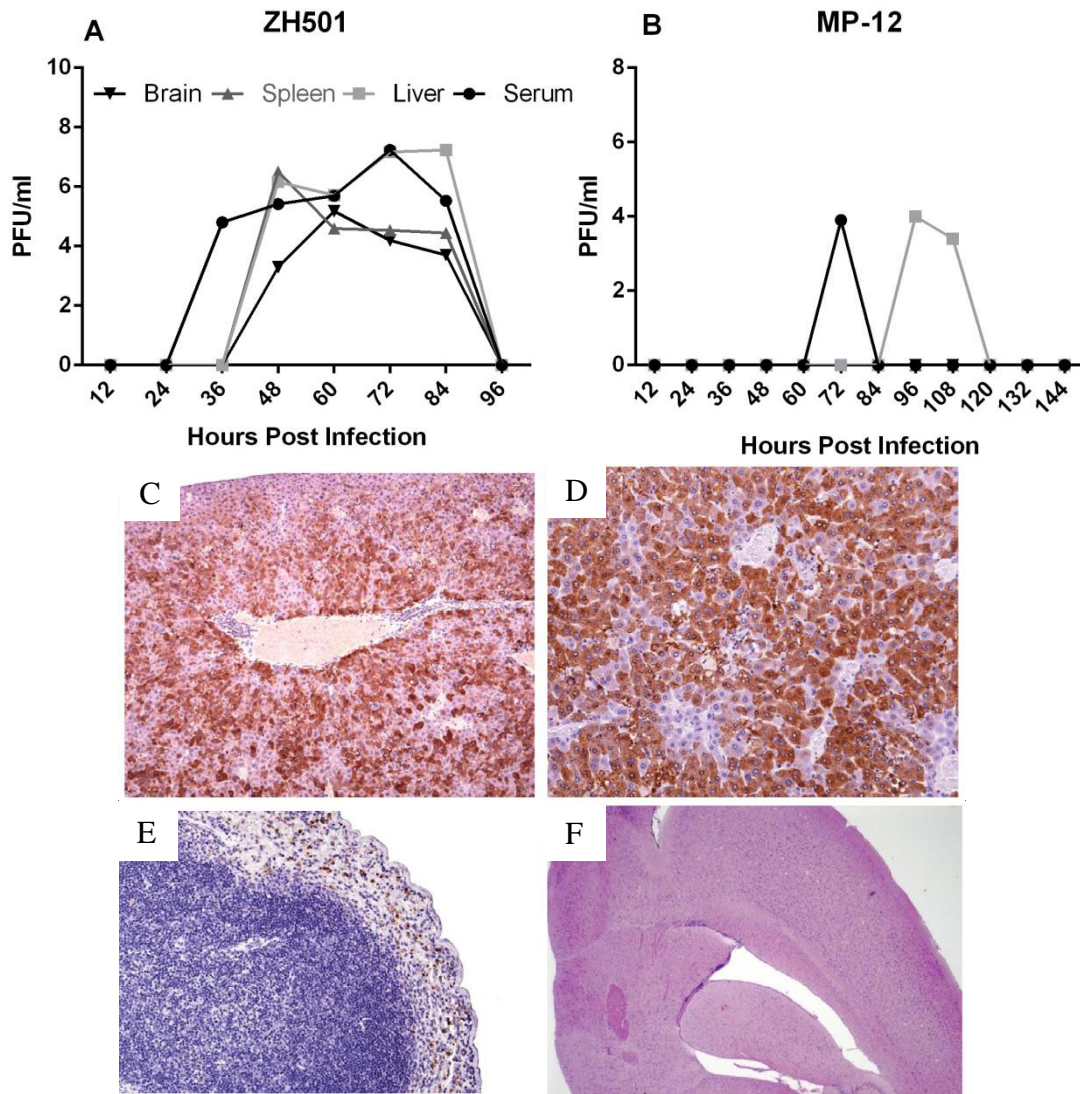


Figure 5.5. Viral Distribution

Viral titers in the serum, liver, spleen, and brain after infection with (A) ZH501 or (B) MP-12. (C) Immunohistochemical stain of liver from a ZH501-infected mouse at 60 HPI. Intracytoplasmic viral antigen is depicted by brown staining, 10X. (D) Immunohistochemical stain of liver from a ZH501-infected mouse at 84 HPI. Intracytoplasmic viral antigen is depicted by brown staining, 20X. (E) Immunohistochemical stain of spleen for RVFV antigen from a ZH501-infected mouse at 84 HPI. The red pulp sinusoids contain numerous cells with cytoplasmic brown, granular material depicting viral antigen. There are no viral antigen positive cells in the lymphoid follicle. Note the increased lymphocytolysis depicted by pyknotic nuclei and cellular fragments, 20X. (F) Brain from a ZH501-infected animal at 84 HPI with no pathologic changes, H&E 2.5X.

Immunohistochemical stains for RVFV antigen in formalin-fixed tissues collected from the three study groups were examined microscopically (Figure 5.5C-F). Seven out of a total of 11 MP-12-infected mice analyzed, had no viral antigen in their livers, spleens, or brains; while four mice had occasional antigen-positive cells in splenic red pulp sinusoids and white pulp lymphoid follicles (data not shown). One MP-12-infected animal exhibited cytoplasmic antigen staining in small numbers of cells within multiple hepatic microgranulomas. Seven out of eight ZH501-infected mice sacrificed from 48 to 84 HPI exhibited diffuse granular cytoplasmic viral antigen staining in most hepatocytes (from 75% to 95% of cells affected) (Figure 5.5C and D). While two out of eight ZH501-infected animals had no splenic viral antigen staining, up to 5% of the cells in splenic red pulp sinusoids and white pulp lymphoid follicles in the other six animals contained cytoplasmic viral antigen (Figure 5.5E). Viral antigen was not detected in brain (Figure 5.5F) or spinal cord (data not shown) sections in any mouse from any infection group. While viral antigen has been detected as early as 5 DPI, (Smith, Steele *et al.* 2010; Reed, Steele *et al.* 2012), encephalitis in the mouse model is usually detected more than 10 days after infection if the mouse survives the hepatitis that ZH501 causes (Reed, Steele *et al.* 2012).

Cytokine Profiles

RVFV infection is known to cause a number of pathogenic effects such as liver necrosis and encephalitis that could be correlated with the host immune response to infection. In order to identify potential mechanisms of pathogenesis during RVFV infection, I examined the cytokine response in three major organs (spleen, liver, brain) and the serum. These organs were selected because the spleen plays an important role in the host immune response, RVFV is hepatotropic (McGavran and Easterday 1963) and in some cases causes encephalitis (Maar, Swanepoel *et al.* 1979). The results from these experiments found that wild type ZH501 caused a significant cytokine response in all of

the organs examined compared to MP-12. The responses for each organ are summarized below. Individual graphs for a representative subset of the cytokines examined are shown in Figures 6-9.

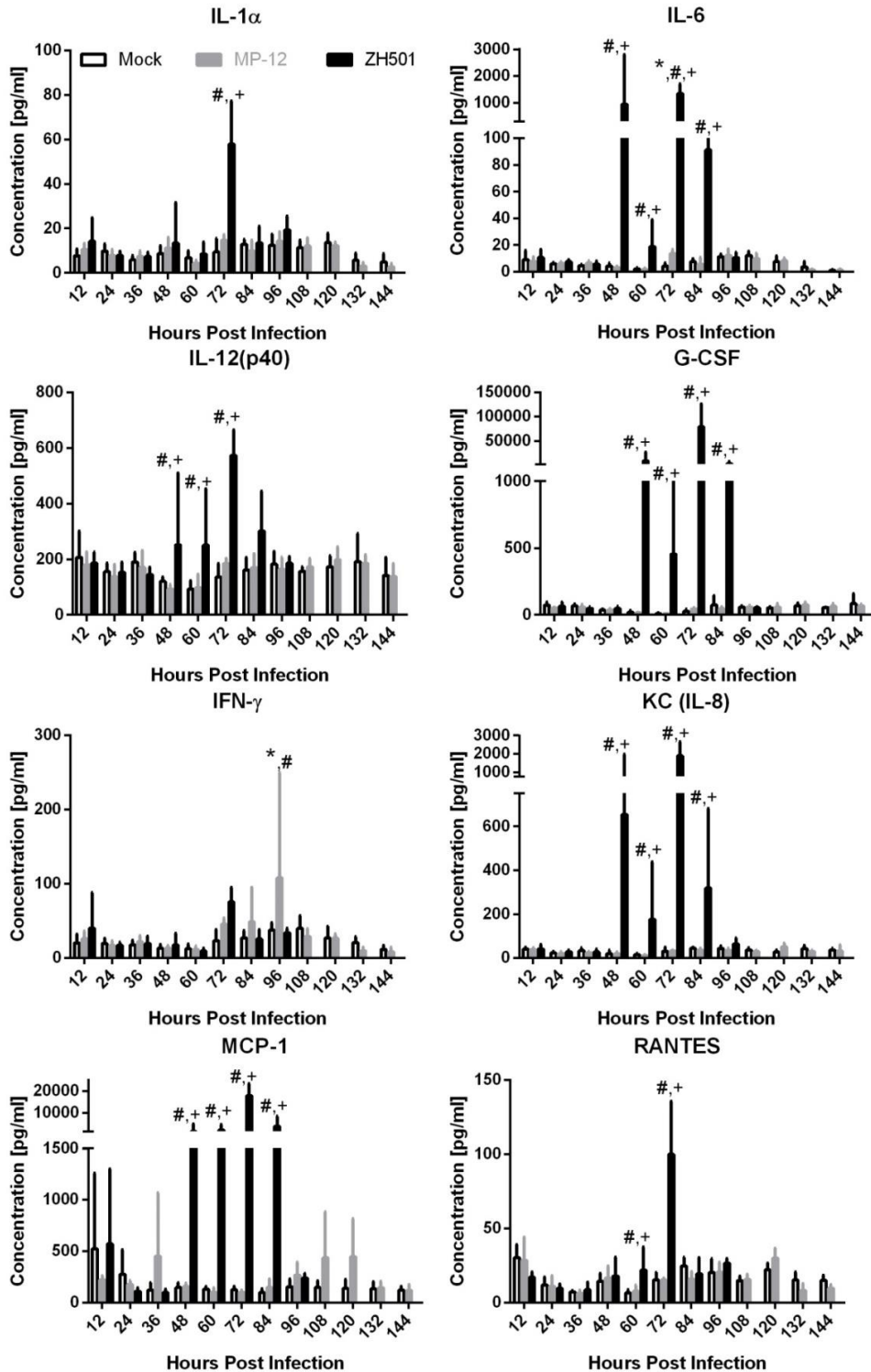


Figure 5.6. Serum Cytokines

The concentration of key cytokines in the serum of mice after mock infection or infection with MP-12 or ZH501. Shown here are the changes in actual concentration [pg/ml]. The values are the average of 5 mice (with the exception of 96 hours post ZH501 infection, where only 3 surviving mice are represented) and the error bars are \pm standard deviation. *, #, and + indicates $p < 0.05$ for mock/MP-12, mock/ZH501, and MP-12/ZH501, respectively.

Serum (Figure 5.6A-H)-The serum from RVFV-infected animals was evaluated for changes in cytokine levels relative to mock-infected animals. These studies indicated a mild and limited inflammatory response in MP-12-infected animals with slight elevations of IL-6, IL-12 and MIP-1 α around 72 HPI. Elevated IL-12(p70) and IFN- γ suggest a Th1 response against viral infection. In contrast, the response against ZH501 infection was very broad with onset evident at 48 HPI with significant elevations of IL-6, KC, MCP-1 and MIP-1 α . By 72 HPI, virtually all cytokines measured in ZH501-infected animals were significantly elevated relative to mock-infected animals. The concentrations of IL-6, G-CSF and MCP-1 indicate a strong inflammatory response and potential response to vascular leakage (Lee, Liu *et al.* 2006). Interestingly, the majority of these cytokines return to non-significant levels in animals sampled at 84 HPI although IL-6, IL-8, G-CSF and MCP-1 remain elevated.

Liver (Figure 5.7A-H)-Samples from MP-12-infected animals showed no significant deviation from mock-infected control animals with the exception of a decrease of IL-12(p70) at 72 HPI. As with serum samples, liver homogenates from ZH501-infected animals had evidence of an inflammatory response with increases in KC, MCP-1 and MIP-1 α . A number of cytokines, such as IL-1 α , IL-12, G-CSF, and KC, became elevated at 48 HPI with most peaking at 72 HPI. G-CSF and KC concentrations were both very high with peak concentrations several hundred fold higher than mock-infected controls. MCP-1 and IL-1 α were also elevated although not to the extent of G-CSF and IL-8.

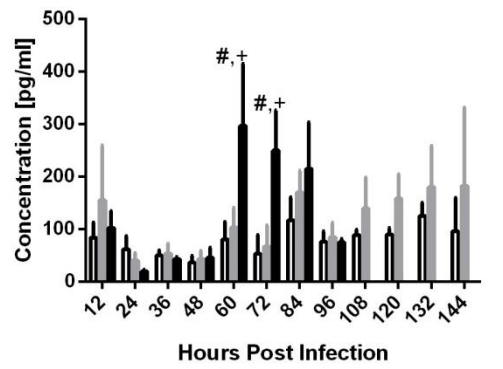
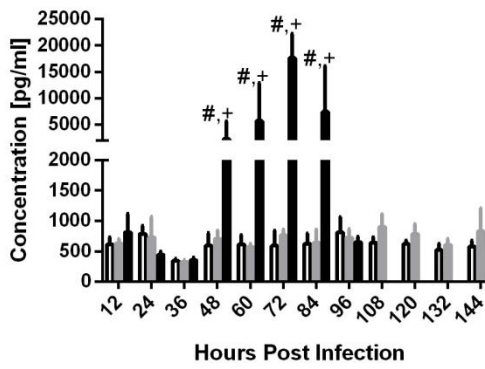
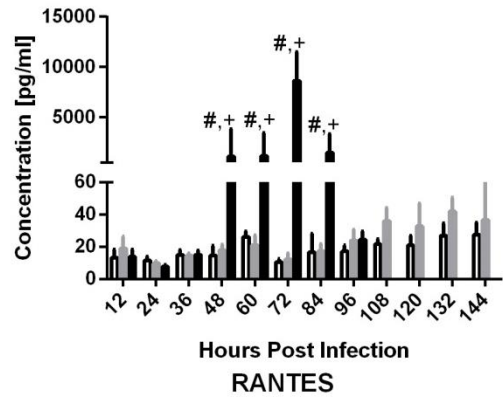
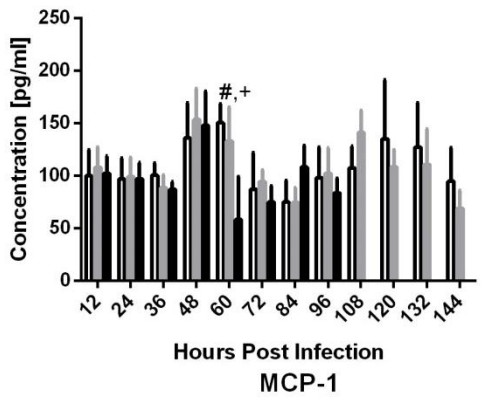
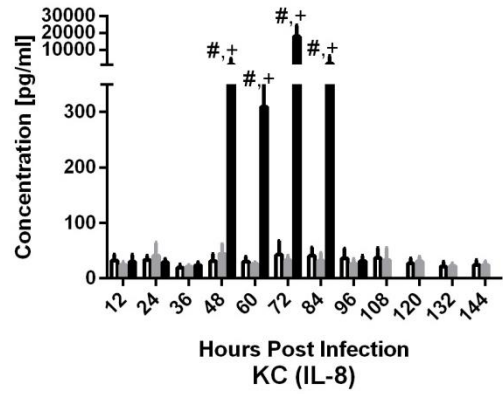
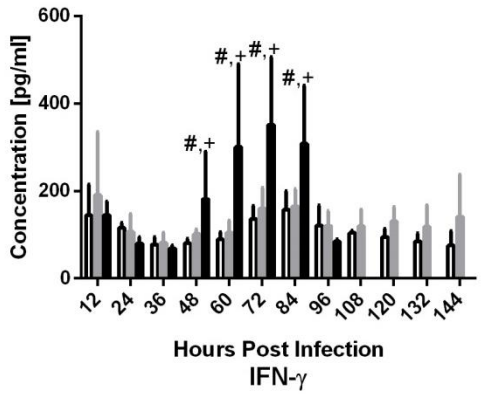
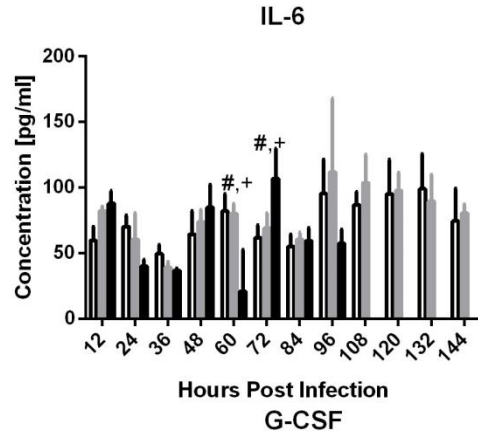
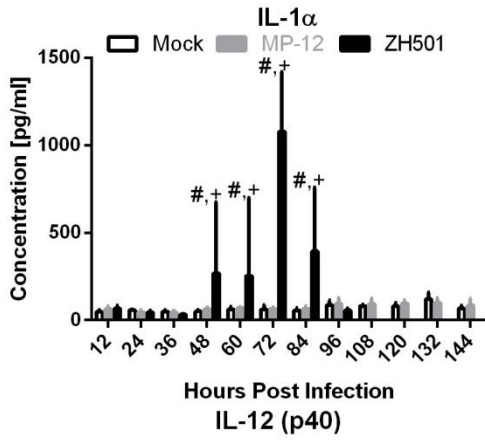


Figure 5.7. Liver Cytokines

The concentration of key cytokines in the serum of mice after mock infection or infection with MP-12 or ZH501. Shown here are the changes in actual concentration [pg/ml]. The values are the average of 5 mice (with the exception of 96 hours post ZH501 infection, where only 3 surviving mice are represented) and the error bars are \pm standard deviation. *, #, and + indicates $p < 0.05$ for mock/MP-12, mock/ZH501, and MP-12/ZH501, respectively.

Spleen (Figure 5.8A-H)-The response to MP-12 infection in the spleen was much like that observed in the serum except that cytokine peaks were delayed by approximately 24 HPI. As seen in the serum, IL-6, IL-12(p70) and IFN- γ concentrations peaked at levels that were significantly higher than in mock-infected animals. In ZH501-infected animals, cytokine concentrations began to increase significantly beginning at 48 HPI. IL-6 and G-CSF displayed the largest fold changes, 200 and 450 times higher, respectively, relative to mock. There was no significant change in concentrations of IL-2, IL-4, IL-12(p70) or IFN- γ suggesting that there was little, if any, stimulation of T- or B-cell activation or differentiation. However, significant induction of IL-6, IL-1 α , and several chemokines, particularly MCP-1, indicates recruitment of pro-inflammatory cells into the spleen. The peak cytokine response in the spleen (72 HPI) correlates with a significant drop in viral titer in the spleen (Figure 5.5B).

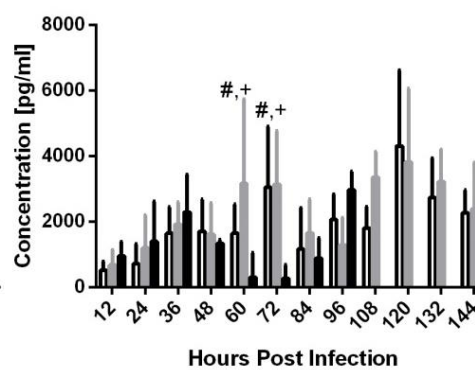
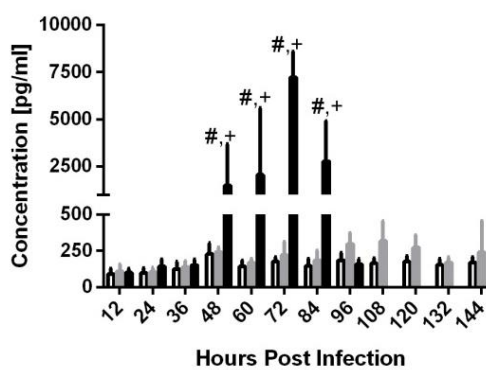
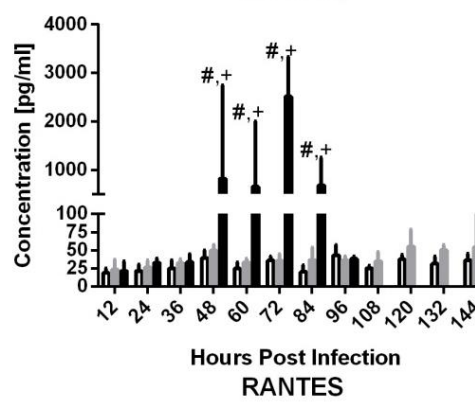
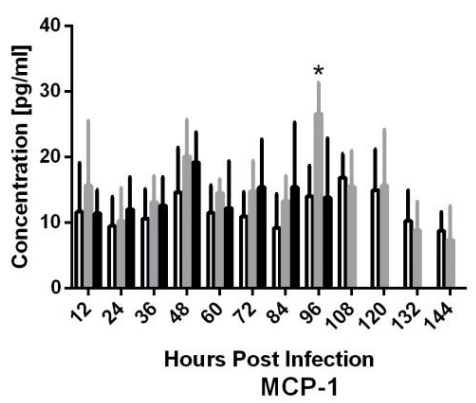
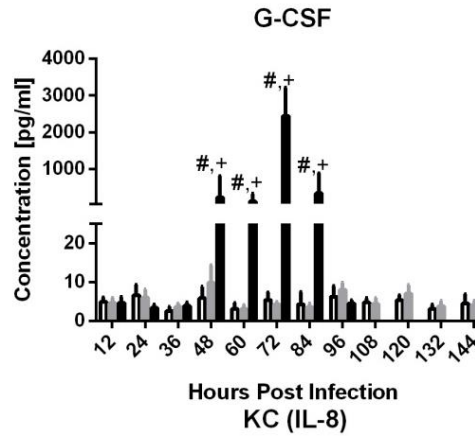
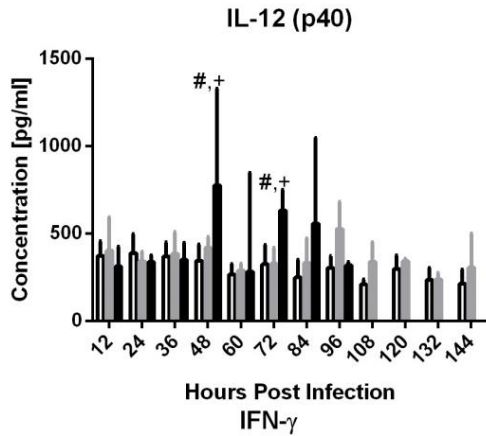
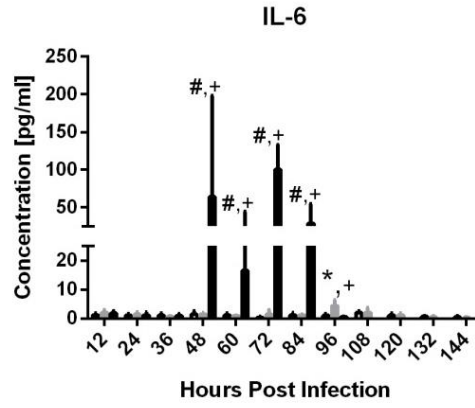
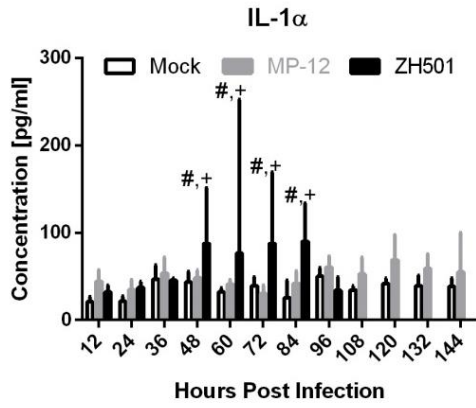


Figure 5.8. Spleen Cytokines

The concentration of key cytokines in the serum of mice after mock infection or infection with MP-12 or ZH501. Shown here are the changes in actual concentration [pg/ml]. The values are the average of 5 mice (with the exception of 96 hours post ZH501 infection, where only 3 surviving mice are represented) and the error bars are \pm standard deviation. *, #, and + indicates $p < 0.05$ for mock/MP-12, mock/ZH501, and MP-12/ZH501, respectively.

Brain (Figure 5.9A-H)-The cytokine response in the brain indicates that the brain is involved during infection with both MP-12 and wild type ZH501. This is particularly interesting given that no virus was detected in the brain of MP-12-infected animals by plaque assay (Figure 5.9) nor was there any signs of neurologic disease. In MP-12-infected animals, IL-2, IL-13 and IL-17 were all elevated along with MCP-1 and MIP-1 α . The presence of IL-2, IL-13 and IL-17 suggests the presence and activation of a B-cell response (Fitzgerald 2001; O'Gorman 2008) or even Th17 cells. Th17 cells have been shown to play a key role in inflammation (Steinman 2007). In addition to Th1 and Th2 cells, Th17 cells are recently discovered T-helper cells (Stockinger and Veldhoen 2007). Th17 cells are potent producers of IL-17 after infection with bacteria and fungi (Siciliano, Skinner *et al.* 2006; Aujla, Dubin *et al.* 2007; Aujla, Dubin *et al.* 2007). They have been shown to be both protective and harmful (causing pathology) in viral infection (Bystrom, Al-Adhoubi *et al.*). Since the discovery of this cell subset is fairly recent, many of its functions remain a mystery.

MCP-1 and MIP-1 α concentrations were elevated soon after infection indicating early onset recruitment of immunomodulatory cells. The brains of ZH501-infected mice showed an early response similar to that seen in MP-12-infected animals, however, concentrations of these cytokines remained elevated and many of their downstream cytokines also became elevated with peak concentrations seen at 60-72 HPI. IL-6 was not evident in the brains of MP-12-infected animals and IL-8 did not deviate significantly from mock-infected animals. In ZH501-infected animals both cytokines were elevated significantly indicating a strong pro-inflammatory response. G-CSF levels were also

extremely high 48-72 HPI (over 2,500 times higher than mock and MP-12-infected mice) suggesting stimulation of a strong protective anti-apoptotic response in the brain that is associated with neurogenesis (Schabitz, Kollmar *et al.* 2003; Schneider, Kruger *et al.* 2005; Henriques, Pitzer *et al.* 2010). Although I found no clear clinical or histological evidence that the ZH501-infected animals developed neurologic disease, the cytokine response strongly suggests that they were going down a path that could lead to encephalitis.

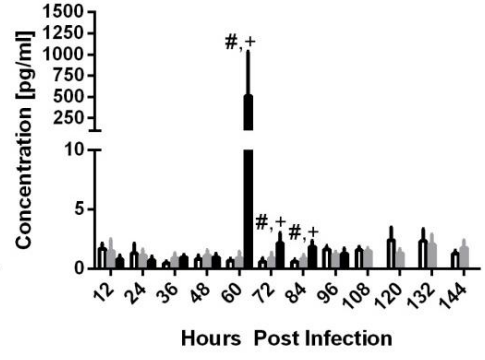
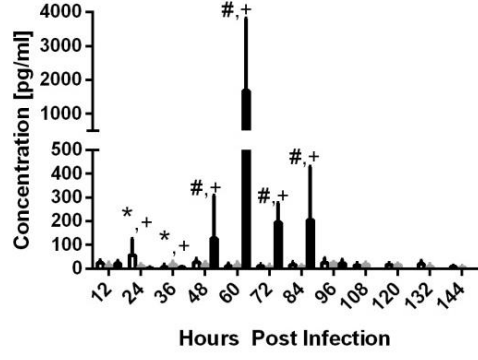
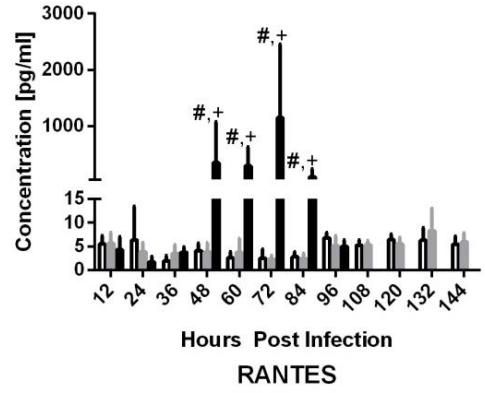
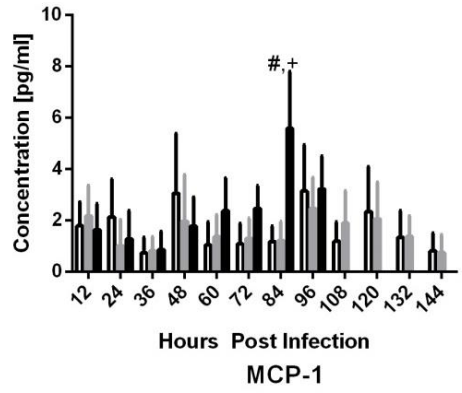
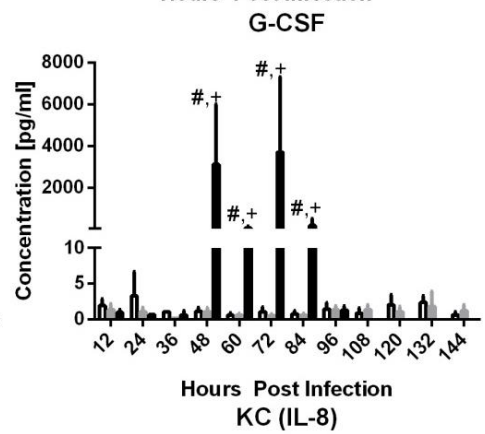
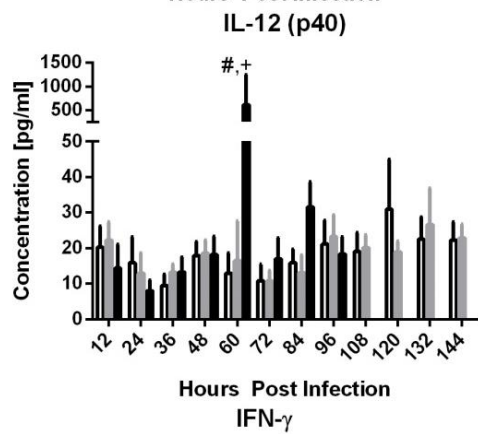
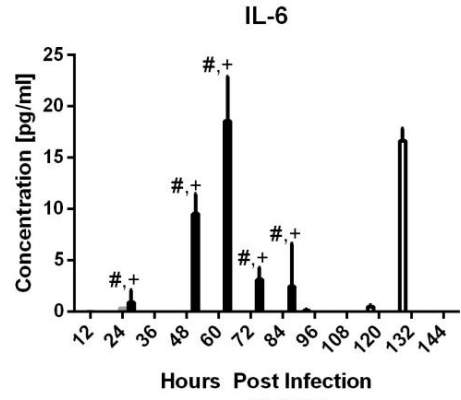
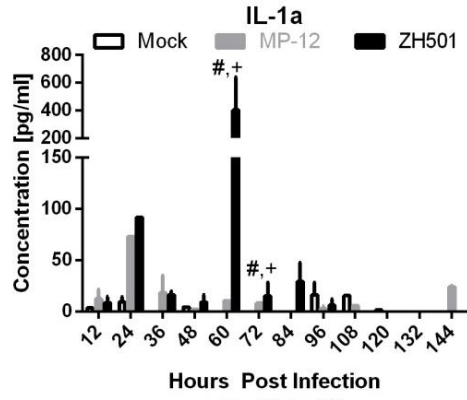


Figure 5.9. Brain Cytokines

The concentration of key cytokines in the serum of mice after mock infection or infection with MP-12 or ZH501. Shown here are the changes in actual concentration [pg/ml]. The values are the average of 5 mice (with the exception of 96 hours post ZH501 infection, where only 3 surviving mice are represented) and the error bars are \pm standard deviation. *, #, and + indicates $p < 0.05$ for mock/MP-12, mock/ZH501, and MP-12/ZH501, respectively.

IFN- β (Figure 5.10) –As wild type RVFV has been demonstrated to have type I IFN antagonist properties (Bouloy, Janzen *et al.* 2001; Billecocq, Spiegel *et al.* 2004), I examined IFN- β production in the liver, spleen and brain. One out of five ZH501-infected animals had elevated IFN- β in the brain at 84 HPI (Figure 5.10A). Three mock-infected animals had slightly elevated IFN- β concentrations in the brain while none of the other mock-infected animals exceeded 75 pg/ml in any sample tested. Similar results were seen in MP-12-infected animals, but one animal had elevated IFN- β in the liver at 36 HPI. However, ZH501-infected animals had elevated IFN- β in the liver (Figure 5.10B) and spleen (Figure 5.10C) of the majority of animals tested at 72 and 84 HPI. Mean concentrations of IFN- β in the spleens of ZH501-infected mice were significantly higher (2-5 fold increase) than both mock and MP-12-infected animals between 48-96 HPI, while in the liver a significant difference was only seen at 72 HPI.

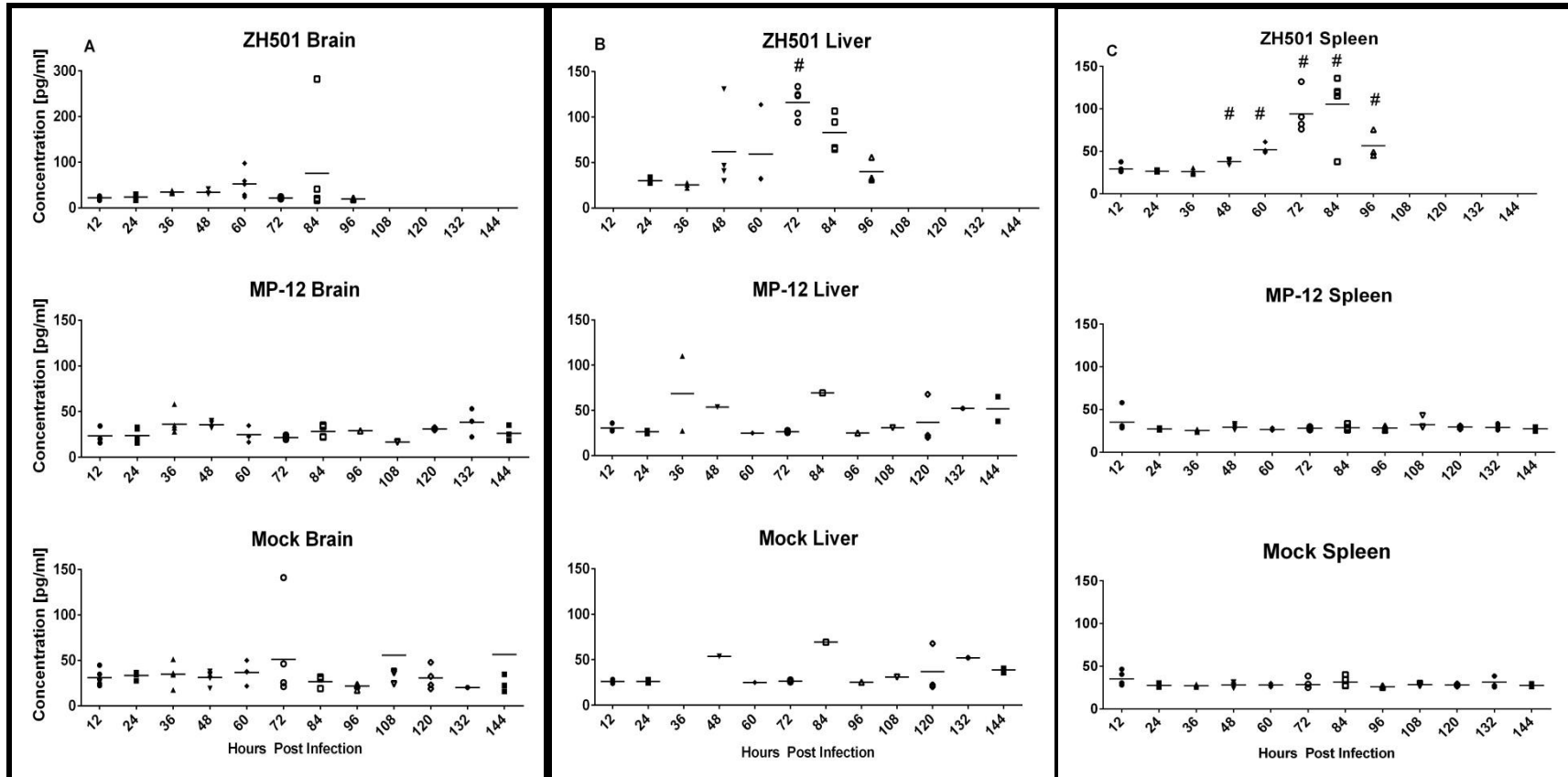


Figure 5.10. IFN- β concentration following infection.

IFN- β concentration in the (A) liver, (B) spleen, and (C) brain in mice after infection. The first row represents mock-infected mice, the second row represents MP-12-infected mice, and the third is ZH501-infected mice. Each symbol represents an individual mouse. There were five mice in each group with the exception of the 96 time-point for ZH501 when only three animals were surviving. The horizontal bar represents the average of the mice for each group. The # indicate that $p < 0.05$ for the average value of ZH501-infected animals compared to both mock and MP-12-infected animals.

Histopathology

Examination of H&E stained sections from the liver, spleen and brain largely supported clinical and cytokine response observations indicating significant damage to the liver and spleen of ZH501-infected animals while tissues from mock and MP-12-infected animals were essentially normal (Figure 5.11A and B).

ZH501-infected mice had evidence of necrosis and hepatocellular change as early as 48 HPI (Figure 5.11C). Histological findings correlated well with the cytokine response in that ZH501-infected animals with the more significant cytokine response also had increased tissue damage. This trend was seen throughout the course of infection. At 48 HPI, mouse 60 presented with the highest cytokine levels (IL-1 α , IL-6, IL-8, IL-12, IFN- γ , eotaxin, and G-CSF) and had moderate necrosis in the liver as opposed to mild microgranulomas with approximately 70% of hepatocytes having cytoplasmic vacuolation that was seen in the mouse 56, which had lower cytokine levels at the same time point. At 60 HPI, the mouse with higher levels of IL-1 α , IL-6, IL-8, IFN- γ , and various chemokines in the liver (mouse 71) had moderate necrosis and hepatocyte degeneration while other ZH501-infected animals (mouse 73 and 75) had minimal microgranulomas that were made up of neutrophils, Kupffer cells, and lymphocytes that had no effect on surrounding tissue (Figure 5.11C). The foci of hepatocyte degeneration and necrosis had occasional neutrophils, Kupffer cells and lymphocytes present (Figure 5.11C). At 72 HPI, the livers of ZH501-infected mice had evidence of severe architectural disruption and most of the hepatocytes were in the process of degeneration and necrosis. There was disassociation of hepatocytes, expansion of sinusoidal lumens and accumulation of hemorrhage within dilated hepatic sinusoids. Most of the nuclei that were still intact contained a single, centrally-located, intranuclear eosinophilic inclusion. At 84 HPI, the livers looked similar to those collected at 72 HPI with architectural disruption and necrosis (Figure 5.11C).

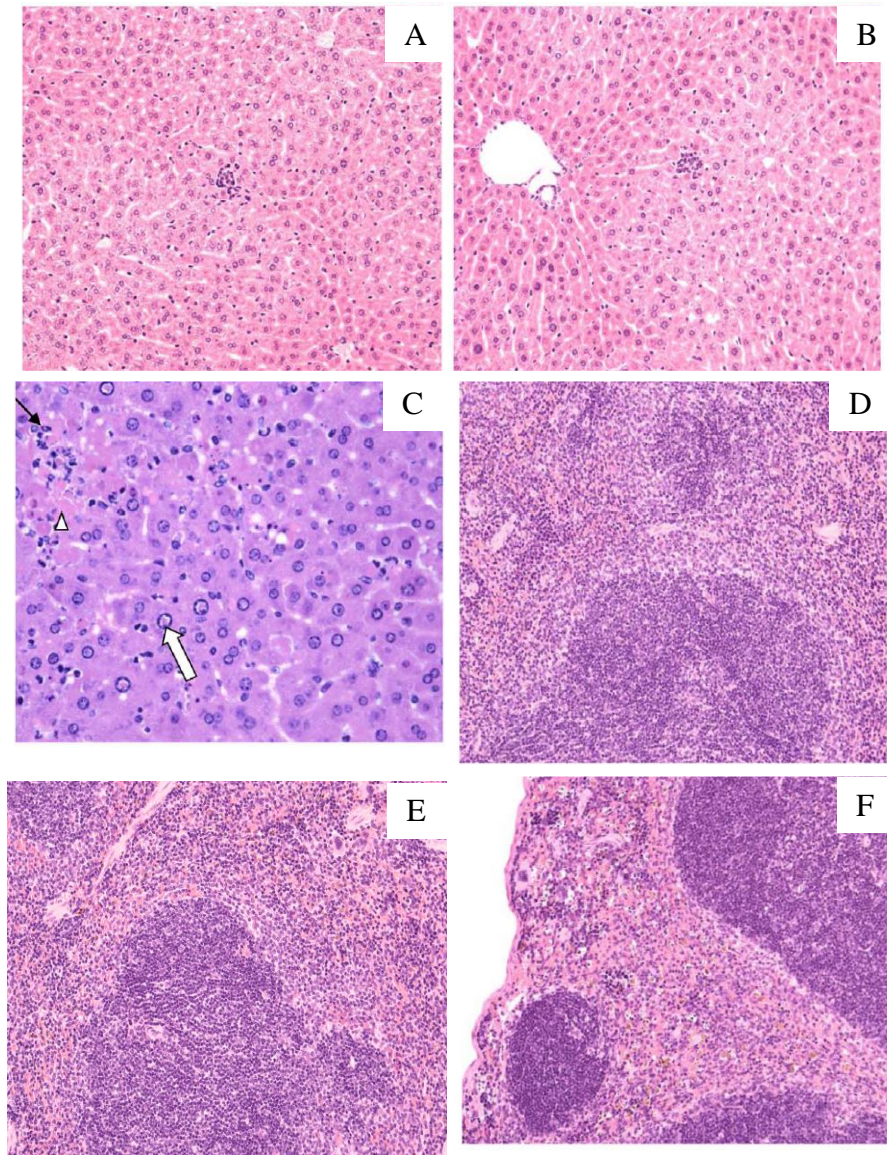


Figure 5.11. Liver and spleen pathology

(A) Liver from a mock-infected mouse at 84 HPI. The liver is essentially normal H&E 20x. (B) Liver from an MP-12-infected mouse at 84 HPI. The random, small microgranulomas composed of individually necrotic hepatocytes surrounded by a small number of neutrophils and mononuclear cells are unrelated to the study, H&E 20x. (C) Liver from a ZH501-infected mouse at 84 HPI, showing piecemeal hepatocyte necrosis (white arrowhead), hepatocellular intranuclear eosinophilic inclusions (white arrow). Note the presence of neutrophils (black arrow) within foci of necrosis, H&E stain 40x. (D) Spleen from a mock-infected mouse at 84 HPI. The spleen is essentially normal, H&E 20x. (E) Spleen from an MP-12-infected mouse at 84 HPI. The spleen is essentially normal, H&E 20x. (F) Spleen from a WT RVFV ZH501-infected mouse at 84 HPI with moderate amounts of necrotic cellular debris and macrophages containing hemosiderin (brown pigment) within red pulp sinusoids, H&E 10x.

The spleens of the mock- (Figure 5.11D) and MP-12-infected (Figure 5.11E) mice remained essentially normal throughout the study. The only pathologic change observed was in mice infected with ZH501 (Figure 5.11F). At 48-84 HPI, the spleens of mice infected with ZH501 that had the highest levels of cytokines (IL-1 α , IL-1 β , IL-6, eotaxin, MCP, and MIP-1 α) with corresponding increases in pathology. Observations included mildly enlarged spleens with moderate amounts of necrotic cellular debris. This pathology was not evident in animals with a limited cytokine response. At later time points (i.e. 72 and 84 HPI), there was increased evidence of neutrophils and macrophages containing hemosiderin (Figure 5.11F).

The brains of all the mice examined appeared essentially normal during the course of this study despite evidence of a high viral titer and significantly increased inflammatory cytokine concentrations in the brain (data not shown).

DISCUSSION

Rift Valley fever virus is a highly pathogenic virus that causes large scale outbreaks in livestock with frequently associated epidemics in humans. The mouse is an established model for RVFV infection where animals succumb to wild type RVFV infection within a matter of days with disease characteristics similar to that seen in fatal cases of human disease and in infected newborn lambs (Ikegami and Makino 2011). While the mouse is an accepted model for disease, the host response to infection has not been well characterized in this or any model. Some studies have evaluated clotting time, mortality, and disease progression, but none have focused on the host immune response to RVFV infection (Morrill, Jennings *et al.* 1987; Peters, Jones *et al.* 1988; Morrill, Jennings *et al.* 1989; Morrill, Jennings *et al.* 1990; Smith, Steele *et al.* 2010; Ikegami and Makino 2011). Smith *et al.* described the pathogenesis of ZH501 infection in BALB/c mice following subcutaneous challenge (Smith, Steele *et al.* 2010; Reed, Steele *et al.*

2012), but did not have the benefit of cytokine profiles to correlate the pathogenesis to the host response. To my knowledge, this is the first study to provide a broad examination of the host response to RVFV infection in the mouse model. This study identifies very significant differences between the host response to infection with wild type ZH501 or the live-attenuated vaccine strain MP-12 and clearly demonstrates that a significant and systemic pro-inflammatory immune response is likely a major contributor to the progression to lethal disease.

As other studies examining the clinical response to viral infection have shown (Tigabu, Juelich *et al.* 2009), clinical analysis is not particularly useful for predicting or analyzing disease progression in this model. In this study, there was no significant change in body weight or temperature in any of the challenge groups despite the ZH501-infected animals showing clear indications of disease. There was an insignificant, although constant, slight decrease in body temperature in the RVFV-infected mice when compared to mock-infected mice. While RVFV is known to cause febrile illness, it is possible that the mice were not febrile because body temperature can decrease as organ systems shut down. Hematological analysis appeared to show that wild type RVFV infection stimulates depletion of lymphocytes and platelets over the course of disease. The depletion in WBC could be the result of lymphopenia during the mid-stages of disease in ZH501-infected animals. Smith *et al.* has shown virus is present in thymus and the bone marrow as early as three days after infection of BALB/c mice with ZH501 (Smith, Steele *et al.* 2010). There appears to be a decrease in both total WBC and lymphocyte numbers between 48 and 60 HPI in ZH501-infected mice (Table 1) with a gradual recovery toward the end of the study. Lymphocyte recovery may be the result of stimulation of the hematopoietic system as significantly increased concentrations of G-CSF were found in the serum and tissues of ZH501-infected animals. Hematology results in the C57BL/6 mouse model correlate somewhat with previously published studies in the BALB/c mouse (Smith, Steele *et al.* 2010) and rhesus macaque (Morrill, Jennings *et*

al. 1989). Infected macaques had an initial leukocytosis and then a sharp decrease to leukopenia at 5 dpi that slowly began to recover and was back to normal by 7 dpi. In another study, looking at WBC counts in ZH501-infected rhesus macaques, animals with a fatal outcome had evidence of leukocytosis at 2 dpi which remained elevated until death or returned to baseline levels just prior to death. Animals which showed clinical illness, but survived infection had only a transient leukocytosis (Morrill, Jennings *et al.* 1990).

The transient decrease in platelet concentration in ZH501-infected mice was a bit surprising. Generally, DIC will cause the platelet count to decrease as the platelets are used to form small clots in the blood vessels throughout the organism. Morrill *et al.* reported a drop in platelet counts in RVFV-infected macaques which was in direct proportion to the severity of the disease (Morrill, Jennings *et al.* 1990). Smith *et al.* observed a decrease in platelet count in BALB/c mice infected with ZH501 when compared to uninfected mice (Smith, Steele *et al.* 2010). In this study utilizing the mouse model, I found no difference between MP-12- and mock-infected animals yet a significant decrease in the mean platelet count in ZH501-infected animals relative to mock-infected animals but only at 72 HPI. Examination of individual ZH501-infected animals found that mice with liver damage indicated by elevated ALT, low glucose and high total bilirubin levels in the serum also had low platelets counts. However, not all mice with low platelet counts had evidence of severe liver damage. My data also seem to indicate a correlation between liver disease and low platelet counts in mice infected with wild type RVFV, but not the reverse. When it appeared that the mice had large amounts of liver necrosis, the number of platelets in circulation was low. The liver produces the glycoprotein thrombopoietin. This protein stimulates the production of the platelet precursor cells, megakaryocytes (Kaushansky 2006). When the liver is not functioning properly, it more than likely cannot produce thrombopoietin, and therefore the number of platelets will drop as they are used up. Similar results have been seen in humans where

approximately half of the patients with laboratory confirmed RVF present with abnormal platelet counts (Al-Hazmi, Ayoola *et al.* 2003).

Clinical chemistry data seemed to indicate liver and kidney disease in ZH501-infected animals, but no evidence of similar disease in MP-12- or mock-infected animals. Liver necrosis has been shown to be a large contributor to the mortality seen after infection with wild type RVFV (McGavran and Easterday 1963; Abdel-Wahab, El Baz *et al.* 1978; McIntosh, Russell *et al.* 1980; Peters, Liu *et al.* 1989; Morrill, Jennings *et al.* 1990; Bouloy, Janzen *et al.* 2001; Al-Hazmi, Ayoola *et al.* 2003; Smith, Steele *et al.* 2010). In studies with ZH501-infected non-human primates or sheep, serum aminotransferases were increased in animals with fatal infections (Cosgriff, Morrill *et al.* 1989; Kortekaas, Antonis *et al.* 2012; Smith, Bird *et al.* 2012). One of the studies showed a correlation between the amount of liver damage (using ALT values) and viremia (Cosgriff, Morrill *et al.* 1989). ZH501-infected mice with elevated ALT and bilirubin concentrations appeared to have histological indications of hepatitis, liver necrosis and possible hepatitis associated jaundice that are characteristic of infection in mice. In Saudi Arabia, 95% of patients with confirmed RVFV infections also had increased ALT levels and 75% of them were diagnosed with hepatic failure (Al-Hazmi, Ayoola *et al.* 2003). Animals with extremely elevated (above 600 U/L) serum ALT also had increased virus titers and a stronger cytokine response in the liver indicating a strong correlation with the onset of liver disease. Macroscopic examination of liver tissues during necropsy showed them to be black in color in the later stages of disease, which was the consequence of the livers being congested with blood. This finding was supported by histopathology with accumulation of hemorrhage present throughout the liver in conjunction with significant levels of viral antigen (Figure 5.5C-D).

ZH501-infected animals presented with elevated BUN and creatinine levels at times when liver enzymes were the highest and cytokine response was at its peak. Marmosets and sheep both show increases in BUN and creatinine amounts in the serum

after infection with ZH501 (Kortekaas, Antonis *et al.* 2012; Smith, Bird *et al.* 2012). While I did not test for viral titers in the kidneys of C57BL/6 mice, BALB/c mice do have detectable amounts of virus in the kidneys 3-8 days post infection (Smith, Steele *et al.* 2010). These findings lead me to believe that in addition to the liver failure, the animals might also be in the process of developing kidney disease and are experiencing multi-organ failure (which could account for the low body temperatures) as virus has also been found in every major organ in RVFV-infected animals (brain, spleen, lung, thymus, heart, pancreas, large intestine, adrenal gland, lymph nodes, sex organs (ovary and testis) skeletal muscle, and bone marrow) (Smith, Steele *et al.* 2010; Gomet, Billecocq *et al.* 2011; Reed, Steele *et al.* 2012; Smith, Bird *et al.* 2012).

In order to characterize the host immune response to RVFV infection and to differentiate infection with MP-12 vaccine strain from wild type ZH501, the concentration of a panel of cytokines in tissue homogenates and serum was determined. The response to ZH501 infection was significant and dramatic in all of the tissues tested while the response to MP-12 infection was largely unremarkable. The response seen in livers from ZH501-infected animals was not anticipated. Given the nature of the wild type RVFV infection, I expected evidence of a significant inflammatory response in the liver. The induction of a pro-inflammatory response was not evident; however, a significant chemokine response focused on recruitment of T-cells, neutrophils and monocytes was pronounced. Histological evaluation of livers from ZH501-infected mice identified significant cellular infiltration and congestion with the appearance of neutrophils, macrophages, and lymphocytes within disrupted sinusoids and eosinophilic intranuclear inclusion bodies that are characteristic of RVFV infections (Ishak, Walker *et al.* 1982). These data were strongly correlated to the observed chemokine response and were also consistent with studies in the BALB/c mouse model (Smith, Steele *et al.* 2010).

Morphologically, the spleen was enlarged with a large amount of cellular debris and a moderate number of neutrophils and macrophages containing hemosiderin (Figure

5.11F). Hemosiderin is commonly found in macrophages when they break down hemoglobin and release heme and bilirubin after conditions that result in hemorrhage (Stewart, Fawcett *et al.* 1985; Turkmen, Eren *et al.* 2008). The presence of hemosiderin containing macrophages in the spleen is indicative of hemorrhage following ZH501 infection.

As with the liver, the level of serum cytokines was significantly increased in ZH501-infected animals. The levels of IL-6, IL-12(p40), G-CSF and several chemokines were elevated indicating the onset of a strong inflammatory response and recruitment of immunomodulatory cells. I have found only one study that examines the cytokine response in ruminant animals to compare these data to. In the serum of goats infected with RVFV (ZH501 strain), Nfon *et al.* recorded an increase in IL-6, IL-12, IFN- γ , TNF- α , and IL-1 β , but they did not see an increase in the type I IFN, IFN- α (Nfon, Marszal *et al.* 2012). The concentrations of all the analytes I examined, with the exception of IL-5 and IL-13, were significantly elevated in serum at 72 HPI supporting the hypothesis of a strong unregulated immune response following ZH501 infection when compared to MP-12 infection. Interestingly, animals sampled at 84 HPI did not have this broad cytokine response and animals sampled at 96 HPI had normal cytokine levels. These data suggest that there might be a critical transition period for RVFV pathogenesis that occurs around 72 HPI in this experimental model. Although exactly what this transition entails or the associated mechanism is unclear, it is possibly a release of neutralizing antibodies and the start of a Th2 response. Antibody titers and cell types present after infection were not measured, therefore this is not definitive conclusion.

Despite a slight cytokine response in the brain following MP-12 infection, which could indicate initiation of cellular recruitment, correlating pathology was not observed. The results from MP-12-infected animals were in striking contrast to the response seen in ZH501-infected mice. A very significant pro-inflammatory cytokine response was stimulated in the brains of ZH501-infected mice and it was maintained through the course

of disease. Despite the pronounced cytokine and chemokine response in the brain beginning around 48 HPI, I did not find any viral antigen or histological evidence of meningoencephalitis as was observed in BALB/c mice (Smith, Steele *et al.* 2010). It is surprising that I could not detect viral antigen in brain sections, but viral titers reached 5 logs in the brain when evaluated via plaque assay. Studies done by Smith *et al.* and Morrill *et al.* show that virus appears in the brains of infected mice on day 5 or 7 post infection, respectively (Morrill, Ikegami *et al.* 2010; Smith, Steele *et al.* 2010). While Smith detected virus in the brain via plaque assay as early as 3 dpi, virus was not detected in immunolabeled sections of the brain until 5 dpi. BALB/c did not have any prominent brain lesions and meningoencephalitis until 8 dpi (Smith, Steele *et al.* 2010). Here, animals did not survive beyond 4 dpi, therefore not detecting virus or pathological changes in immunolabeled brain sections is not surprising. It is possible that the C57BL/6 mice would have developed neurological disease had they survived longer.

Previously published studies have shown that the NSs protein of wild type RVFV has type I IFN (both IFN- α and - β) antagonist properties, while the MP-12 vaccine strain induces type I IFN in in-bred mouse strains (Bouloy, Janzen *et al.* 2001; Billecocq, Spiegel *et al.* 2004; Ikegami, Narayanan *et al.* 2009). Monkeys that produce IFN- α soon after infection with RVFV do not develop clinical disease (Morrill, Jennings *et al.* 1990). High susceptibility in MBT/Pas mice to wild type infection is thought to be caused by defects in both the early and late IFN responses after RVFV infection, even though the mice typically produce and respond to IFN (do Valle, Billecocq *et al.* 2010). Here, I found that wild type ZH501 induced a modest IFN- β response in the liver and spleen while the IFN- β response in MP-12-infected animals was negligible in the tested tissues. The induction of the IFN- β response was not evident until 72 HPI. This delayed IFN response gives the virus an opportunity in a small window of time to replicate to high titers. This suggests that production of measurable IFN- β could be correlated to increases in virus titer. Previous work has shown that the initial inhibition of type I IFN occurs

shortly after infection allowing the virus to become established with the resulting release of IFN- β coming from bystander cells (Bouloy, Janzen *et al.* 2001; Billecocq, Spiegel *et al.* 2004). The lack of an IFN- β response in MP-12-infected animals is curious as I had anticipated that I would see an induction of this cytokine as reported by others. However, the lack of a strong generalized immune response suggests a key role for IFN- β at the very onset of viral infection of macrophages or dendritic cells which could limit virus propagation and dissemination, subsequently eliminating the induction of a broad response. Evidence of virus in the spleen of some MP-12-infected animals and the moderate Th-1 type response in the brain suggests that some virus escapes initial control measures, but that the particle numbers are insufficient to trouble a competent immune system.

With these experiments, I have identified significant host response differences in the mouse model following infection with either wild type RVFV or the attenuated vaccine strain. I have also identified a temporal correlation between increased virus titers in ZH501-infected mice, a decrease in WBC and platelets, architectural disruption and necrosis in the liver, and the onset of a significant systemic cytokine response. The specific mechanisms driving these physiological changes still need to be elucidated. However, many of the responses that were identified can be directly correlated to disease outcome. Clearly, there is a significant amount of cellular infiltration into and necrosis of the liver that likely limits organ function, disrupts regulation of the acute phase response and the ability of the coagulation cascade to limit hemorrhaging, regardless of the mechanism associated with vascular leakage. There is evidence of a systemic pro-inflammatory response in both the liver and the serum, but there is also evidence that neurologic disease may play a role in the demise of ZH501-infected animals despite a lack of gross signs of neurologic disease. This finding is generally not surprising as I have observed a number of studies with vaccines and attenuated viruses where animals that survive the first phase of disease following ZH501 infection are only partially

protected and may succumb to neurologic disease 10-14 dpi (M. Holbrook, unpublished observations (Gowen, Bailey *et al.* 2013). There have also been published reports of humans developing neurologic (Alrajhi May 2004) and ocular disease (Siam and Meegan 1980; Al-Hazmi, Al-Rajhi *et al.* 2005) as a result of RVFV infection.

This experiment has demonstrated that RVFV vaccine strain MP-12 infects and replicates in adult C57BL/6 mice, but does not cause acute disease while the wild type strain ZH501 is highly pathogenic and causes a significant innate immune response. Given that there are only 11 amino acid differences between the MP-12 strain and ZH548, and the high homology between ZH501 and ZH548 (nucleotide difference of 0.26%), the differences in the host response are quite impressive (Bird, Khristova *et al.* 2007). This study makes it clear that MP-12 has the potential to be further developed and evaluated as a safe and effective vaccine and clinical trials will hopefully provide additional support for the use of MP-12 as a vaccine for RVFV in humans. This study also gives evidence that rMP12-C13type virus could also be a good candidate vaccine candidate. Recent studies have shown that virus lacking NSs provides protection in mice post-exposure (Gowen, Bailey *et al.* 2013). The data published in that study along with the cytokine response that I showed rMP12-C13type virus exhibited in primary macrophage cells could provide a basis for more studies involving rMP12-13type virus.

It has been shown that the early innate response is important in survival rates of those infected with RVFV, but there is very little published data on the immune response of the primary host of RVFV (sheep, cattle, goats and humans). Recent studies have shown a strong correlation between an increased pro-inflammatory response and survival of infection in humans (McElroy and Nichol 2012). Knowing the pathology of the virus and how the immune response has a hand in this pathogenesis is vital for better devised treatments and vaccines. A single dose, immunogenic vaccine is needed because of the sporadic nature of and quick spread of infection during outbreaks. The number of casualties from RVFV infection can be decrease if a virus can be created that will

decrease the number of animals that are infected and/or decrease the levels of viremia in these animals. If virus amplification in the animals is reduced, then transmission by mosquitoes can also be reduced. Small mammal studies are where these studies have to begin in an effort to eliminate any treatments that may not be advantageous.

Chapter 6 Conclusions and Future Studies

OVERVIEW

The aim of this project was to examine host responses against pathogenic and attenuated RVF virus infection with the long-term goal of identifying specific host factors that play an important role in protection and viral clearance. To examine these processes, I utilized mouse macrophage (RAW 264.7) and mouse dendritic cell (DC 2.4) lines as well as primary mouse BMD macrophages and dendritic cells for *in vitro* studies. To examine cytokine secretion *in vivo*, C57BL/6 mice were used. The purpose of using both cells and mice was to characterize the cytokine response in cells with the expectation that the cytokine response that is seen *in vivo* could be attributed to immunomodulatory cells. For these studies I used γ -irradiated MP-12, MP-12, rMP12-C13type virus or ZH501. I have shown that primary mouse BMD DCs appear not to be permissive to RVFV infection, while primary mouse BMD macrophages are susceptible and productive infection can be measured. While MP-12 and ZH501 had similar growth kinetics and grew to comparable titers in primary macrophage cells (Figure 3.9), these similarities in virus growth did not translate into the mouse system as ZH501 replicates to higher titers more rapidly in the serum, liver, and spleen of infected mice. I also observed stark differences in the cytokine response mounted against MP-12 and ZH501 both *in vivo* and *in vitro*. This is likely due to the fact that infection of additional and more relevant targets cells (such as hepatocytes and endothelial cells) contribute to the overall viremia and therefore result in increased viral titers of ZH501. Furthermore, infection with the attenuated MP-12 strain does not result in the development of clinical signs of disease in mice and replication in immuno-competent mice is normally controlled very effectively.

In these studies I tried to discriminate protective host responses following RVFV infection to those that could contribute to development of severe disease. To obtain a better understanding of the host response to RVFV infection, various signaling proteins (Chapter 3) and secreted cytokines (Chapter 4) were characterized in macrophages and dendritic cells *in vitro*, and compared with findings of blood chemistry, serum electrolyte, and cytokine analysis from mouse *in vivo* studies (Chapter 5). ZH501 infection caused a decrease in the concentration of all cytokines examined in primary macrophages, while ZH501 infection caused large increases in the same cytokines (with the exception of IL-5) systemically *in vivo*. The opposite was observed in MP-12 infection. MP-12 caused an increase in the concentration of cytokines examined *in vitro* and a decrease in those cytokines *in vivo* (with the exception of IFN- γ). By understanding these host cellular responses to RVFV infection, it will be possible to identify specific pathways and mediators that are important for viral clearance in response to infection.

CELL SIGNALING

To examine the effects of RVFV infection on the response of specific immunomodulatory cells, macrophage cell lines (RAW 264.7), dendritic cell lines (DC 2.4) and primary BMD macrophage cells were used. In the cells examined, pro-apoptotic pathways appeared to be activated viral replication as the phosphorylation levels increase ≤ 24 HPI. These results are in accordance with other studies published by Popova *et al.* that show an increase in the phosphorylation of p53 and its upstream effectors p38 MAPK and JNK which are associated with pro-apoptotic pathways (Popova, Turell *et al.* 2010). The phosphorylation of JNK leads to phosphorylation of both p53 and c-Jun. It appears that a competition for activation by JNK occurs, in terms of when JNK activates c-Jun, p-p53 concentration decreases leading to cell proliferation. The same is true in that the absence of c-Jun leads to the increase of phosphorylation of p53 by JNK and cellular apoptosis (Schreiber, Kolbus *et al.* 1999). When evaluating primary BMD

macrophages I also found an inverse correlation between p-p53 and p-c-Jun. I concluded that the initial signaling steps of pro-apoptotic pathways are activated after MP-12 infection in primary mouse macrophages due to an increase in p-p53, interference from RVFV NSm may prevent the final steps of the pro-apoptotic pathway. Won *et al.* demonstrated that the NSm protein of RVFV has anti-apoptotic properties by blocking the cleavage of caspases 3, 8, and 9 (Won, Ikegami *et al.* 2007). This down-regulation of apoptosis allows the virus to more efficiently replicate before expending all the cell's resources (Engdahl, Naslund *et al.* 2012).

While the pro-apoptotic pathways appear to be activated, the STAT pathways I examined are either not activated, or activated late in the course of infection of primary macrophages. STAT proteins are phosphorylated when IFNs and other cytokines bind to their receptors and activate their specific signal transduction pathways. Of the STAT proteins that I examined, only STAT2 was phosphorylated, and that occurred 48 hours or more after MP-12 infection of primary macrophage cells. Normally, STAT proteins are activated by IFN- α/β and once phosphorylated, they translocate into the nucleus to activate transcription of antiviral genes. The late increase in phosphorylation of STAT2 protein after infection of RAW 264.7 cells with γ -irradiated MP-12 could be due to an antiviral response that is initiated when the virus first enters the cells. Uptake of the irradiated virus causes exposed cells to release IFN, and via paracrine signaling, JAK/STAT pathways are activated in nearby cells. The cell lines infected with irradiated MP-12 show an increase in IFN- γ secretion. While I did not measure the IFN- α/β concentration in the RAW 264.7 cells, the increase in STAT2 is expected following the increase in IFN- γ concentration (Lehtonen, Matikainen *et al.* 1997). STAT3 was not phosphorylated in the primary macrophages during the course of infection. It is possible that no phosphorylation was detected because STAT3 activation is inhibited by JNK, and I did detect increases in the phosphorylation of JNK (Figure 3.11).

The expression of IFN- α/β and many other cytokines such as RANTES, MCP-1, and MIP-1 α is controlled by NF- κ B. NF- κ B is phosphorylated in response to TNF α and controls inflammation by regulation of cytokines. An increase in the phosphorylation of NF- κ B was detected 48 hours after MP-12 infection of primary macrophage cells, which correlates with the observed increase in TNF α at 48 HPI. While no change in NF- κ B phosphorylation could be detected after ZH501 infection, decreases in IFN- γ , MCP-1, and MIP-1 α concentrations were observed. Additionally, NF- κ B has also been shown to induce IL-6 (Han, Runge *et al.* 1999; Brasier, Recinos *et al.* 2002; Brasier 2006), which was detected at 48 HPI after MP-12 infection (discussed below).

CYTOKINE SECRETION

The NSs protein of ZH548 (a wild type strain of RVFV that was isolated during the same outbreak as ZH501) has been shown to antagonize IFN- α/β production *in vivo* while MP-12 infection has been shown to induce IFN- α/β (Bouloy, Janzen *et al.* 2001). That same study identified the target of the NSs protein as IFN- α/β system as opposed to the IFN- γ system. It is thought that, even though other mutations have been acquired in other segments of the genome of the attenuated MP-12 strain, the induction of IFN- α/β by MP-12 is due to the mutation at position 513 of the NSs protein, which results in an valine-to-alanine point mutation (Bouloy, Janzen *et al.* 2001). Studies using Pas mice demonstrated the importance of low IFN levels released after infection. A delay in survival by two or four days could be observed in comparison to ZH548 infections in IFN competent C57BL/6 mice and BALB/c mice, respectively. The MBT/Pas mice had a higher viremia and began to die earlier than the inbred mouse strains, which expressed a broader array of interferon stimulated genes. Mouse embryonic fibroblasts (MEFs) isolated from the MBT/Pas mice had a weaker IFN-dependent response at 9 HPI when compared to BALB/c MEFs after infection with ZH548. These results show that RVFV interferes with IFN- β production as early as 3 HPI (Le May, Mansuroglu *et al.* 2008).

Genetic variations that cause a difference in innate cellular antiviral response lead to a difference in the expression of IFN response genes (*Ifnb1* and *Ifna4*) after ZH548 infection that can be translated to a difference in survival. The expression of these IFN genes, although lower than the IFN induction after infection with a NSs-deficient virus, was detectable after infection of BALB/c and MBT/Pas mice (do Valle, Billecoq *et al.* 2010). While there is only a small amount of stimulation of IFN genes after infection with ZH548 when compared to West Nile virus infection (Fredericksen, Keller *et al.* 2008; do Valle, Billecoq *et al.* 2010), there is a detectable difference in IFN response that will result in a difference in disease progression.

Very few studies have been done that examine the secretion of cytokines *in vivo* after infection with RVFV. Cytokines are the signaling molecules of the immune system and are produced by almost every nucleated cell in the body (Boyle 2005). In this study, very low response for Th1 cytokines (IFN- γ and IL-12) was measured in the examined organs (brain, liver, spleen) after MP-12 or ZH501 infection of C57BL/6 mice. The only exception was a detectable increase at 60 hours post ZH501 infection in the brain. These data suggest for a potential restriction in Th1 cell proliferation *in vivo* after infection with RVFV, which could allow the virus to replicate in an attempt to overwhelm the host response before a Th2 response can develop. The Th2 cytokines (IL-6 and IL-10) did not show an increase in secretion until 48 hours after infection *in vivo* and 24 HPI in primary macrophage cell cultures. Since IL-6 is a pro-inflammatory cytokine, it is not surprising that after infection of C57BL/6 mice, an increase in the secretion of IL-6 could be measured. The increase of IL-6 could also contribute to the increase seen in IL-10. The anti-inflammatory cytokine IL-10 could be released in an attempt to regulate inflammation and to counteract the effects of IL-6.

The decrease of Th1 cytokines could be at least partially responsible for the decrease in WBCs that was observed after infection with ZH501, but absent after MP-12 infection. A decrease in Th1 cytokines causes a decrease in the number of WBCs that

mature. There are no new cells to replace the dying WBCs that are in circulation combating infection. As previously described in other studies (Morrill, Jennings *et al.* 1989; Smith, Steele *et al.* 2010), there is a decrease, followed by a subsequent increase (to levels higher than in mock-infected mice), in the number of the WBCs that are circulating after infection with ZH501. Just before the number of WBCs increases, an increase in the amount of G-CSF can be measured. The increase that is seen in G-CSF could lead to the increase of pJNK. G-CSF binds to its receptor and then causes the activation of intracellular pathways including the JNK pathway (Kendrick and Bogoyevitch 2007). The G-CSF increase could stimulate the hematopoietic system which would explain the rebound in the numbers of WBCs that were detected after infection with ZH501.

The decrease in Th1 cytokines *in vivo* does not correlate with *in vitro* macrophage studies. When comparing *in vivo* and *in vitro* data, contrary to infections in C57BL/6 mice, macrophages secreted low levels of Th1 cytokines after ZH501 infection. It has been suggested that this down-regulation of cytokines *in vitro* is a direct result of the presence of the NSs protein (McElroy and Nichol 2012). I did not see this down-regulation after MP-12 infection in cells, but rather a large increase in the secretion of all cytokines examined with the exception of IFN- γ . These data suggest that the primary macrophages might not be the primary source of cytokines after ZH501 infection *in vivo*. ZH501 could also be blocking the functionality of the primary macrophages since they show a decrease in the concentration of all cytokines examined after infection. This effect has also been observed by McElroy and Nichol (McElroy and Nichol 2012). *In vivo*, hepatocytes or endothelial cells are both possible target cells that could be responsible for the increase in pro-inflammatory cytokine secretion, but supporting data have not been published. The hepatocytes were clearly infected with high titers of RVFV during the experiments discussed here. The ZH501-infected macrophages are not

secreting pro-inflammatory cytokines and have become a center of viral replication because they are not signaling bystander cells to defend against viral infection.

In my studies I also found that TNF α was not secreted from infected primary macrophages, with the exception of cells infected with rMP12-C13type virus. MP-12 and ZH501, which both contain an intact NSs protein, did not exhibit any change in TNF α concentration, until late in the infection when there was an increase in TNF α in MP-12-infected cells at 48 hpi. The NSs protein of MP-12 and ZH501 do not have the same suppressing function on IFN- α/β , but both viruses could have a similar effect on TNF α secretion. Since I did not use rMP12-C13type virus in my mouse challenge studies, no definite statement can be made, to whether these findings could be translated to the mouse system. However, no change in TNF α concentration could be detected in mice infected with MP-12 or ZH501. Inhibition of TNF α in macrophages is a recent finding by McElroy and Nichol that needs to be investigated further (McElroy and Nichol 2012).

In the cell lines (RAW 264.7 and DC 2.9) infected with MP-12 and ZH501, a decrease in the secretion of pro-inflammatory cytokines compared to mock-infected cells was observed. Pro-inflammatory cytokines did not increase after ZH501 infection in primary macrophages, but did increase after MP-12 infection later in the experiment (\geq 48 HPI). While it looks like that both MP-12 and ZH501 are down regulating the immune response after infection in cell lines, it appears that the immune response is only down-regulated after ZH501 infection in primary macrophages. Conversely, macrophages infected with MP-12 elicited a response suggesting an attempt to clear the virus.

IN VIVO

Studies of other hemorrhagic fever diseases, such as CCHF and Ebola, show that an increase in the secretion of pro-inflammatory cytokines after infection *in vivo* can be

observed as the mortality rate increases (Villinger, Rollin *et al.* 1999; Gupta, Mahanty *et al.* 2001; Stroher, West *et al.* 2001; Ergonul, Tuncbilek *et al.* 2006; Papa, Bino *et al.* 2006; Hutchinson and Rollin 2007; Connolly-Andersen, Douagi *et al.* 2009). Results from these studies support my findings with ZH501 *in vivo*. While the serum, livers and spleens of infected mice all had high levels of cytokines and chemokines secreted and evidence of necrosis after ZH501 infection, the brain involvement in the course of the infection with MP-12 or ZH501 was minimal with no observed pathology. Some cytokines present in the brain after MP-12 infection, such as IL-1 α , were only elevated early in infection. This could have been a protective mechanism initiated by the brain in the presence of systemic infection. No virus was detected in the brains of MP-12-infected mice. Brains from ZH501-infected mice exhibited an increase in the pro-inflammatory cytokines examined between 48 and 84 HPI. These samples also displayed a peak in viral titer at 60 HPI. The virus was not detected in the brains at 96 HPI. This would fit with the pathology of the disease as all mice infected with ZH501 succumbed to disease by 4 dpi and the virus had yet to invade the brain. The encephalitic cases observed in humans and livestock, represent a secondary condition that is often seen after the host appears to clear the virus and make a recovery.

Of note is that the immune response appears as if it should be able to produce antibodies via B cells after infection with ZH501 *in vivo* when the spleens of infected mice are examined. Recent studies have shown that the B cells are critical for viral clearance after infection with ZH501 that is lacking the NSs gene (Dodd, McElroy *et al.* 2013). The spleens of mice infected with ZH501 only have a small amount of necrosis and the spleens of mice infected with MP-12 looked normal throughout the course of the experiment. There was no viral antigen detected in the lymphoid follicles of the spleen after MP-12 or ZH501 infection. The lymphoid follicles, in the white pulp of the spleen, are filled with B-lymphocytes. In mice, the spleen can hold up to half of the animal's monocytes (Swirski, Nahrendorf *et al.* 2009). After infection, these monocytes migrate

to the site of infection and then mature into dendritic cells or macrophages (Jia and Pamer 2009; Swirski, Nahrendorf *et al.* 2009). The ZH501-infected mice would likely still be able to mount a Th2 response if they would survive for an extended time. The three mice that did not succumb to ZH501 infection and were sacrificed at 96 HPI cleared the virus and all had normal cytokine and blood chemistry levels. With a functioning immune response, treatments given after infection could be effective if the proper therapeutics are found.

The damage that is seen after RVFV infection could be due to the early effects of TNF- α or viral replication itself. TNF- α has been shown to increase in patients that have alcoholic hepatitis (Felver, Mezey *et al.* 1990). It has been shown that it is produced by mononuclear cells infiltrating the liver (Yoshioka, Kakumu *et al.* 1990). I saw an increase early in the course of infection. This TNF- α secretion by the macrophages could be a contributing factor to the hepatitis that is seen after infection. Of note is the decrease in anti-inflammatory cytokines that is seen after ZH501 infection in primary macrophages. This decrease in anti-inflammatory cytokines that appears to be mediated by the virus could be done to allow the virus more time to replicate. The more viral replication that there is, the more damage the virus itself can cause. The balance between damage caused by the immune response and by the virus is intricate and needs further study to be better understood.

The study represented here demonstrates that MP-12 causes neither a release of large amounts of chemokines nor does it cause any pathology in the liver, spleen, or brain. The lack of pathology and the protection provided by MP-12 against lethal infection with ZH501 in most laboratory strains of mice are good indicators that MP-12 vaccines will be effective and have few adverse reactions (Vialat, Billecocq *et al.* 2000; Bouloy, Janzen *et al.* 2001; Flick and Bouloy 2005; Bhardwaj, Heise *et al.* 2010; Smith, Steele *et al.* 2010; Ikegami and Makino 2011; Gray, Worthy *et al.* 2012).

		MP-12	ZH501
Primary Macrophages	Titer	2-5 PFU	2-5 PFU
	Pro-Inflammatory cytokines	+	-
	Anti-Inflammatory cytokines	++	-
	Th1 cytokines	++	-
	Th2 cytokines	+	-
	Cell death	+	+++
C57BL/6 Mice	Titer	≤ 4 PFU	4-7 PFU
	Pro-Inflammatory cytokines	-/+	+++
	Anti-Inflammatory cytokines	-/+	-/+
	Th1 cytokines	-/+	+
	Th2 cytokines	-/+	+++
	Pathology	Liver, spleen, and brain - no obvious pathology	Liver - Moderate necrosis and hepatocellular degeneration
			Spleen - Midly enlarged with moderate necrosis
			Brain - Essentially normal
	Viral dissemination	+	+++
	Survival	Alive	Death

Table 6.1. Comparison of the host response to MP-12 and ZH501 infections

Summary of the host response to RVFV infection in primary BMD macrophage cells and C57BL/6 mice.

While some severe manifestations are induced by RVFV cytotoxicity, it is believed that a large percentage of the manifestations in RVFV disease are caused by an overactive host immune system response *in vivo* (Morrill, Jennings *et al.* 1990). It appears that while ZH501 causes the secretion of many different cytokines and chemokines *in vivo*, macrophages are not the cells that are responsible for this release. The studies that were performed examined cytokine response in both primary macrophage cells as well as in the C57BL/6 mouse model. These data demonstrate the importance of using the whole organism to analyze the effect of RVFV on the host immune system. The high levels of chemokines *in vivo* were in stark contrast to what

was seen *in vitro*. The macrophage and dendritic cells were not secreting high levels of chemokines after infection with either MP-12 or ZH501, but high levels of chemokines could be detected in mice after ZH501 infection in serum, liver, spleen, and brain. This leads to the conclusion that the macrophages and dendritic cells *in vivo* may not be responsible for the high level of chemokines detected. The macrophages may be responsible for localized cytokine production but not for the cytokine storm that is seen in infected humans and animals. As macrophage and dendritic cells are the first line of defense against infection, other host cells must be responsible for the high quantity of cytokines released after ZH501 infection because increased cytokine responses were measured *in vivo* after the virus has grown to high titers. *In vivo* the host response was severely unbalanced. There was a large increase in the amount of released pro-inflammatory cytokines, but the proper complement of Th1 cytokines (IFN- γ and IL-12) is not seen. While the type-II IFN response was not as expected, the story behind type I IFN function correlates well between *in vivo* and *in vitro* studies. Since ZH501 shuts-off host gene expression, the virus grows to high titers in the mouse. The type I IFN induction was late in the course of infection *in vivo*. This delay in type I IFN induction could allow for the hepatitis that is seen *in vivo*. As with any complex system, when one component is removed to study its functionality, the results may or may not be the same as if it were possible to keep the entire system intact and to study the response.

FUTURE STUDIES

Future studies should be performed focusing on cytokines secreted by hepatocytes. In this study, I used liver homogenates, the cytokines presents could be from hepatocytes, resident macrophages, or other immune cell infiltrates. Co-culture studies could also be performed to examine the interaction between the hepatocytes and macrophage. These studies could investigate the cytokines secreted by macrophages alone, hepatocytes alone, and then cytokines secreted by the two when cultured together.

Careful attention should be paid to IFN- γ , IL-12, and TNF α . These studies would be important in determining how the macrophage cells behave in the presence of other cells that are also reacting to viral infection. It would also be interesting to determine if the dendritic cells, while not actively infected, are facilitating a niche for the virus to gain access to lymph nodes in the host. While it did not appear that the primary DCs that were used in these experiments were infected, future attempts should include RT-PCR to demonstrate the absence of transcription of viral genes before a definitive conclusion can be made.

The cytokine profiles should also be characterized in other RVFV animal models (such as the rat, hamster or non-human primate), to demonstrate that the results that I observed in the C57BL/6 mice could potentially be translated to other species. Future studies should also include the examination of therapies using different cytokines such as TNF α . TNF α is not increased *in vivo* but there are significant increases in TNF α concentration after infection with MP-12 in primary macrophages. TNF α treatment that is given earlier in infection may be able to control viral infection as it has been shown to control and protect against lethal West Nile viral infection in mice (Shrestha, Zhang *et al.* 2008). It seems that in the case of RVFV an early treatment is crucial to result in increased survival. If a therapeutic could be devised that is directed against RVFV specific biomarkers and could be given even before symptoms appear, as a preventative measure during an outbreak, the better the outcome would be. This treatment needs to be cost effective, temperature stable, and immunologically effective. This study and others like it could lead to the development of a preventative inexpensive human and livestock vaccine that can be given to prevent the spread of RVF disease.

IN SUMMARY

While still in the early stages, it appears that RVFV does not replicate in primary BMD DCs. I have shown that primary BMD macrophage cells do support an active

RVFV infection and infection with MP-12 or rMP12-C13type virus leads to the activation of pro-apoptotic pathways and the secretion of pro-inflammatory cytokines. In the primary macrophage cells, ZH501 replication decreases cellular signaling and cytokine secretion. While a down-regulation of the immune response is seen after ZH501 infection in primary macrophage cells, the opposite is seen after ZH501 infection in C57BL/6 mice. In the serum, livers, spleens, and brains of ZH501-infected mice, large increases in pro-inflammatory cytokines were seen in stark contrast to what was seen in MP-12-and mock-infected mice. The organs of MP-12-infected mice had no obvious pathology while the livers and spleens of ZH501-infected mice had large patches of necrosis. There appeared to be no pathology in the brains of ZH501-infected mice. While the function of the macrophages is important after infection *in vivo*, it appears that the large amounts of cytokines that are seen after infection cannot be contributed to the macrophages alone.

References

- Abdel-Wahab, K. S., El Baz L.M., El-Tayeb E.M., Omar H., Ossman M.A., and Yasin W. (1978). "Rift Valley Fever virus infections in Egypt: Pathological and virological findings in man." Trans R Soc Trop Med Hyg **72**: 392-396.
- Abdel-Wahab, K. S., L. M. El Baz, E. M. El-Tayeb, H. Omar, M. A. Ossman and W. Yasin (1978). "Rift Valley Fever virus infections in Egypt: Pathological and virological findings in man." Trans R Soc Trop Med Hyg **72**(4): 392-396.
- Adam, A. A., M. S. Karsany and I. Adam (2010). "Manifestations of severe Rift Valley fever in Sudan." Int J Infect Dis **14**(2): e179-180.
- Aggarwal, B. B., W. J. Kohr, P. E. Hass, B. Moffat, S. A. Spencer, W. J. Henzel, T. S. Bringman, G. E. Nedwin, D. V. Goeddel and R. N. Harkins (1985). "Human tumor necrosis factor. Production, purification, and characterization." J Biol Chem **260**(4): 2345-2354.
- Al-Hazmi, A., A. A. Al-Rajhi, E. B. Abboud, E. A. Ayoola, M. Al-Hazmi, R. Saadi and N. Ahmed (2005). "Ocular complications of Rift Valley fever outbreak in Saudi Arabia." Ophthalmology **112**(2): 313-318.
- Al-Hazmi, M., E. A. Ayoola, M. Abdurahman, S. Banzal, J. Ashraf, A. El-Bushra, A. Hazmi, M. Abdullah, H. Abbo, A. Elamin, *et al.* (2003). "Epidemic Rift Valley fever in Saudi Arabia: a clinical study of severe illness in humans." Clin Infect Dis **36**(3): 245-252.
- Alrajhi, A. A., A. Al-Semari, J. Al-Watban. (May 2004). "Rift Valley fever encephalitis." Emerging Infectious Disease, from <http://www.cdc.gov/ncidod/EID/vol10no3/02-0817.htm>.
- Anderson, G. W., Jr., J. O. Lee, A. O. Anderson, N. Powell, J. A. Mangiafico and G. Meadors (1991). "Efficacy of a Rift Valley fever virus vaccine against an aerosol infection in rats." Vaccine **9**(10): 710-714.
- Anderson, G. W., Jr. and C. J. Peters (1988). "Viral determinants of virulence for Rift Valley fever (RVF) in rats." Microb Pathog **5**(4): 241-250.
- Anderson, G. W., Jr. and J. F. Smith (1987). "Immunoelectron microscopy of Rift Valley fever viral morphogenesis in primary rat hepatocytes." Virology **161**(1): 91-100.
- Aujla, S. J., P. J. Dubin and J. K. Kolls (2007). "Interleukin-17 in pulmonary host defense." Exp Lung Res **33**(10): 507-518.

- Aujla, S. J., P. J. Dubin and J. K. Kolls (2007). "Th17 cells and mucosal host defense." Semin Immunol **19**(6): 377-382.
- Austin, D., A. Baer, L. Lundberg, N. Shafagati, A. Schoonmaker, A. Narayanan, T. Popova, J. J. Panthier, F. Kashanchi, C. Bailey, *et al.* (2012). "p53 Activation following Rift Valley fever virus infection contributes to cell death and viral production." PLoS One **7**(5): e36327.
- Baer, A., D. Austin, A. Narayanan, T. Popova, M. Kainulainen, C. Bailey, F. Kashanchi, F. Weber and K. Kehn-Hall (2012). "Induction of DNA Damage Signaling upon Rift Valley Fever Virus Infection Results in Cell Cycle Arrest and Increased Viral Replication." J Biol Chem **287**(10): 7399-7410.
- Bales, J. M., D. S. Powell, L. M. Bethel, D. S. Reed and A. L. Hartman (2012). "Choice of inbred rat strain impacts lethality and disease course after respiratory infection with Rift Valley Fever Virus." Front Cell Infect Microbiol **2**: 105.
- Barnard, B. J. and M. J. Botha (1977). "An inactivated rift valley fever vaccine." J S Afr Vet Assoc **48**(1): 45-48.
- Bartelloni, P. J. and R. B. Tesh (1976). "Clinical and serologic responses of volunteers infected with phlebotomus fever virus (Sicilian type)." Am J Trop Med Hyg **25**(3): 456-462.
- Baskerville, A., K. A. Hubbard and J. R. Stephenson (1992). "Comparison of the pathogenicity for pregnant sheep of Rift Valley fever virus and a live attenuated vaccine." Res Vet Sci **52**(3): 307-311.
- Belakova, J., M. Horynova, M. Krupka, E. Weigl and M. Raska (2007). "DNA vaccines: are they still just a powerful tool for the future?" Arch Immunol Ther Exp (Warsz) **55**(6): 387-398.
- Benferhat, R., T. Josse, B. Albaud, D. Gentien, Z. Mansuroglu, V. Marcato, S. Soues, B. Le Bonniec, M. Bouloy and E. Bonnefoy (2012). "Large-scale chromatin immunoprecipitation with promoter sequence microarray analysis of the interaction of the NSs protein of Rift Valley fever virus with regulatory DNA regions of the host genome." J Virol **86**(20): 11333-11344.
- Bhardwaj, N., M. T. Heise and T. M. Ross (2010). "Vaccination with DNA plasmids expressing Gn coupled to C3d or alphavirus replicons expressing gn protects mice against Rift Valley fever virus." PLoS Negl Trop Dis **4**(6): e725.
- Billecocq, A., M. Spiegel, P. Vialat, A. Kohl, F. Weber, M. Bouloy and O. Haller (2004). "NSs protein of Rift Valley fever virus blocks interferon production by inhibiting host gene transcription." J Virol **78**(18): 9798-9806.
- Bird, B. H., C. G. Albarino, A. L. Hartman, B. R. Erickson, T. G. Ksiazek and S. T. Nichol (2008). "Rift valley fever virus lacking the NSs and NSm genes is highly attenuated, confers protective immunity from virulent virus challenge, and allows for differential identification of infected and vaccinated animals." J Virol **82**(6): 2681-2691.

- Bird, B. H., M. L. Khristova, P. E. Rollin, T. G. Ksiazek and S. T. Nichol (2007). "Complete genome analysis of 33 ecologically and biologically diverse Rift Valley fever virus strains reveals widespread virus movement and low genetic diversity due to recent common ancestry." J Virol **81**(6): 2805-2816.
- Bird, B. H., T. G. Ksiazek, S. T. Nichol and N. J. Maclachlan (2009). "Rift Valley fever virus." J Am Vet Med Assoc **234**(7): 883-893.
- Boshra, H., G. Lorenzo, F. Rodriguez and A. Brun (2011). "A DNA vaccine encoding ubiquitinated Rift Valley fever virus nucleoprotein provides consistent immunity and protects IFNAR(-/-) mice upon lethal virus challenge." Vaccine **29**(27): 4469-4475.
- Botros, B., A. Omar, K. Elian, G. Mohamed, A. Soliman, A. Salib, D. Salman, M. Saad and K. Earhart (2006). "Adverse response of non-indigenous cattle of European breeds to live attenuated Smithburn Rift Valley fever vaccine." J Med Virol **78**(6): 787-791.
- Bouloy, M. (2011). Molecular Biology of Phleboviruses. Bunyaviridae molecular and cellular biology. A. Plyusnin, Richard M. Elliott ed. Norfolk, UK, Caister Academic Press: 95-128.
- Bouloy, M., C. Janzen, P. Vialat, H. Khun, J. Pavlovic, M. Huerre and O. Haller (2001). "Genetic evidence for an interferon-antagonistic function of rift valley fever virus nonstructural protein NSs." J Virol **75**(3): 1371-1377.
- Boyle, J. J. (2005). "Macrophage activation in atherosclerosis: pathogenesis and pharmacology of plaque rupture." Curr Vasc Pharmacol **3**(1): 63-68.
- Brasier, A. R. (2006). "The NF-kappaB regulatory network." Cardiovasc Toxicol **6**(2): 111-130.
- Brasier, A. R., A. Recinos, 3rd and M. S. Eledrisi (2002). "Vascular inflammation and the renin-angiotensin system." Arterioscler Thromb Vasc Biol **22**(8): 1257-1266.
- Brown, J. L., J. W. Dominik and R. L. Morrissey (1981). "Respiratory infectivity of a recently isolated Egyptian strain of Rift Valley fever virus." Infect Immun **33**(3): 848-853.
- Bystrom, J., N. Al-Adhoubi, M. Al-Bogami, A. S. Jawad and R. A. Mageed "Th17 lymphocytes in respiratory syncytial virus infection." Viruses **5**(3): 777-791.
- Caplen, H., C. J. Peters and D. H. Bishop (1985). "Mutagen-directed attenuation of Rift Valley fever virus as a method for vaccine development." J Gen Virol **66** (Pt 10): 2271-2277.
- Capstick, P. B. and D. Gosden (1962). "Neutralizing antibody response of sheep to pantropic and neutrotropic rift valley fever virus." Nature **195**: 583-584.
- CDC. (2009). "Rift Valley Fever encephalitis." Retrieved May, 2012, from [<http://www.cdc.gov/ncidod/EID/vol10no3/02-0817.htm>].

- Chehab, N. H., A. Malikzay, M. Appel and T. D. Halazonetis (2000). "Chk2/hCds1 functions as a DNA damage checkpoint in G(1) by stabilizing p53." Genes Dev **14**(3): 278-288.
- Chia, J. K., M. Pollack, G. Guelde, N. L. Koles, M. Miller and M. E. Evans (1989). "Lipopolysaccharide (LPS)-reactive monoclonal antibodies fail to inhibit LPS-induced tumor necrosis factor secretion by mouse-derived macrophages." J Infect Dis **159**(5): 872-880.
- Coackley, W., A. Pini and D. Gosden (1967). "The immunity induced in cattle and sheep by inoculation of neurotropic or pantropic Rift Valley fever viruses." Res Vet Sci **8**(4): 406-414.
- Coetzer, J. A. and B. J. Barnard (1977). "Hydrops amnii in sheep associated with hydranencephaly and arthrogryposis with wesselsbron disease and rift valley fever viruses as aetiological agents." Onderstepoort J Vet Res **44**(2): 119-126.
- Coetzer, J. A. and K. G. Ishak (1982). "Sequential development of the liver lesions in new-born lambs infected with Rift Valley fever virus. I. Macroscopic and microscopic pathology." Onderstepoort J Vet Res **49**(2): 103-108.
- Connolly-Andersen, A. M., I. Douagi, A. A. Kraus and A. Mirazimi (2009). "Crimean Congo hemorrhagic fever virus infects human monocyte-derived dendritic cells." Virology **390**(2): 157-162.
- Cosgriff, T. M., J. C. Morrill, G. B. Jennings, L. A. Hodgson, M. V. Slayter, P. H. Gibbs and C. J. Peters (1989). "Hemostatic derangement produced by Rift Valley fever virus in rhesus monkeys." Rev Infect Dis **11 Suppl 4**: S807-814.
- Dash, S., R. Prabhu, S. Hazari, F. Bastian, R. Garry, W. Zou, S. Haque, V. Joshi, F. G. Regenstein and S. N. Thung (2005). "Interferons alpha, beta, gamma each inhibit hepatitis C virus replication at the level of internal ribosome entry site-mediated translation." Liver Int **25**(3): 580-594.
- Daubney, R., Hudson, J.R., Garnham, P.C. (1931). "Enzootic hepatitis or Rift Valley fever. An undescribed disease of sheep, cattle, and man from East Africa." J Path Bact **34**(2): 545-579.
- Davenport, F. M., A. V. Hennessy and T. Francis, Jr. (1953). "Epidemiologic and immunologic significance of age distribution of antibody to antigenic variants of influenza virus." J Exp Med **98**(6): 641-656.
- Davies, F. G., B. Clausen and L. J. Lund (1972). "The pathogenicity of Rift Valley fever virus for the baboon." Trans R Soc Trop Med Hyg **66**(2): 363-365.
- Davies, F. G. and R. B. Highton (1980). "Possible vectors of Rift Valley fever in Kenya." Trans R Soc Trop Med Hyg **74**(6): 815-816.
- Davies, F. G., K. J. Linthicum and A. D. James (1985). "Rainfall and epizootic Rift Valley fever." Bull World Health Organ **63**(5): 941-943.
- Davies, F. G., V. Martin (2003). Recognizing Rift Valley fever. Food and Agriculture Organization. Rome, Food and Agriculture organization of the United Nations.

- de Boer, S. M., J. Kortekaas, A. F. Antonis, J. Kant, J. L. van Oploo, P. J. Rottier, R. J. Moormann and B. J. Bosch (2010). "Rift Valley fever virus subunit vaccines confer complete protection against a lethal virus challenge." Vaccine **28**(11): 2330-2339.
- Dessau, M. and Y. Modis (2013). "Crystal structure of glycoprotein C from Rift Valley fever virus." Proc Natl Acad Sci U S A **110**(5): 1696-1701.
- Digoutte, J. P. and C. J. Peters (1989). "General aspects of the 1987 Rift Valley fever epidemic in Mauritania." Res Virol **140**(1): 27-30.
- do Valle, T. Z., A. Billecocq, L. Guillemot, R. Alberts, C. Gomet, R. Geffers, K. Calabrese, K. Schughart, M. Bouloy, X. Montagutelli, *et al.* (2010). "A new mouse model reveals a critical role for host innate immunity in resistance to Rift Valley fever." J Immunol **185**(10): 6146-6156.
- Dodd, K. A., A. K. McElroy, M. E. Jones, S. T. Nichol and C. F. Spiropoulou (2013). "Rift Valley fever virus clearance and protection from neurologic disease are dependent on CD4+ T cell and virus-specific antibody responses." J Virol **87**(11): 6161-6171.
- Donnelly, R. P., H. Dickensheets and D. S. Finbloom (1999). "The interleukin-10 signal transduction pathway and regulation of gene expression in mononuclear phagocytes." J Interferon Cytokine Res **19**(6): 563-573.
- Dungu, B., I. Louw, A. Lubisi, P. Hunter, B. F. von Teichman and M. Bouloy (2010). "Evaluation of the efficacy and safety of the Rift Valley Fever Clone 13 vaccine in sheep." Vaccine **28**(29): 4581-4587.
- Easterday, B. C. (1965). "Rift valley fever." Adv Vet Sci **10**: 65-127.
- El-Karamany, R., IZE Imam, AH Farid, *et al.* (1981). "Production of inactivated RVF vaccine." J Egypt Publ Health Assoc **56**(5-6): 495-525.
- Engdahl, C., J. Naslund, L. Lindgren, C. Ahlm and G. Bucht (2012). "The Rift Valley Fever virus protein NSm and putative cellular protein interactions." Virol J **9**: 139.
- Ergonul, O., S. Tuncbilek, N. Baykam, A. Celikbas and B. Dokuzoguz (2006). "Evaluation of serum levels of interleukin (IL)-6, IL-10, and tumor necrosis factor-alpha in patients with Crimean-Congo hemorrhagic fever." J Infect Dis **193**(7): 941-944.
- Feduchi, E., M. A. Alonso and L. Carrasco (1989). "Human gamma interferon and tumor necrosis factor exert a synergistic blockade on the replication of herpes simplex virus." J Virol **63**(3): 1354-1359.
- Felver, M. E., E. Mezey, M. McGuire, M. C. Mitchell, H. F. Herlong, G. A. Veech and R. L. Veech (1990). "Plasma tumor necrosis factor alpha predicts decreased long-term survival in severe alcoholic hepatitis." Alcohol Clin Exp Res **14**(2): 255-259.
- Ferron, F., Z. Li, E. I. Danek, D. Luo, Y. Wong, B. Coutard, V. Lantez, R. Charrel, B. Canard, T. Walz, *et al.* (2011). "The hexamer structure of Rift Valley fever virus

- nucleoprotein suggests a mechanism for its assembly into ribonucleoprotein complexes." PLoS Pathog **7**(5): e1002030.
- Findlay, G. M. (1932). "The infectivity of rift valley fever for monkeys." Trans. Roy. Soc. Trop. Med. Hyg. **26**: 161-168.
- Findlay, G. M., R. Daubney (1931). "The virus of rift valley fever or enzootic hepatitis." Lancet **221**: 1350-1351.
- Fitzgerald, K. A., Juke A.J. O'Neill, Andy J.H. Gearing, and Robin E. Callard, Ed. (2001). The Cytokine Facts Book. San Diego, CA, Academic Press.
- Flick, R. and M. Bouloy (2005). "Rift Valley fever virus." Curr Mol Med **5**(8): 827-834.
- Fontenille, D., M. Traore-Lamizana, M. Diallo, J. Thonnon, J. P. Digoutte and H. G. Zeller (1998). "New vectors of Rift Valley fever in West Africa." Emerg Infect Dis **4**(2): 289-293.
- Fredericksen, B. L., B. C. Keller, J. Fornek, M. G. Katze and M. Gale, Jr. (2008). "Establishment and maintenance of the innate antiviral response to West Nile Virus involves both RIG-I and MDA5 signaling through IPS-1." J Virol **82**(2): 609-616.
- Freiberg, A. N., M. B. Sherman, M. C. Morais, M. R. Holbrook and S. J. Watowich (2008). "Three-dimensional organization of Rift Valley fever virus revealed by cryoelectron tomography." J Virol **82**(21): 10341-10348.
- Gear, J. H. (1977). "Haemorrhagic fevers of Africa: an account of two recent outbreaks." J S Afr Vet Assoc **48**(1): 5-8.
- Gemmell, E., T. A. Winning, C. L. Carter, P. J. Ford, P. S. Bird, R. B. Ashman, D. A. Grieco and G. J. Seymour (2003). "Differences in mouse strain influence leukocyte and immunoglobulin phenotype response to *Porphyromonas gingivalis*." Oral Microbiol Immunol **18**(6): 364-370.
- Gerdes, G. H. (2004). "Rift Valley fever." Rev Sci Tech **23**(2): 613-623.
- Giese, M. (1998). "DNA-antiviral vaccines: new developments and approaches--a review." Virus Genes **17**(3): 219-232.
- Gommet, C., A. Billecocq, G. Jouvion, M. Hasan, T. Zaverucha do Valle, L. Guillemot, C. Blanchet, N. van Rooijen, X. Montagutelli, M. Bouloy, *et al.* (2011). "Tissue tropism and target cells of NSs-deleted rift valley fever virus in live immunodeficient mice." PLoS Negl Trop Dis **5**(12): e1421.
- Gowen, B. B., K. W. Bailey, D. Scharon, Z. Vest, J. B. Westover, R. Skirpstunas and T. Ikegami (2013). "Post-exposure vaccination with MP-12 lacking NSs protects mice against lethal Rift Valley fever virus challenge." Antiviral Res **98**(2): 135-143.
- Gras, G. and M. Kaul (2010). "Molecular mechanisms of neuroinvasion by monocytes-macrophages in HIV-1 infection." Retrovirology **7**: 30.
- Gray, K. K., M. N. Worthy, T. L. Juelich, S. L. Agar, A. Poussard, D. Ragland, A. N. Freiberg and M. R. Holbrook (2012). "Chemotactic and inflammatory responses

- in the liver and brain are associated with pathogenesis of Rift Valley fever virus infection in the mouse." *PLoS Negl Trop Dis* **6**(2): e1529.
- Gro, M. C., P. Di Bonito, L. Accardi and C. Giorgi (1992). "Analysis of 3' and 5' ends of N and NSs messenger RNAs of Toscana Phlebovirus." *Virology* **191**(1): 435-438.
- Gupta, M., S. Mahanty, R. Ahmed and P. E. Rollin (2001). "Monocyte-derived human macrophages and peripheral blood mononuclear cells infected with ebola virus secrete MIP-1alpha and TNF-alpha and inhibit poly-IC-induced IFN-alpha in vitro." *Virology* **284**(1): 20-25.
- Habjan, M., N. Penski, V. Wagner, M. Spiegel, A. K. Overby, G. Kochs, J. T. Huiskonen and F. Weber (2009). "Efficient production of Rift Valley fever virus-like particles: The antiviral protein MxA can inhibit primary transcription of bunyaviruses." *Virology* **385**(2): 400-408.
- Habjan, M., A. Pichlmair, R. M. Elliott, A. K. Overby, T. Glatter, M. Gstaiger, G. Superti-Furga, H. Unger and F. Weber (2009). "NSs protein of rift valley fever virus induces the specific degradation of the double-stranded RNA-dependent protein kinase." *J Virol* **83**(9): 4365-4375.
- Han, Y., M. S. Runge and A. R. Brasier (1999). "Angiotensin II induces interleukin-6 transcription in vascular smooth muscle cells through pleiotropic activation of nuclear factor-kappa B transcription factors." *Circ Res* **84**(6): 695-703.
- Hartley, D. M., J. L. Rinderknecht, T. L. Nipp, N. P. Clarke and G. D. Snowder (2011). "Potential effects of Rift Valley fever in the United States." *Emerg Infect Dis* **17**(8): e1.
- Hayashi, Y. and K. Koike (1989). "Interferon inhibits hepatitis B virus replication in a stable expression system of transfected viral DNA." *J Virol* **63**(7): 2936-2940.
- Heinzel, F. P., M. D. Sadick, B. J. Holaday, R. L. Coffman and R. M. Locksley (1989). "Reciprocal expression of interferon gamma or interleukin 4 during the resolution or progression of murine leishmaniasis. Evidence for expansion of distinct helper T cell subsets." *J Exp Med* **169**(1): 59-72.
- Henriques, A., C. Pitzer, L. Dupuis and A. Schneider (2010). "G-CSF protects motoneurons against axotomy-induced apoptotic death in neonatal mice." *BMC Neurosci* **11**: 25.
- Hsieh, C. S., S. E. Macatonia, C. S. Tripp, S. F. Wolf, A. O'Garra and K. M. Murphy (1993). "Development of TH1 CD4+ T cells through IL-12 produced by Listeria-induced macrophages." *Science* **260**(5107): 547-549.
- Hubbard, K. A., A. Baskerville and J. R. Stephenson (1991). "Ability of a mutagenized virus variant to protect young lambs from Rift Valley fever." *Am J Vet Res* **52**(1): 50-55.
- Huiskonen, J. T., A. K. Overby, F. Weber and K. Grunewald (2009). "Electron cryo-microscopy and single-particle averaging of Rift Valley fever virus: evidence for GN-GC glycoprotein heterodimers." *J Virol* **83**(8): 3762-3769.

- Hunter, P., B. J. Erasmus and J. H. Vorster (2002). "Teratogenicity of a mutagenised Rift Valley fever virus (MVP 12) in sheep." Onderstepoort J Vet Res **69**(1): 95-98.
- Hutchinson, K. L. and P. E. Rollin (2007). "Cytokine and chemokine expression in humans infected with Sudan Ebola virus." J Infect Dis **196 Suppl 2**: S357-363.
- Ikegami, T. (2012). "Molecular biology and genetic diversity of Rift Valley fever virus." Antiviral Res **95**(3): 293-310.
- Ikegami, T. and S. Makino (2009). "Rift valley fever vaccines." Vaccine **27 Suppl 4**: D69-72.
- Ikegami, T. and S. Makino (2011). "The Pathogenesis of Rift Valley Fever." Viruses **3**(5): 493-519.
- Ikegami, T., K. Narayanan, S. Won, W. Kamitani, C. J. Peters and S. Makino (2009). "Dual functions of Rift Valley fever virus NSs protein: inhibition of host mRNA transcription and post-transcriptional downregulation of protein kinase PKR." Ann N Y Acad Sci **1171 Suppl 1**: E75-85.
- Ikegami, T., K. Narayanan, S. Won, W. Kamitani, C. J. Peters and S. Makino (2009). "Rift Valley fever virus NSs protein promotes post-transcriptional downregulation of protein kinase PKR and inhibits eIF2alpha phosphorylation." PLoS Pathog **5**(2): e1000287.
- Ikegami, T., S. Won, C. J. Peters and S. Makino (2005). "Rift Valley fever virus NSs mRNA is transcribed from an incoming anti-viral-sense S RNA segment." J Virol **79**(18): 12106-12111.
- Ikegami, T., S. Won, C. J. Peters and S. Makino (2006). "Rescue of infectious rift valley fever virus entirely from cDNA, analysis of virus lacking the NSs gene, and expression of a foreign gene." J Virol **80**(6): 2933-2940.
- Ishak, K. G., D. H. Walker, J. A. Coetzer, J. J. Gardner and L. Gorelkin (1982). "Viral hemorrhagic fevers with hepatic involvement: pathologic aspects with clinical correlations." Prog Liver Dis **7**: 495-515.
- Jansen van Vuren, P., C. T. Tiemessen and J. T. Paweska (2011). "Anti-nucleocapsid protein immune responses counteract pathogenic effects of Rift Valley fever virus infection in mice." PLoS One **6**(9): e25027.
- Jia, T. and E. G. Pamer (2009). "Immunology. Dispensable but not irrelevant." Science **325**(5940): 549-550.
- Kalveram, B., O. Lihoradova and T. Ikegami (2011). "NSs protein of rift valley fever virus promotes posttranslational downregulation of the TFIIF subunit p62." J Virol **85**(13): 6234-6243.
- Kalveram, B., O. Lihoradova, S. V. Indran, N. Lokugamage, J. A. Head and T. Ikegami (2013). "Rift Valley fever virus NSs inhibits host transcription independently of the degradation of dsRNA-dependent protein kinase PKR." Virology **435**(2): 415-424.

- Kamal, S. A. (2009). "Pathological studies on postvaccinal reactions of Rift Valley fever in goats." *Virol J* **6**: 94.
- Kant, S., W. Swat, S. Zhang, Z. Y. Zhang, B. G. Neel, R. A. Flavell and R. J. Davis (2011). "TNF-stimulated MAP kinase activation mediated by a Rho family GTPase signaling pathway." *Genes Dev* **25**(19): 2069-2078.
- Karin, M. and E. Gallagher (2005). "From JNK to pay dirt: jun kinases, their biochemistry, physiology and clinical importance." *IUBMB Life* **57**(4-5): 283-295.
- Karin, M. and F. R. Greten (2005). "NF-kappaB: linking inflammation and immunity to cancer development and progression." *Nat Rev Immunol* **5**(10): 749-759.
- Kark, J. D., Y. Aynor and C. J. Peters (1982). "A rift Valley fever vaccine trial. I. Side effects and serologic response over a six-month follow-up." *Am J Epidemiol* **116**(5): 808-820.
- Kark, J. D., Y. Aynor and C. J. Peters (1985). "A Rift Valley fever vaccine trial: 2. Serological response to booster doses with a comparison of intradermal versus subcutaneous injection." *Vaccine* **3**(2): 117-122.
- Kasari, T. R., D. A. Carr, T. V. Lynn and J. T. Weaver (2008). "Evaluation of pathways for release of Rift Valley fever virus into domestic ruminant livestock, ruminant wildlife, and human populations in the continental United States." *J Am Vet Med Assoc* **232**(4): 514-529.
- Kaushansky, K. (2006). "Hematopoietic growth factors, signaling and the chronic myeloproliferative disorders." *Cytokine Growth Factor Rev* **17**(6): 423-430.
- Kendrick, T. S. and M. A. Bogoyevitch (2007). "Activation of mitogen-activated protein kinase pathways by the granulocyte colony-stimulating factor receptor: mechanisms and functional consequences." *Front Biosci* **12**: 591-607.
- Koenig, S., H. E. Gendelman, J. M. Orenstein, M. C. Dal Canto, G. H. Pezeshkpour, M. Yungbluth, F. Janotta, A. Aksamit, M. A. Martin and A. S. Fauci (1986). "Detection of AIDS virus in macrophages in brain tissue from AIDS patients with encephalopathy." *Science* **233**(4768): 1089-1093.
- Konishi, H., K. Okamoto, Y. Ohmori, H. Yoshino, H. Ohmori, M. Ashihara, Y. Hirata, A. Ohta, H. Sakamoto, N. Hada, *et al.* (2012). "An orally available, small-molecule interferon inhibits viral replication." *Sci Rep* **2**: 259.
- Kortekaas, J., A. F. Antonis, J. Kant, R. P. Vloet, A. Vogel, N. Oreshkova, S. M. de Boer, B. J. Bosch and R. J. Moormann (2012). "Efficacy of three candidate Rift Valley fever vaccines in sheep." *Vaccine* **30**(23): 3423-3429.
- Koukuntla, R., R. B. Mandell and R. Flick (2012). "Virus-like particle-based countermeasures against Rift Valley fever virus." *Zoonoses Public Health* **59 Suppl 2**: 142-150.
- Lagerqvist, N., J. Naslund, A. Lundkvist, M. Bouloy, C. Ahlm and G. Bucht (2009). "Characterisation of immune responses and protective efficacy in mice after immunisation with Rift Valley Fever virus cDNA constructs." *Virol J* **6**: 6.

- Laughlin, L. W., J. M. Meegan, L. J. Strausbaugh, D. M. Morens and R. H. Watten (1979). "Epidemic Rift Valley fever in Egypt: observations of the spectrum of human illness." Trans R Soc Trop Med Hyg **73**(6): 630-633.
- Le May, N., S. Dubaele, L. Proietti De Santis, A. Billecocq, M. Bouloy and J. M. Egly (2004). "TFIIH transcription factor, a target for the Rift Valley hemorrhagic fever virus." Cell **116**(4): 541-550.
- Le May, N., Z. Mansuroglu, P. Leger, T. Josse, G. Blot, A. Billecocq, R. Flick, Y. Jacob, E. Bonnefoy and M. Bouloy (2008). "A SAP30 complex inhibits IFN-beta expression in Rift Valley fever virus infected cells." PLoS Pathog **4**(1): e13.
- Lee, Y. R., M. T. Liu, H. Y. Lei, C. C. Liu, J. M. Wu, Y. C. Tung, Y. S. Lin, T. M. Yeh, S. H. Chen and H. S. Liu (2006). "MCP-1, a highly expressed chemokine in dengue haemorrhagic fever/dengue shock syndrome patients, may cause permeability change, possibly through reduced tight junctions of vascular endothelium cells." J Gen Virol **87**(Pt 12): 3623-3630.
- Lehtonen, A., S. Matikainen and I. Julkunen (1997). "Interferons up-regulate STAT1, STAT2, and IRF family transcription factor gene expression in human peripheral blood mononuclear cells and macrophages." J Immunol **159**(2): 794-803.
- Lin, K., A. D. Kwong and C. Lin (2004). "Combination of a hepatitis C virus NS3-NS4A protease inhibitor and alpha interferon synergistically inhibits viral RNA replication and facilitates viral RNA clearance in replicon cells." Antimicrob Agents Chemother **48**(12): 4784-4792.
- Linthicum, K. J., F. G. Davies, A. Kairo and C. L. Bailey (1985). "Rift Valley fever virus (family Bunyaviridae, genus Phlebovirus). Isolations from Diptera collected during an inter-epizootic period in Kenya." J Hyg (Lond) **95**(1): 197-209.
- Liu, L., J. Spurrier, T. R. Butt and J. E. Strickler (2008). "Enhanced protein expression in the baculovirus/insect cell system using engineered SUMO fusions." Protein Expr Purif **62**(1): 21-28.
- Locksley, R. M., F. P. Heinzl, B. J. Holaday, S. S. Mutha, S. L. Reiner and M. D. Sadick (1991). "Induction of Th1 and Th2 CD4+ subsets during murine Leishmania major infection." Res Immunol **142**(1): 28-32.
- Lokugamage, N., A. N. Freiberg, J. C. Morrill and T. Ikegami (2012). "Genetic subpopulations of Rift Valley fever virus strains ZH548 and MP-12 and recombinant MP-12 strains." J Virol **86**(24): 13566-13575.
- Lozach, P. Y., A. Kuhbacher, R. Meier, R. Mancini, D. Bitto, M. Bouloy and A. Helenius (2011). "DC-SIGN as a receptor for phleboviruses." Cell Host Microbe **10**(1): 75-88.
- Lubroth, J., M. M. Rweyemamu, G. Viljoen, A. Diallo, B. Dungu and W. Amanfu (2007). "Veterinary vaccines and their use in developing countries." Rev Sci Tech **26**(1): 179-201.
- Maar, S. A., R. Swanepoel and M. Gelfand (1979). "Rift Valley fever encephalitis. A description of a case." Cent Afr J Med **25**(1): 8-11.

- Madani, T. A., Y. Y. Al-Mazrou, M. H. Al-Jeffri, A. A. Mishkhas, A. M. Al-Rabeah, A. M. Turkistani, M. O. Al-Sayed, A. A. Abodahish, A. S. Khan, T. G. Ksiazek, *et al.* (2003). "Rift Valley fever epidemic in Saudi Arabia: epidemiological, clinical, and laboratory characteristics." Clin Infect Dis **37**(8): 1084-1092.
- Mandell, R. B., R. Koukuntla, L. J. Mogler, A. K. Carzoli, A. N. Freiberg, M. R. Holbrook, B. K. Martin, W. R. Staplin, N. N. Vahanian, C. J. Link, *et al.* (2010). "A replication-incompetent Rift Valley fever vaccine: chimeric virus-like particles protect mice and rats against lethal challenge." Virology **397**(1): 187-198.
- Mansuroglu, Z., T. Josse, J. Gilleron, A. Billecocq, P. Leger, M. Bouloy and E. Bonnefoy (2010). "Nonstructural NSs protein of rift valley fever virus interacts with pericentromeric DNA sequences of the host cell, inducing chromosome cohesion and segregation defects." J Virol **84**(2): 928-939.
- Mathieu, C., C. Pohl, J. Szecsi, S. Trajkovic-Bodennec, S. Devergnas, H. Raoul, F. L. Cosset, D. Gerlier, T. F. Wild and B. Horvat (2011). "Nipah virus uses leukocytes for efficient dissemination within a host." J Virol **85**(15): 7863-7871.
- McElroy, A. K. and S. T. Nichol (2012). "Rift Valley fever virus inhibits a pro-inflammatory response in experimentally infected human monocyte derived macrophages and a pro-inflammatory cytokine response may be associated with patient survival during natural infection." Virology **422**(1): 6-12.
- McGavran, M. H. and B. C. Easterday (1963). "Rift Valley Fever Virus Hepatitis: Light and Electron Microscopic Studies in the Mouse." Am J Pathol **42**(5): 587-607.
- McIntosh, B. M., D. Russell, I. dos Santos and J. H. Gear (1980). "Rift Valley fever in humans in South Africa." S Afr Med J **58**(20): 803-806.
- Medeot, S. I., M. S. Contigiani, M. S. Sabattini and A. Camara (1995). "The role of mononuclear blood cells in experimental Junin virus spread to the central nervous system." Viral Immunol **8**(2): 101-108.
- Meegan, J. M. (1979). "The Rift Valley fever epizootic in Egypt 1977-78. 1. Description of the epizootic and virological studies." Trans R Soc Trop Med Hyg **73**(6): 618-623.
- Meegan, J. M. (1979). "The Rift Valley fever epizootic in Egypt 1977-78. 1. Description of the epizootic and virological studies." Trans R Soc Trop Med Hyg **73**(6): 618-623.
- Meegan, J. M., Bailey CL (1989). "Rift Valley fever." Monath TP, ed. The arboviruses: epidemiology and ecology **IV**: 51-76.
- Meegan, J. M., C.J. Bailey (1988). Rift Valley Fever. Boca Raton, FL, CRC Press Inc.
- Meegan, J. M., H. Hoogstraal and M. I. Moussa (1979). "An epizootic of Rift Valley fever in Egypt in 1977." Vet Rec **105**(6): 124-125.
- Miagostovich, M. P., R. G. Ramos, A. F. Nicol, R. M. Nogueira, T. Cuzzi-Maya, A. V. Oliveira, R. S. Marchevsky, R. P. Mesquita and H. G. Schatzmayr (1997). "Retrospective study on dengue fatal cases." Clin Neuropathol **16**(4): 204-208.

- Milstone, L. M. and B. H. Waksman (1970). "Release of virus inhibitor from tuberculin-sensitized peritoneal cells stimulated by antigen." J Immunol **105**(5): 1068-1071.
- Mims, C. A. (1956). "Rift Valley Fever virus in mice. I. General features of the infection." Br J Exp Pathol **37**(2): 99-109.
- Misslitz, A. C., K. Bonhagen, D. Harbecke, C. Lippuner, T. Kamradt and T. Aebischer (2004). "Two waves of antigen-containing dendritic cells in vivo in experimental *Leishmania major* infection." Eur J Immunol **34**(3): 715-725.
- Morrill, J. C., L. Carpenter, D. Taylor, H. H. Ramsburg, J. Quance and C. J. Peters (1991). "Further evaluation of a mutagen-attenuated Rift Valley fever vaccine in sheep." Vaccine **9**(1): 35-41.
- Morrill, J. C., C. W. Czarniecki and C. J. Peters (1991). "Recombinant human interferon-gamma modulates Rift Valley fever virus infection in the rhesus monkey." J Interferon Res **11**(5): 297-304.
- Morrill, J. C., T. Ikegami, N. Yoshikawa-Iwata, N. Lokugamage, S. Won, K. Terasaki, A. Zamoto-Niikura, C. J. Peters and S. Makino (2010). "Rapid accumulation of virulent rift valley Fever virus in mice from an attenuated virus carrying a single nucleotide substitution in the m RNA." PLoS One **5**(4): e9986.
- Morrill, J. C., G. B. Jennings, H. Caplen, M. J. Turell, A. J. Johnson and C. J. Peters (1987). "Pathogenicity and immunogenicity of a mutagen-attenuated Rift Valley fever virus immunogen in pregnant ewes." Am J Vet Res **48**(7): 1042-1047.
- Morrill, J. C., G. B. Jennings, T. M. Cosgriff, P. H. Gibbs and C. J. Peters (1989). "Prevention of Rift Valley fever in rhesus monkeys with interferon-alpha." Rev Infect Dis **11 Suppl 4**: S815-825.
- Morrill, J. C., G. B. Jennings, A. J. Johnson, T. M. Cosgriff, P. H. Gibbs and C. J. Peters (1990). "Pathogenesis of Rift Valley fever in rhesus monkeys: role of interferon response." Arch Virol **110**(3-4): 195-212.
- Morrill, J. C., B. K. Johnson, C. Hyams, F. Okoth, P. M. Tukei, M. Mugambi and J. Woody (1991). "Serological evidence of arboviral infections among humans of coastal Kenya." J Trop Med Hyg **94**(3): 166-168.
- Morrill, J. C., C. A. Mebus and C. J. Peters (1997). "Safety and efficacy of a mutagen-attenuated Rift Valley fever virus vaccine in cattle." Am J Vet Res **58**(10): 1104-1109.
- Morrill, J. C., C. A. Mebus and C. J. Peters (1997). "Safety of a mutagen-attenuated Rift Valley fever virus vaccine in fetal and neonatal bovids." Am J Vet Res **58**(10): 1110-1114.
- Morrill, J. C. and C. J. Peters (2003). "Pathogenicity and neurovirulence of a mutagen-attenuated Rift Valley fever vaccine in rhesus monkeys." Vaccine **21**(21-22): 2994-3002.
- Moussa, M. I., K. S. Abdel-Wahab and O. L. Wood (1986). "Experimental infection and protection of lambs with a minute plaque variant of Rift Valley fever virus." Am J Trop Med Hyg **35**(3): 660-662.

- Moutailler, S., G. Krida, F. Schaffner, M. Vazeille and A. B. Failloux (2008). "Potential vectors of Rift Valley fever virus in the Mediterranean region." Vector Borne Zoonotic Dis **8**(6): 749-753.
- Muller, R., J. F. Saluzzo, N. Lopez, T. Dreier, M. Turell, J. Smith and M. Bouloy (1995). "Characterization of clone 13, a naturally attenuated avirulent isolate of Rift Valley fever virus, which is altered in the small segment." Am J Trop Med Hyg **53**(4): 405-411.
- Narayanan, A., T. Popova, M. Turell, J. Kidd, J. Chertow, S. G. Popov, C. Bailey, F. Kashanchi and K. Kehn-Hall (2011). "Alteration in superoxide dismutase 1 causes oxidative stress and p38 MAPK activation following RVFV infection." PLoS One **6**(5): e20354.
- Naslund, J., N. Lagerqvist, M. Habjan, A. Lundkvist, M. Evander, C. Ahlm, F. Weber and G. Bucht (2009). "Vaccination with virus-like particles protects mice from lethal infection of Rift Valley Fever Virus." Virology **385**(2): 409-415.
- Nfon, C. K., P. Marszal, S. Zhang and H. M. Weingartl (2012). "Innate immune response to Rift Valley fever virus in goats." PLoS Negl Trop Dis **6**(4): e1623.
- NICD. (2011, May 20, 2011). "Interim report on the 2011 Rift valley fever (RVF) outbreak in South Africa." Rift Valley fever outbreak Retrieved June 26, 2011, from http://www.nicd.ac.za/?page=rift_valley_fever_outbreak&id=94.
- Niklasson, B. S., G. F. Meadors and C. J. Peters (1984). "Active and passive immunization against Rift Valley fever virus infection in Syrian hamsters." Acta Pathol Microbiol Immunol Scand C **92**(4): 197-200.
- O'Gorman, M. R. G. a. A. D. D., Ed. (2008). Handbook of Human Immunology. Boca Raton, FL, CRC Press, Taylor & Francis Group.
- Olajide, O. A., H. S. Bhatia, A. C. de Oliveira, C. W. Wright and B. L. Fiebich (2013). "Anti-neuroinflammatory properties of synthetic cryptolepine in human neuroblastoma cells: Possible involvement of NF-kappaB and p38 MAPK inhibition." Eur J Med Chem **63C**: 333-339.
- Olsson, A., C. Manzl, A. Strasser and A. Villunger (2007). "How important are post-translational modifications in p53 for selectivity in target-gene transcription and tumour suppression?" Cell Death Differ **14**(9): 1561-1575.
- Pan, C. H., E. S. Kim, S. H. Jung, C. W. Nho and J. K. Lee (2008). "Tectorigenin inhibits IFN-gamma/LPS-induced inflammatory responses in murine macrophage RAW 264.7 cells." Arch Pharm Res **31**(11): 1447-1456.
- Papa, A., S. Bino, E. Velo, A. Harxhi, M. Kota and A. Antoniadis (2006). "Cytokine levels in Crimean-Congo hemorrhagic fever." J Clin Virol **36**(4): 272-276.
- Patterson, J. L., B. Holloway and D. Kolakofsky (1984). "La Crosse virions contain a primer-stimulated RNA polymerase and a methylated cap-dependent endonuclease." J Virol **52**(1): 215-222.
- Peters, C. J., GW Anderson Jr (1981). "Pathogenesis of Rift Valley fever." Contr epidem Biostatist **3**: 21-41.

- Peters, C. J., D. Jones, R. Trotter, J. Donaldson, J. White, E. Stephen and T. W. Slone, Jr. (1988). "Experimental Rift Valley fever in rhesus macaques." Arch Virol **99**(1-2): 31-44.
- Peters, C. J., KJ Linthicum (1994). Rift Valley Fever. Handbook of zoonoses, section B. Viral 2nd ed. G. W. Beran, JH Steele. Boca Raton, FL, CRC Press: 125-138.
- Peters, C. J., C. T. Liu, G. W. Anderson, Jr., J. C. Morrill and P. B. Jahrling (1989). "Pathogenesis of viral hemorrhagic fevers: Rift Valley fever and Lassa fever contrasted." Rev Infect Dis **11 Suppl 4**: S743-749.
- Peters, C. J. and T. W. Slone (1982). "Inbred rat strains mimic the disparate human response to Rift Valley fever virus infection." J Med Virol **10**(1): 45-54.
- Peters, C. J., Spertzel R., Patrick W. (2002). Aerosol technology and biological weapons. Biological Threats and Terrorism: Assessing the Science and Response Capabilities. S. L. Knobler, AAF Mahmoud, LA Pray. Washington, National Academy Press: 66-77.
- Pichlmair, A., M. Habjan, H. Unger and F. Weber (2010). "Virus-like particles expressing the nucleocapsid gene as an efficient vaccine against Rift Valley fever virus." Vector Borne Zoonotic Dis **10**(7): 701-703.
- Pinto, E. F., M. de Mello Cortezia and B. Rossi-Bergmann (2003). "Interferon-gamma-inducing oral vaccination with *Leishmania amazonensis* antigens protects BALB/c and C57BL/6 mice against cutaneous leishmaniasis." Vaccine **21**(25-26): 3534-3541.
- Piper, M. E., D. R. Sorenson and S. R. Gerrard (2011). "Efficient cellular release of Rift Valley fever virus requires genomic RNA." PLoS One **6**(3): e18070.
- Pittman, P., CT Liu, TL Cannon, RS Makuch, JA Mangiafico, PH Gibbs et. al (2000). "Immunogenicity of an inactivated Rift Valley fever vaccine in humans: a 12-year experience." Vaccine **18**(1-2): 181-189.
- Popova, T. G., M. J. Turell, V. Espina, K. Kehn-Hall, J. Kidd, A. Narayanan, L. Liotta, E. F. Petricoin, 3rd, F. Kashanchi, C. Bailey, *et al.* (2010). "Reverse-phase phosphoproteome analysis of signaling pathways induced by Rift valley fever virus in human small airway epithelial cells." PLoS One **5**(11): e13805.
- Randall, R., C. J. Gibbs, Jr., C. G. Aulisio, L. N. Binn and V. R. Harrison (1962). "The development of a formalin-killed Rift Valley fever virus vaccine for use in man." J Immunol **89**: 660-671.
- Raymond, D. D., M. E. Piper, S. R. Gerrard, G. Skiniotis and J. L. Smith (2012). "Phleboviruses encapsidate their genomes by sequestering RNA bases." Proc Natl Acad Sci U S A **109**(47): 19208-19213.
- Raymond, D. D., M. E. Piper, S. R. Gerrard and J. L. Smith (2010). "Structure of the Rift Valley fever virus nucleocapsid protein reveals another architecture for RNA encapsidation." Proc Natl Acad Sci U S A **107**(26): 11769-11774.
- Reed, C., K. Lin, C. Wilhelmsen, B. Friedrich, A. Nalca, A. Keeney, G. Donnelly, J. Shamblin, L. E. Hensley, G. Olinger, *et al.* (2013). "Aerosol exposure to Rift

- Valley fever virus causes earlier and more severe neuropathology in the murine model, which has important implications for therapeutic development." PLoS Negl Trop Dis **7**(4): e2156.
- Reed, C., K. E. Steele, A. Honko, J. Shamblin, L. E. Hensley and D. R. Smith (2012). "Ultrastructural study of Rift Valley fever virus in the mouse model." Virology **431**(1-2): 58-70.
- Ritchie, A. J., A. O. Yam, K. M. Tanabe, S. A. Rice and M. A. Cooley (2003). "Modification of in vivo and in vitro T- and B-cell-mediated immune responses by the *Pseudomonas aeruginosa* quorum-sensing molecule N-(3-oxododecanoyl)-L-homoserine lactone." Infect Immun **71**(8): 4421-4431.
- Ritter, M., M. Bouloy, P. Vialat, C. Janzen, O. Haller and M. Frese (2000). "Resistance to Rift Valley fever virus in *Rattus norvegicus*: genetic variability within certain 'inbred' strains." J Gen Virol **81**(Pt 11): 2683-2688.
- Ross, T. M., N. Bhardwaj, S. J. Bissel, A. L. Hartman and D. R. Smith (2012). "Animal models of Rift Valley fever virus infection." Virus Res **163**(2): 417-423.
- Rusu, M., R. Bonneau, M. R. Holbrook, S. J. Watowich, S. Birmanns, W. Wriggers and A. N. Freiberg (2012). "An assembly model of rift valley Fever virus." Front Microbiol **3**: 254.
- Schabitz, W. R., R. Kollmar, M. Schwaninger, E. Juettler, J. Bardutzky, M. N. Scholzke, C. Sommer and S. Schwab (2003). "Neuroprotective effect of granulocyte colony-stimulating factor after focal cerebral ischemia." Stroke **34**(3): 745-751.
- Schmaljohn, C. S., S. T. Nichol (2007). Bunyaviridae. Field's Virology. D. M. Knipe, P.M. Howley. Philadelphia, Pa, Wolters Kluwer. **2**: 1741-1790.
- Schneider, A., C. Kruger, T. Steigleder, D. Weber, C. Pitzer, R. Laage, J. Aronowski, M. H. Maurer, N. Gassler, W. Mier, *et al.* (2005). "The hematopoietic factor G-CSF is a neuronal ligand that counteracts programmed cell death and drives neurogenesis." J Clin Invest **115**(8): 2083-2098.
- Schreiber, M., A. Kolbus, F. Piu, A. Szabowski, U. Mohle-Steinlein, J. Tian, M. Karin, P. Angel and E. F. Wagner (1999). "Control of cell cycle progression by c-Jun is p53 dependent." Genes Dev **13**(5): 607-619.
- Schwentker, F. F. and T. M. Rivers (1934). "Rift Valley Fever in Man : Report of a Fatal Laboratory Infection Complicated by Thrombophlebitis." J Exp Med **59**(3): 305-313.
- Shen, Z., G. Reznikoff, G. Dranoff and K. L. Rock (1997). "Cloned dendritic cells can present exogenous antigens on both MHC class I and class II molecules." J Immunol **158**(6): 2723-2730.
- Sherman, M. B., A. N. Freiberg, M. R. Holbrook and S. J. Watowich (2009). "Single-particle cryo-electron microscopy of Rift Valley fever virus." Virology **387**(1): 11-15.

- Shirakawa, F. and S. B. Mizel (1989). "In vitro activation and nuclear translocation of NF-kappa B catalyzed by cyclic AMP-dependent protein kinase and protein kinase C." Mol Cell Biol **9**(6): 2424-2430.
- Shirazi, Y. and P. M. Pitha (1992). "Alpha interferon inhibits early stages of the human immunodeficiency virus type 1 replication cycle." J Virol **66**(3): 1321-1328.
- Shoemaker, T., C. Boulianne, M. J. Vincent, L. Pezzanite, M. M. Al-Qahtani, Y. Al-Mazrou, A. S. Khan, P. E. Rollin, R. Swanepoel, T. G. Ksiazek, *et al.* (2002). "Genetic analysis of viruses associated with emergence of Rift Valley fever in Saudi Arabia and Yemen, 2000-01." Emerg Infect Dis **8**(12): 1415-1420.
- Shrestha, B., B. Zhang, W. E. Purtha, R. S. Klein and M. S. Diamond (2008). "Tumor necrosis factor alpha protects against lethal West Nile virus infection by promoting trafficking of mononuclear leukocytes into the central nervous system." J Virol **82**(18): 8956-8964.
- Siam, A. L. and J. M. Meegan (1980). "Ocular disease resulting from infection with Rift Valley fever virus." Trans R Soc Trop Med Hyg **74**(4): 539-541.
- Siciliano, N. A., J. A. Skinner and M. H. Yuk (2006). "Bordetella bronchiseptica modulates macrophage phenotype leading to the inhibition of CD4+ T cell proliferation and the initiation of a Th17 immune response." J Immunol **177**(10): 7131-7138.
- Simons, J. F. and R. F. Pettersson (1991). "Host-derived 5' ends and overlapping complementary 3' ends of the two mRNAs transcribed from the ambisense S segment of Uukuniemi virus." J Virol **65**(9): 4741-4748.
- Smith, D. R., B. H. Bird, B. Lewis, S. C. Johnston, S. McCarthy, A. Keeney, M. Botto, G. Donnelly, J. Shamblin, C. G. Albarino, *et al.* (2012). "Development of a novel nonhuman primate model for Rift Valley fever." J Virol **86**(4): 2109-2120.
- Smith, D. R., K. E. Steele, J. Shamblin, A. Honko, J. Johnson, C. Reed, M. Kennedy, J. L. Chapman and L. E. Hensley (2010). "The pathogenesis of Rift Valley fever virus in the mouse model." Virology **407**(2): 256-267.
- Smithburn, K. C. (1949). "Rift Valley fever; the neurotropic adaptation of the virus and the experimental use of this modified virus as a vaccine." Br J Exp Pathol **30**(1): 1-16.
- Smithburn, K. C., A. J. Haddow and W. H. Lumsden (1949). "Rift Valley fever; transmission of the virus by mosquitoes." Br J Exp Pathol **30**(1): 35-47.
- Smithburn, K. C., A. F. Mahaffy and *et al.* (1949). "Rift Valley fever; accidental infections among laboratory workers." J Immunol **62**(2): 213-227.
- Spik, K., A. Shurtleff, A. K. McElroy, M. C. Guttieri, J. W. Hooper and C. SchmalJohn (2006). "Immunogenicity of combination DNA vaccines for Rift Valley fever virus, tick-borne encephalitis virus, Hantaan virus, and Crimean Congo hemorrhagic fever virus." Vaccine **24**(21): 4657-4666.

- Steinman, L. (2007). "A brief history of T(H)17, the first major revision in the T(H)1/T(H)2 hypothesis of T cell-mediated tissue damage." Nat Med **13**(2): 139-145.
- Stewart, S., J. Fawcett and W. Jacobson (1985). "Interstitial haemosiderin in the lungs of sudden infant death syndrome: a histological hallmark of 'near-miss' episodes?" J Pathol **145**(1): 53-58.
- Stockinger, B. and M. Veldhoen (2007). "Differentiation and function of Th17 T cells." Curr Opin Immunol **19**(3): 281-286.
- Strandin, T., J. Hepojoki and A. Vaheri (2013). "Cytoplasmic tails of bunyavirus Gn glycoproteins-Could they act as matrix protein surrogates?" Virology **437**(2): 73-80.
- Stroher, U., E. West, H. Bugany, H. D. Klenk, H. J. Schnittler and H. Feldmann (2001). "Infection and activation of monocytes by Marburg and Ebola viruses." J Virol **75**(22): 11025-11033.
- Struthers, J. K. and R. Swanepoel (1982). "Identification of a major non-structural protein in the nuclei of Rift Valley fever virus-infected cells." J Gen Virol **60**(Pt 2): 381-384.
- Sugarman, B. J., B. B. Aggarwal, P. E. Hass, I. S. Figari, M. A. Palladino, Jr. and H. M. Shepard (1985). "Recombinant human tumor necrosis factor-alpha: effects on proliferation of normal and transformed cells in vitro." Science **230**(4728): 943-945.
- Swanepoel, R., Coetzer, J.A.W. (1994). Rift Valley fever. Infectious Diseases of Livestock with Special Reference to South Africa. J. A. Coetzer, G.R. Thomson, and R.C. Tustin. Cape Town, Oxford University Press: 688-717.
- Swanepoel, R., J.A.W. Coetzer (2004). Rift Valley fever. Infectious Diseases of Livestock. J. A. coetzer, R. Tustin. Cape Town, Oxford University Press: 1038-1070.
- Swanepoel, R., J. K. Struthers, M. J. Erasmus, S. P. Shepherd, G. M. McGillivray, A. J. Shepherd, D. E. Hummitzsch, B. J. Erasmus and B. J. Barnard (1986). "Comparative pathogenicity and antigenic cross-reactivity of Rift Valley fever and other African phleboviruses in sheep." J Hyg (Lond) **97**(2): 331-346.
- Swirski, F. K., M. Nahrendorf, M. Etzrodt, M. Wildgruber, V. Cortez-Retamozo, P. Panizzi, J. L. Figueiredo, R. H. Kohler, A. Chudnovskiy, P. Waterman, *et al.* (2009). "Identification of splenic reservoir monocytes and their deployment to inflammatory sites." Science **325**(5940): 612-616.
- Terasaki, K., S. Won and S. Makino (2012). "The C-terminal region of Rift Valley fever virus NSm protein targets the protein to the mitochondrial outer membrane and exerts antiapoptotic function." J Virol **87**(1): 676-682.
- Tigabu, B., T. Juelich, J. Bertrand and M. R. Holbrook (2009). "Clinical evaluation of highly pathogenic tick-borne flavivirus infection in the mouse model." J Med Virol **81**(7): 1261-1269.

- Turkmen, N., B. Eren, R. Fedakar and S. Akgoz (2008). "The significance of hemosiderin deposition in the lungs and organs of the mononucleated macrophage resorption system in infants and children." J Korean Med Sci **23**(6): 1020-1026.
- van Velden, D. J., J. D. Meyer, J. Olivier, J. H. Gear and B. McIntosh (1977). "Rift Valley fever affecting humans in South Africa: a clinicopathological study." S Afr Med J **51**(24): 867-871.
- Vialat, P., A. Billecocq, A. Kohl and M. Bouloy (2000). "The S segment of rift valley fever phlebovirus (Bunyaviridae) carries determinants for attenuation and virulence in mice." J Virol **74**(3): 1538-1543.
- Vialat, P., R. Muller, T. H. Vu, C. Prehaud and M. Bouloy (1997). "Mapping of the mutations present in the genome of the Rift Valley fever virus attenuated MP12 strain and their putative role in attenuation." Virus Res **52**(1): 43-50.
- Villinger, F., P. E. Rollin, S. S. Brar, N. F. Chikkala, J. Winter, J. B. Sundstrom, S. R. Zaki, R. Swanepoel, A. A. Ansari and C. J. Peters (1999). "Markedly elevated levels of interferon (IFN)-gamma, IFN-alpha, interleukin (IL)-2, IL-10, and tumor necrosis factor-alpha associated with fatal Ebola virus infection." J Infect Dis **179** **Suppl 1**: S188-191.
- von Stebut, E., Y. Belkaid, B. V. Nguyen, M. Cushing, D. L. Sacks and M. C. Udey (2000). "Leishmania major-infected murine langerhans cell-like dendritic cells from susceptible mice release IL-12 after infection and vaccinate against experimental cutaneous Leishmaniasis." Eur J Immunol **30**(12): 3498-3506.
- Wallace, D. B., C. E. Ellis, A. Espach, S. J. Smith, R. R. Greyling and G. J. Viljoen (2006). "Protective immune responses induced by different recombinant vaccine regimes to Rift Valley fever." Vaccine **24**(49-50): 7181-7189.
- WHO. (2007). "Rift Valley fever fact sheet." Retrieved August 20, 2007.
- WHO. (2007). "Rift Valley fever fact sheet." August 20, 2007, from <http://www.who.int/mediacentre/factsheets/fs207/en/>.
- WHO. (2007, January 31, 2007). "Rift Valley Fever in Kenya and Somalia - update 3." Global Alert and Response, from http://www.who.int/csr/don/2007_01_31/en/index.html.
- WHO. (2013, May 2013). "Rift Valley fever in Mauritania." Global Alert and Response Retrieved 4/12, 2013, from http://www.who.int/csr/don/2012_11_01/en/index.html.
- Won, S., T. Ikegami, C. J. Peters and S. Makino (2006). "NSm and 78-kilodalton proteins of Rift Valley fever virus are nonessential for viral replication in cell culture." J Virol **80**(16): 8274-8278.
- Won, S., T. Ikegami, C. J. Peters and S. Makino (2007). "NSm protein of Rift Valley fever virus suppresses virus-induced apoptosis." J Virol **81**(24): 13335-13345.
- Wu, G. S. (2004). "The functional interactions between the p53 and MAPK signaling pathways." Cancer Biol Ther **3**(2): 156-161.

- Yadani, F. Z., A. Kohl, C. Prehaud, A. Billecocq and M. Bouloy (1999). "The carboxy-terminal acidic domain of Rift Valley Fever virus NSs protein is essential for the formation of filamentous structures but not for the nuclear localization of the protein." J Virol **73**(6): 5018-5025.
- Yang, X., Y. Zhao, Y. Zhou, Y. Lv, J. Mao and P. Zhao (2007). "Component and antioxidant properties of polysaccharide fractions isolated from *Angelica sinensis* (OLIV.) DIELS." Biol Pharm Bull **30**(10): 1884-1890.
- Yi, P. F., W. Y. Bi, H. Q. Shen, Q. Wei, L. Y. Zhang, H. B. Dong, H. L. Bai, C. Zhang, Z. Song, Q. Q. Qin, *et al.* (2013). "Inhibitory effects of sulfated 20(S)-ginsenoside Rh2 on the release of pro-inflammatory mediators in LPS-induced RAW 264.7 cells." Eur J Pharmacol **712**(1-3): 60-66.
- Yoshioka, K., S. Kakumu, M. Arao, Y. Tsutsumi, M. Inoue, T. Wakita, T. Ishikawa and M. Mizokami (1990). "Immunohistochemical studies of intrahepatic tumour necrosis factor alpha in chronic liver disease." J Clin Pathol **43**(4): 298-302.

Vita

Kimberly Kershea Gray was born on July 26, 1982 in Houston, Texas to Erroll and Ella Cunningham. Kimberly graduated in the top of her class with honors from Flour Bluff High School in Corpus Christi, Texas in 2000. She then attended Southern Arkansas University in Magnolia, Arkansas. She was awarded a Bachelor's degree in biological science in May 2004. Kimberly then went on to Texas A&M-Kingsville and earned her Master's degree in molecular biology in May 2006. While at TAMUK, Kimberly taught microbiology labs to undergraduate students. Kimberly was also the recipient of a Bridges to Doctoral grant while at TAMUK. Kimberly then enrolled at the University of Texas-Medical Branch in the Ph.D. program in August of 2006.

While at UTMB, Kimberly obtained outside funding for her research and education in the form of a NIAID F31 fellowship. Kimberly became a senator for the graduate school in the student government association and a member of the student life advisory committee. During her studies for her Ph.D., Kimberly has published one paper in the online peer-reviewed journal PLoS. After entering UTMB, Kimberly became a member of American Society for Microbiology (ASM), American Society for Virology (ASV), and American Association for Clinical Chemistry (AACC). While at UTMB, Kimberly met and married her husband and changed her last name to Roberts.

Permanent address: 6806 Laughlin Drive

Missouri City, TX 77489

Email address: KKGray726@hotmail.com

Education

B.S., May 2004, Southern Arkansas University, Magnolia, Arkansas

M.S., May 2006, Texas A&M University-Kingsville, Kingsville, Texas

Publications

GRAY KIMBERLY, Worthy MN, Juelich TL, Agar SL, Poussard A, Ragland D, Freiberg AN and Holbrook MR: Chemotactic and inflammatory responses in the liver and brain are associated with pathogenesis of Rift Valley fever virus infection in the mouse. February 28, 2012, PLoS Neglected Tropical Diseases.

Presentations at Scientific Meetings

1. **Gray KK**, Freiberg AN, and Holbrook MR: Host signaling response after Rift Valley Fever virus infection. Presentation at American Society for Virology 31st annual meeting, Madison, Wisconsin, 2012. [**Oral** Presentation]
2. **Gray KK**, Freiberg AN, and Holbrook MR: Host signaling response after Rift Valley Fever virus infection. Presentation at American Society for Virology 30th annual meeting, Minneapolis, Minnesota, 2011. [**Oral** Presentation]
3. **Gray KK**, Freiberg AN, and Holbrook MR: Innate immune response to Rift Valley Fever virus infection. Presentation at American Society for Virology 29th annual meeting, Bozeman, Montana, 2010. [**Oral** Presentation]

4. **Gray KK**, Freiberg AN, and Holbrook MR: Innate immune response to Rift Valley Fever virus infection. Presentation at American Society for Tropical Medicine and Health, Atlanta, Georgia, 2010. [**Oral** Presentation]

5. **Gray KK** and Holbrook MR: Cellular Immune Response to Rift Valley Fever Virus Infection, American Society for Tropical Medicine and Hygiene. Washington, D.C. November 2009. [**Poster** Presentation]

This dissertation was typed by Kimberly K. Roberts